AD-A252 840

SYNTHESIS AND STRUCTURAL CHARACTERIZATION OF NEW HIGH-VALENT INORGANIC FLUORINE COMPOUNDS AND THEIR OXIDIZING PROPERTIES:

VOLUME 1.

Prof. G.J. Schrobilgen

McMaster University
Department of Chemistry
Hamilton, Ontario L8S 4M1
Canada

DTIC
ELECTE
JUN 16 1992
S
A
D

February 1992

Final Report

92-15509

92 6 15 048

PHILLIPS LABORATORY
Propulsion Directorate
AIR FORCE SYSTEMS COMMAND
EDWARDS AIR FORCE BASE CA 93523-5000

NOTICE

When U.S. Government drawings, specifications, or other data are used for any purpose other than a definitely related Government procurement operation, the fact that the Government may have formulated, furnished, or in any way supplied the said drawings, specifications, or other data, is not to be regarded by implication or otherwise, or in any way licensing the holder or any other person or corporation, or conveying any rights or permission to manufacture, use or sell any patented invention that may be related thereto.

FOREWORD

This final report was prepared by McMaster University, Hamilton, Ontario, Canada under contract F49620-87-C-0049 for Operating Location AC, Phillips Laboratory (AFSC), Edwards AFB CA 93523-5000. OLAC PL Project Manager was 1Lt Robert A. mantz.

This report has been reviewed and is approved for release and distribution in accordance with the distribution statement on the cover and on the SF Form 298.
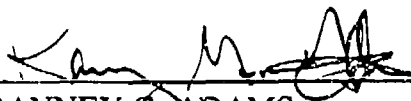

ROBERT A. MANTZ, 1Lt, USAF
Project Manager

STEPHEN L. RODGERS
Chief, Emerging Technologies Branch

FOR THE COMMANDER

DAVID W. LEWIS, Major, USAF
Acting Director,
Fundamental Technologies Division

RANNEY G. ADAMS
Public Affairs Director

REPORT DOCUMENTATION PAGE

Public reporting burden for this collection of information is estimated to average 1 hour per response, including the time for reviewing instructions, searching existing data sources, gathering and maintaining the data needed, and completing and reviewing the collection of information. Send comments regarding this burden estimate or any other aspect of this collection of information, including suggestions for reducing this burden, to Washington Headquarters Services, Directorate for Information Operations and Reports, 1215 Jefferson Davis Highway, Suite 1204, Arlington, VA 22202-4302, and to the Office of Management and Budget, Paperwork Reduction Project (0704-0188), Washington, DC 20503.

1. AGENCY USE ONLY (Leave blank)	2. REPORT DATE February 1992	3. REPORT TYPE AND DATES COVERED Final-1 May 1987 to 30 April 1991

4. TITLE AND SUBTITLE	5. FUNDING NUMBERS
SYNTHESIS AND STRUCTURAL CHARACTERIZATION OF NEW HIGH-VALENT INORGANIC FLUORINE COMPOUNDS AND THEIR OXIDIZING PROPERTIES	C - F49620-87-C-0049 PR- 5730 TA- 007G

6. AUTHOR(S)

G.J. Schrobilgen

7. PERFORMING ORGANIZATION NAME(S) AND ADDRESS(ES)	8. PERFORMING ORGANIZATION REPORT NUMBER
McMaster University Department of Chemistry Hamilton, Ontario L8S 4MI Canada	

9. SPONSORING/MONITORING AGENCY NAME(S) AND ADDRESS(ES)	10. SPONSORING/MONITORING AGENCY REPORT NUMBER
Phillips Laboratory (AFSC) OLAC PL/RKFE Edwards AFB CA 93523-5000	PL-TR-91-3108 Volume 1

11. SUPPLEMENTARY NOTES

Phillips Laboratory, Edwards is the former Astronautics Laboratory.
COSATI Code: 07/02

12a. DISTRIBUTION/AVAILABILITY STATEMENT	12b. DISTRIBUTION CODE
Approved for Public Release; Distribution is unlimited.	

13. ABSTRACT (Maximum 200 words)

Noble gas fluorine oxidizers of Neon, Krypton, Argon, and Xenon have been synthesized and characterized. KrF^+ and XeF^+ cations have been made with neutral organic bases. Kr-N and Kr-O bonded molecules are also synthesized and characterized. The hypervalent compounds ClF_6^- and XeF_5^- are made. The anions IF_6O^-, TeF_6O^{2-}, TeF_7^- and TeF_8^{2-} anions are also made. Proof that the ClF_6^- anion exists is also presented. The photoelectron spectra of XeF_2, XeF_4, and XeF_6 are obtained using monochromatized synchrotron radiation. The synthesis and characterization of $Sb(OTeF_5)_6^-$ Et_4N^+, and $Bi(OTeF_5)_6^-$ Et_4N^+ salts is completed. Radiotracer experiments involving ^{18}F are also accomplished to show the inability to synthesize NF_5 is due to mainly steric reasons.

14. SUBJECT TERMS		15. NUMBER OF PAGES 170
fluorine, oxidizers, noble gas, NMR, photoelectron, HEDM.		16. PRICE CODE

17. SECURITY CLASSIFICATION OF REPORT	18. SECURITY CLASSIFICATION OF THIS PAGE	19. SECURITY CLASSIFICATION OF ABSTRACT	20. LIMITATION OF ABSTRACT
UNCLASSIFIED	UNCLASSIFIED	UNCLASSIFIED	SAR

NSN 7540-01-280-5500

Standard Form 298 (Rev 2-89)
Prescribed by ANSI Std 239-18
298-102

OVERVIEW OF THE REPORT

The following annual report encompasses eleven areas of research funded by the United States Air Force Astronautics Laboratory, Edwards Air Force Base, California under Contract F49620-87-C-0049. Where possible published or about to be published work is included in this Report under each of the eleven appropriate subheadings. The basic philosophy underpinning this work has been to develop the technology for the synthesis, storage and handling of new high-energy density materials. The importance of performing the "easier" heavy element chemistry as the ground work to synthesizing the more challenging and potentially more useful lighter analogs has been stressed throughout much of this work. The validity of this approach is best illustrated in Part I where the synthesis of $HC{\equiv}N\text{-}XeF^+$ is described. The synthesis of the xenon compound has made possible the realization of the lighter and more energetic krypton analog, $HC{\equiv}N\text{-}KrF^+$. The publication of these results in turn precipitated a total of four theoretical papers on $HC{\equiv}N\text{-}NgF^+$ (Ng = Ne, Ar, Kr, Xe). While the neon analog is forecast to be unstable, the argon analog, $HC{\equiv}N\text{-}ArF^+$ is predicted to be stable. The hope of binding ArF^+ (also presently unknown), potentially an oxidant of unprecedented strength, to a fuel moiety, HCN, is intriguing and the direct consequence of having done a thorough job delineating the chemistry of the heavier congeners.

Part I is concerned with the syntheses and characterization of noble-gas species in novel bonding situations, more specifically, the investigation of the interactions of the strong oxidant Lewis acid noble-gas cations, KrF^+ and XeF^+, with neutral organic nitrogen bases. This work has been summarized previously in two Annual Technical Reports: May 1, 1987 - April 30, 1988 and May 1, 1988 - April 30, 1989. These and the present report outline the syntheses and characterization of a large number of new xenon compounds that had been prepared by the interaction of the strong oxidant Lewis acid cation XeF^+ with a number of organic nitrogen bases. The majority of the bases that had been selected for study were oxidatively resistant perfluoro-organic nitrogen bases with first ionization potentials exceeding 10-11 eV. These recent findings represent a major extension of Group VIII (18) chemistry in that they (1) significantly extend the range of known Xe-N bonded species, (2) demonstrate that a large range of fluoro-organic ligands are capable of stabilizing Xe(II), (3) produce several examples of the first compounds in which a noble-gas atom serves as an aromatic substituent; (4) provide new series of model compounds which may aid in developing synthetic approaches to the

1

formation of new xenon-carbon and krypton-oxygen bonds; (5) provide the first examples of Kr-N bonded species, which, in turn provided the impetus for us to successfully attempt the synthesis of the first compound containing a Kr-O bond. Most importantly from the viewpoint of practical impact on the field of propellants and monopropellants, this aspect of our research has demonstrated that under the appropriate conditions, strongly oxidizing Lewis acid cations can be bound to fuel substrates containing a base center. The best illustration of this which we have discovered in the course of this work has been the $F-Kr-N\equiv CH^+$ cation, where KrF^+ represents the most potent chemical oxidant known.

The syntheses and attempted syntheses of adduct cations with other xenon Lewis acids are also described in Part I, namely $XeOTeF_5^+$ and XeF_3^+. Using the $XeOTeF_5^+$ cation as an acceptor, two novel compounds containing the first examples of N-Xe-O linkages were prepared, $s-C_3F_3N_2N-XeOTeF_5^+AsF_6^-$ and $s-C_3F_3N_2N-XeOTeF_5^+Sb(OTeF_5)_6^-$. The novel salt, $XeOTeF_5^+Sb(OTeF_5)_6^-$, was also synthesized in the course of this work, and is the only noble-gas salt known which is soluble at low temperatures in a low polarity solvent and also represents the first ionic fully -$OTeF_5$ substituted derivative. These compounds were characterized by ^{19}F NMR, [129]Xe NMR and low-temperature laser Raman spectroscopy.

Part II describes the syntheses and characterization of the first Kr-N bonded species, $HC\equiv N-KrF^+$ and three further examples of Kr-N bonds in which the KrF^+ cation is bonded to an organic moiety, namely, $R_FC\equiv N-KrF^+$ ($R_F = CF_3$, C_2F_5, $n-C_3F_7$) and their xenon analogs.

Part III describes our recently published theoretical findings relating to the $HC\equiv N-KrF^+$ and $HC\equiv N-XeF^+$ cations.

Part IV describes the preparation and characterization of $Kr(OTeF_5)_2$. This compound provides the first example of a species containing a Kr-O bond and has been prepared by the reaction of KrF_2 with natural abundance and [17]O-enriched $B(OTeF_5)_3$ at -90 to -112 °C in SO_2ClF solvent. Characterization of thermally unstable $Kr(OTeF_5)_2$ and its decomposition products has been achieved using ^{19}F and ^{17}O NMR spectroscopy.

In view of the reported Lewis base properties of $N\equiv SF_3$ and its resistance to oxidation (first adiabatic ionization potential, 12.50 eV), it was considered likely that $N\equiv SF_3$ would form adducts with the noble-gas cations XeF^+, $XeOTeF_5^+$ and $XeOSeF_5^+$ which would be stable to redox degradation. No estimates of electron affinity (EA) other than for XeF^+ (10.9 ev), KrF^+ (13.2 eV) and ArF^+ (13.6

2

eV) are available. However, the EA values of $XeOSeF_5^+$ and $XeOTeF_5^+$ are predicted to be less than that of XeF^+, and all xenon(II) cations are below the first ionization potential (IP) of $N\equiv SF_3$. Consequently, the xenon(II) cations were expected to form redox-stable adduct cations with $N\equiv SF_3$. In Part V, the ligand, $N\equiv SF_3$, was also studied in a variety of oxidatively resistant solvents deemed suitable for noble-gas compound syntheses, and adducted with the Lewis acid AsF_5 to assess the base character of the ligand. Aspects of this work were reported on in our Annual Technical Report, May 1, 1989 - April 30, 1990. The $F_5SeO-Xe-N\equiv SF_3^+$ and $F-Xe-N\equiv SF_3^+$ cations have been synthesized in BrF_5 solvent and fully characterized by ^{129}Xe, ^{14}N and ^{19}F NMR spectroscopy. The salt, $F-Xe-N\equiv SF_3^+AsF_6^-$, was also synthesized by the direct combination of $XeF^+AsF_6^-$ and $N\equiv SF_3$ at -20 °C and the vibrational spectrum was studied using low-temperature Raman spectroscopy. In addition, the solvolysis of $F-Xe-N\equiv SF_3^+$ has been studied in anhydrous HF and has lead to the novel $F_4S=N(H)-Xe-I^+$ cation. The latter cation has been characterized in solution by ^{129}Xe, ^{14}N and ^{19}F NMR spectroscopy. Based on the ^{19}F and ^{129}Xe NMR spectroscopic data, further solvolysis of this cation in HF gives rise to the $F_5S-N(H_2)-Xe-F^+$ cation, the first example of an sp^3-nitrogen bonded to a noble gas. Based on our understanding of Lewis acid-base adduct chemistry incorporating the strongly oxidizing noble-gas cations as acceptor centers, it should be possible to extend the range of bases coordinated to noble-gas cations and to other strong oxidizers such as chlorine fluoro-cations to include related bases having heats of formation that are more endothermic such as NH_2F ($\Delta H^o_{f(g)}$ = -9.1 kcal mol^{-1}, as a pure compound NH_2F is a violent detonator; cf., gas phase heats of formation for $HC\equiv N$, -31.2; NF_3, -31.9; NF_2H, -15.5; NH_3, -11.0 kcal mol^{-1}). Although the latter chemistry has not yet been achieved, much of the ground work has been laid by demonstrating that the higher molecular weight analogs exist. In this instance that XeF^+ can be coordinated to the SF_5 analog, F_5SNH_2, and to $F_4S=NH$ in their respective novel cations $FXe-N(H_2)SF_5^+$ and $FXe-N(H)=SF_4^+$.

In Parts VI and VII the hypervalent anions ClF_6^- and XeF_5^- were prepared and studied for the first time. Aspects of the work described in Parts VI and VII were carried out in collaboration with Drs. K.O. Christe and W.W. Wilson, Rocketdyne Division, North American Rockwell, Canoga Park, California. This work has previously been summarized in our Annual Technical Report, May 1, 1989 - April 30, 1990. Hypervalent fluoro- and oxofluoro-anions are known to offer the best possibility for stabilizing high oxidation states of the elements. These species are of particular importance as they serve to extend our knowledge of the interrelation of valence electron lone pair

3

stereochemical activity and coordination number in strong oxidizer fluorides. The ClF_6^- anion was determined to possess a stereochemically inactive lone pair while the two valence lone pairs of XeF_5^- are active. Since our last Annual Technical Report, the hypervalent, highly coordinated, high-oxidation state anions IF_6O^-, TeF_6O^{2-}, TeF_7^-, IF_8^- and TeF_8^{2-} have been synthesized in anhydrous $CH_3C \equiv N$ using anhydrous $N(CH_3)_4^+F^-$ as the fluoride ion source and are reported on in Part VII.

In Part VI, the low-temperature reaction of either $N(CH_3)_4F$ or CsF with ClF_5 in $CH_3C \equiv N$ solutions are shown to produce white solids (the $N(CH_3)_4^+$ salt is explosive) which, based on material balances and low-temperature Raman spectra, contain the ClF_6^- anion. The similarity of the Raman spectrum of ClF_6^- to that of the octahedral BrF_6^- ion indicates that ClF_6^- is also octahedral and that the free valence electron pair on chlorine is sterically inactive The existence of the ClF_6^- anion was further supported by an ^{18}F exchange experiment between ClF_5 and ^{18}F-labelled FNO which showed complete randomization of the ^{18}F isotope among the two molecules. A high-field ^{19}F NMR study of neat ClF_5 and ClF_5 in anhydrous HF solution in the presence and absence of excess CsF has provided accurate measurements of the ClF_5 NMR parameters including, for the first time, both $^{37/35}Cl$ secondary isotopic ^{19}F NMR shifts. Moreover, the NMR study also supports the existence of ClF_6^-, showing that ClF_5 undergoes slow chemical exchange with excess CsF in anhydrous HF at room temperature.

In Part VII, the low-temperature reaction of $N(CH_3)_4F$ with XeF_4 in $CH_3C \equiv N$ was shown to produce $N(CH_3)_4^+XeF_5^-$, a stable white crystalline solid at room temperature, but shock-sensitive at -196 °C. The structure of the XeF_5^- anion was determined by X-ray crystallography and shown to be pentagonal planar, representing the first example of an AX_5E_2 (in VSEPR nomenclature) geometry. The anion was also characterized by vibrational spectroscopy and in solution by ^{19}F and ^{129}Xe NMR spectroscopy. The XeF_7^- anion has also been prepared as the $N(CH_3)_4^+$ salt and studied in $CH_3C \equiv N$ solution by ^{129}Xe NMR spectroscopy and shown to be fluxional on the NMR time scale.

Our preparation of the XeF_5^- anion, the first known example of a pentagonal planar AX_5E_2 (where E stands for a free valence electron pair) species, prompted us to study some closely related iodine and tellurium compounds. Furthermore, there are relatively few examples of main-group species which allow the applicability of the valence shell electron pair repulsion (VSEPR) rules to coordination numbers exceeding six to be tested. In Part VIII the IF_6O^-, TeF_6O^{2-}, TeF_7^-, IF_8^- and TeF_8^{2-} anions have been synthesized in anhydrous $CH_3C \equiv N$ using anhydrous $N(CH_3)_4^+F^-$ as the fluoride ion source and characterized by NMR spectroscopy and vibrational spectroscopy and represent examples

of seven- and eight-coordinate species having symmetries C_{5v} (IF_6O^- and TeF_6O^{2-}), D_{5h} (TeF_7^-) and D_{4d} (IF_8^-, TeF_8^{2-}).

Part IX describes the photoelectron spectra of XeF_2, XeF_4 and XeF_6 obtained using monochromatized synchrotron radiation. We have resolved ligand field splittings by photoelectron spectroscopy in relatively deep core levels ($E_B > 30$ eV) for the first time. To resolve these effects required very high resolution not previously attained. The spectra have been characterized using a simple Hamiltonian involving crystal field splitting and spin-orbit splitting. Of particular interest, we have estimated the gas phase structure of XeF_6 from the Xe 4d spectra using an additive model similar to that used in Mossbauer spectroscopy. It has been shown that for a C_{3v} XeF_6 structure, $\Theta_{1,2,3} = 50°$ and $\Theta_{4,5,6} = 76 ±4°$. This is perhaps the best experimental evidence for the distortion of gas phase XeF_6, and it is shown to be in excellent agreement with the recent theoretical calculations.

Part X describes the syntheses and characterization of the fully substituted $-OTeF_5$ derivatives of the powerful Lewis acids SbF_5 and BiF_5, namely $M(OTeF_5)_5$ (M = Sb, Bi) and the isolation of Et_4N^+ salts containing the novel octahedral anions $M(OTeF_5)_6^-$. The properties of these interesting species are described together with their characterization by ^{19}F NMR spectroscopy and, in the case of $M(OTeF_5)_6^-$, by ^{121}Sb and ^{209}Bi NMR spectroscopy. A previous Annual Report (May 1, 1987 - April 31, 1988) described the syntheses and characterization of the fully substituted $-OTeF_5$ derivatives of the powerful Lewis acids SbF_5 and BiF_5, namely $M(OTeF_5)_5$ (M = Sb, Bi) and the isolation of Et_4N^+ salts containing the novel octahedral anions $M(OTeF_5)_6^-$. The properties of these interesting species were described together with their characterization by ^{19}F NMR spectroscopy and, in the case of $M(OTeF_5)_6^-$, by ^{121}Sb and ^{209}Bi NMR spectroscopy. As a continuation of this study, Part X also describes the $[Pb(OTeF_5)_6]^{2-}$ anion, which has been generated in $CH_3C\equiv N$ by means of the reaction of $(Et_4N^+)_2PbCl_6^{2-}$ with (i) $AgOTeF_5$ and (ii) $Xe(OTeF_5)_2$. This is the first example of a Pb(IV) compound containing the highly electronegative, monovalent $OTeF_5$ ligand. The $[Pb(OTeF_5)_6]^{2-}$ anion is a large oxidatively resistant anion which is of great interest for stabilizing strongly oxidizing cations such as the noble-gas cations. The $[Pb(OTeF_5)_6]^{2-}$ anion has thus far been characterized in $CH_3C\equiv N$ by ^{207}Pb and ^{19}F NMR spectroscopy. The inorganic chemistry of Pb(IV) has also been extended by synthesizing mixtures of the previously unknown octahedral anions $[PbCl_nF_{6-n}]^{2-}$. All the above anions have been characterized in $CH_3C\equiv N$ solution by ^{19}F and ^{207}Pb NMR spectroscopy. All of these anions are expected, unlike their fluorine analogs, AsF_6^-, SbF_6^- and BiF_6^-, to be weakly coordinating anions.

For example, $XeF^+SbF_6^-$ is strongly fluorine-bridged in the solid state, i.e., $F-Xe^+---F-SbF_5^-$, whereas the cation and anion in the $OTeF_5$-analog, $XeOTeF_5^+Sb(OTeF_5)_6^-$, are only weakly interacting. It is anticipated that these anions hold considerable promise for the preparation of novel and unusual species by virtue of their weakly coordinating natures. For example, one might anticipate being able to protonate xenon if the following reaction were carried out in a solvent having a proton affinity lower than that of Xe:

$$Xe(OTeF_5)_2 + Sb(OTeF_5)_3 + HOTeF_5 \longrightarrow HXe^+Sb(OTeF_5)_6^- \qquad (1)$$
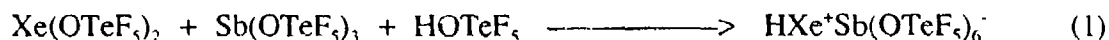
In this instance, $Sb(OTeF_5)_6^-$ could reasonably be expected to have a proton affinity lower than that of Xe; if this were so then so that Xe would be preferentially protonated. These large weakly basic anions may also be useful in stabilizing the methyl analog, $XeCH_3^+$. The XeH^+, $XeCH_3^+$ and $KrCH_3^+$ cations are spectroscopically well characterized in the gas phase and the other NgH^+ cations are also stable gas phase species and one might anticipate using these weakly coordinating anions to protonate lighter noble gases. The isolation of the first salts of the heavy and light noble-gas cations, NgH^+ and $NgCH_3^+$, could be of general interest to the development and storage of monopropellants and fuels.

Part XI represents a collaborative effort with Drs. K.O. Christe and W.W. Wilson, Rocketdyne Division, North American Rockwell, Canoga Park, California. The project is concerned with ^{18}F radiotracer exchange experiments which confirm that the lack of pentacoordinated nitrogen species, namely NF_5, is due mainly to steric reasons.

6

PART I

LEWIS ACID PROPERTIES OF XeL$^+$ (L = F, OSeF$_5$, OTeF$_5$) CATIONS; ADDUCTS WITH ORGANIC AND FLUOROORGANIC NITROGEN BASES AND SOLVOLYTIC BEHAVIOR OF HC≡N-XeF$^+$ IN ANHYDROUS HF

8

LEWIS ACID PROPERTIES OF NOBLE-GAS CATIONS

Gary J. Schrobilgen

Department of Chemistry
McMaster University
Hamilton, Ontario L8S 4M1
Canada

INTRODUCTION

While many examples of xenon bonded to oxygen or fluorine and of xenon bonded to other highly electronegative inorganic ligands through oxygen were synthesized immediately following the discovery of noble-gas reactivity (1), over a decade had elapsed before an example with a ligating atom other than oxygen and fluorine, namely nitrogen, was synthesized (2) and two decades before the Xe-N bond in $FXeN(SO_2F)_2$ was definitively characterized in the solid state by X-ray crystallography and in solution by multinuclear magnetic resonance spectroscopy (3). Other imidodisulfurylfluoride xenon-nitrogen bonded species have since been definitively characterized using primarily NMR spectroscopy, namely, $Xe[N(SO_2F)_2]_2$ (4,5), $F[XeN(SO_2F)_2]_2^+$ (4,5), $XeN(SO_2F)_2^+AsF_6^-$ (6) and $XeN(SO_2F)_2^+Sb_3F_{16}^-$ (6) and the latter salt has also been characterized by single crystal X-ray diffraction. The compound, $Xe[N(SO_2CF_3)_2]_2$ (7), has also been prepared and characterized, and is the most thermally stable of the imido derivatives of xenon.

Recently, a significant extension of noble-gas chemistry, and in particular, noble-gas nitrogen bonds, has been achieved by taking advantage of the Lewis acid properties of noble-gas cations. This has given rise to numerous new examples of xenon-nitrogen and krypton-nitrogen bonds. The

9

adduct salts, which have stabilities ranging from explosive at -60 °C for F-Kr-N≡CH$^+$AsF$_6^-$ (8) to stable at room temperature for s-C$_3$F$_3$N$_2$N-XeF$^+$AsF$_6^-$ (9), have donor-acceptor bonds which are among the weakest bonds that still deserve to be called bonds. The present Review outlines the syntheses, structural characterization and bonding of noble-gas adduct cations for a variety of organic and inorganic nitrogen base centers.

LEWIS ACID AND OXIDANT PROPERTIES OF NOBLE-GAS CATIONS

In view of the propensity of the XeF$^+$ cation to form strong fluorine bridges to counter anions in the solid state (10), the XeF$^+$ cation may be regarded as having a significant Lewis acid strength. Based on considerations of the high electron affinities of the cations (ArF$^+$, 13.7 eV (11); KrF$^+$, 13.2 eV (12); XeF$^+$, 10.9 eV (13)) and first adiabatic ionization potentials of selected bases, where the first adiabatic ionization potential, IP$_1$, determined from photoelectron spectroscopy, is equal to or greater than the estimated electron affinity, EA, of the noble-gas cation; it has been possible to single out specific nitrogen bases and classes of nitrogen bases which offer reasonable promise for preparing noble-gas adduct cations in which the strongly oxidizing noble-gas cations are bound to organic and perfluoro-organic fragments through the nitrogen of the base. A list of some nitrogen bases that have potential or proven compatibility with the estimated electron affinities of the XeF$^+$ and/or KrF$^+$ cations is given in Table 1 along with their IP$_1$ values.

In many ways HC≡N, with IP$_1$ = 13.59 eV (14), is archetypical of the other oxidatively resistant organic and perfluoro-organic nitrogen bases which form adducts with noble-gas Lewis acid centers. For that reason, its interactions

Table 1.   First Adiabatic Ionization Potentials of Some Organic and Inorganic Nitrogen Bases

Compound	1st Ionization Potential	References
$CF_3C\equiv N$	13.90	14
$N\equiv C-C\equiv N$	13.57	15
$HC\equiv N$	13.59	13
trans-N_2F_2	13.10 ± 0.1	16
$CH_2FC\equiv N$	13.00 ± 0.1	17
$CH_2ClC\equiv N$	12.90	17
$N\equiv SF_3$	12.50	18
$ClC\equiv N$	12.49 ± 0.04	19
$CHF_2C\equiv N$	12.40	17
$CD_3C\equiv N$	12.24 ± 0.005	20
$CHCl_2C\equiv N$	12.20 ± 0.1	17
$CH_3C\equiv N$	12.19 ± 0.005	20
N_2F_4	12.04 ± 0.1	21
$BrC\equiv N$	11.95 ± 0.08	19
$C_2H_5C\equiv N$	11.85	15
$N\equiv SF$	11.82	18
$n-C_3H_7C\equiv N$	11.67	22
ND_3	11.52	23
$(CH_3)_2CHC\equiv N$	11.49	22
$s-C_3F_3N_3$	11.50	24
ND_2H	11.47 ± 0.02	23
$N\equiv C-C\equiv C-C\equiv N$	11.45 ± 0.02	25
$N\equiv C-C\equiv C-C\equiv C-C\equiv N$	11.40	25
$S(C\equiv N)_2$	11.32	26
$(CH_3)_3CC\equiv N$	11.11	22
$IC\equiv N$	10.98 ± 0.05	19
$H_2NC\equiv N$	10.76	27
$B-B_3F_3N_3$	10.46	24
NH_3	10.34 ± 0.07	28
C_5F_5N	10.08	24
$s-C_3H_3N_3$	10.07 ± 0.05	29

11

with the XeF^+ and KrF^+ cations will be discussed in considerable detail.

SYNTHETIC APPROACHES AND CHARACTERIZATION

Multi-nuclear magnetic resonance spectroscopy has played an important role in the characterization of noble-gas species (31-33). A substantial portion of the present Review is concerned with structural characterization and inferences regarding bonding derived from NMR studies. The role of NMR in noble-gas chemistry is exemplified by xenon, although the observation of the ^{19}F, $^{14,15}N$, ^{13}C and ^1H NMR spectra is equally crucial. Xenon is the most favorable noble-gas from an NMR standpoint since it has a spin-1/2 nuclide, ^{129}Xe (26.44% natural abundance), with a receptivity of 31.8 relative to that of natural abundance ^{13}C. The high receptivity, non-quadrupolar nature and short spin-lattice relaxation times of ^{129}Xe allow spectral data to be readily acquired using modern FT NMR spectrometers.

The Hydrocyano Cations, $HC≡N-NgF^+$ (Ng = Kr or Xe). Hydrogen cyanide is oxidatively among the most resistant ligands investigated thus far (Table 1), having a first adiabatic ionization potential of 13.59 eV. The estimated electron affinity of XeF^+ (10.9 eV) (13) suggested that $HC≡N$ would be resistant to oxidative attack by the XeF^+ cation and that $HC≡N-XeF^+$ might have sufficient thermal stability to permit its spectroscopic characterization in solution and in the solid state.

The reaction of XeF^+ with $HC≡N$ and the subsequent isolation of $HC≡N-XeF^+AsF_6^-$ and its characterization have indeed been realized. The reactions of

XeF$^+$AsF$_6^-$ and Xe$_2$F$_3^+$AsF$_6^-$ with HC≡N have been reported (34,35) and were carried out according to equations (1) and (2) by combining stoichiometric amounts of the reactants in anhydrous HF (-20 to -10 °C).

$$XeF^+AsF_6^- \quad + \quad HC≡N \quad \longrightarrow \quad HC≡N-XeF^+AsF_6^- \qquad (1)$$

$$Xe_2F_3^+AsF_6^- \quad + \quad HC≡N \quad \longrightarrow \quad HC≡N-XeF^+AsF_6^- \quad + \quad XeF_2 \qquad (2)$$

The compound, HC≡N-XeF$^+$AsF$_6$, has been isolated as a white microcrystalline solid upon removal of the solvent a -30 °C and was stable for up to 4 - 6 hrs. at 0 °C. Solutions of HC≡N-XeF$^+$AsF$_6^-$ in HF solution at ambient temperature slowly decompose over a period of 13 hrs.

Every element in the HC≡N-XeF$^+$ cation possesses at least one nuclide which is suitable for observation by NMR spectroscopy, namely, the spin-1/2 nuclei ^{1}H, ^{13}C, ^{15}N, ^{129}Xe and ^{19}F, and the spin-1 nucleus ^{14}N (Figure 1). Multinuclear magnetic resonance spectra were recorded for HC≡N-XeF$^+$AsF$_6^-$ in HF and BrF$_5$ solvents for all six spin-1/2 nuclei of the cation using natural abundance and ^{13}C and ^{15}N enriched compounds. All possible nuclear spin-spin couplings have been observed, establishing the solution structure of the HC≡N-XeF$^+$ cation (Table 2). Included among these scalar couplings are ^{1}J(^{129}Xe-^{14}N), ^{2}J(^{129}Xe-^{13}C) and ^{3}J(^{129}Xe-^{1}H), representing the first time these scalar couplings have been observed between these nuclides.

An interesting feature of the NMR spectroscopy of the HC≡N-XeF$^+$ cation is the ready observation of the directly bonded ^{129}Xe-^{14}N and ^{14}N-^{13}C scalar couplings. The observation of both couplings and the relative ease of observing ^{1}J(^{129}Xe-^{14}N) in the alkyl nitrile, s-trifluorotriazine and

13
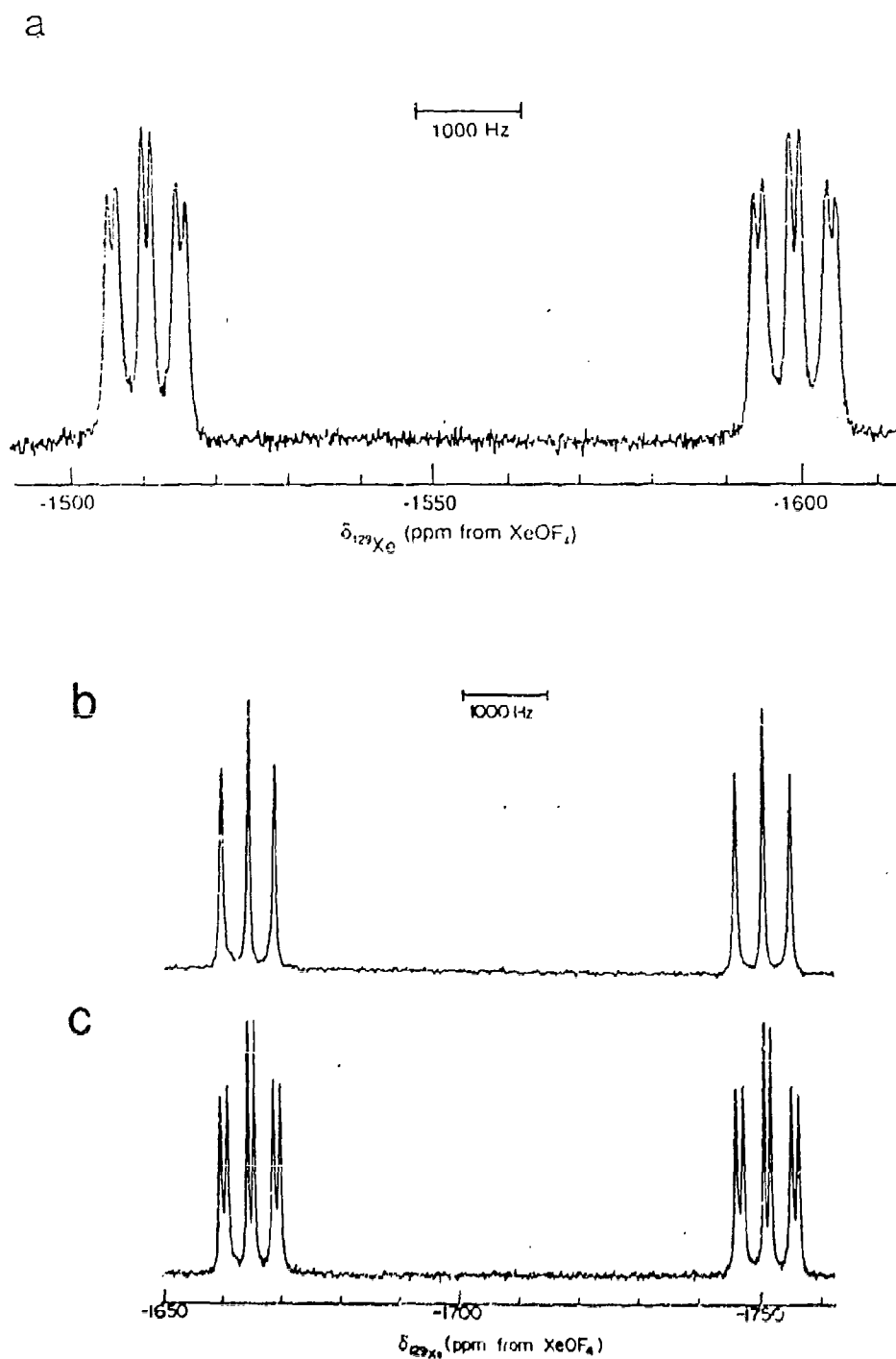
Figure 1.

^{129}Xe NMR spectra (69.563 MHz) recorded in HF solvent at -10 °C for (a) HC≡N-XeF⁺AsF₆⁻ for a 99.2% ^{13}C enriched sample; and CH₃C≡N-XeF⁺AsF₆⁻ where (b) is the natural spectrum and (c) is 99.7% ^{13}C enriched at the 2-carbon. (Reprinted with permission from ref. (34)).

perfluoropyridine adducts of XeF$^+$ (see Spectroscopic Findings and Table 3) is attributed to several factors which minimize quadrupole relaxation of the ^{129}Xe–^{14}N and ^{14}N–^{13}C couplings; the low electric field gradient at the ^{14}N nucleus of the adduct cations, low viscosity of the HF solvent leading to a short molecular correlation time and the small line width factor for ^{14}N (36). However, in the higher viscosity solvent BrF$_5$ (–58 °C), the ^{129}Xe–^{14}N and ^{14}N–^{13}C couplings are quadrupole collapsed into single lines. Because they are generally obscured owing to quadrupolar relaxation caused by the ^{14}N nucleus, ^{15}N enrichment was required for the observation of scalar couplings between nitrogen and non-directly bonded nuclei where the magnitudes of the couplings are small (Table 2).

Prior to the synthesis of the HC≡N–NgF$^+$ cation, no examples of krypton compounds had been reported in which krypton is bonded to an element other than fluorine. In view of the previous success in forming the HC≡N–XeF$^+$ cation (34,35), the synthesis of the krypton(II) analog was undertaken (8). The estimated electron affinity for KrF$^+$ of 13.2 eV suggested that HC≡N might have at least a marginal resistance to oxidative attack by the KrF$^+$ cation and that HC≡N–KrF$^+$ might have sufficient thermal stability to permit its spectroscopic characterization.

Unlike the xenon(II) analog, the direct interaction of KrF$^+$AsF$_6^-$ with HC≡N solutions in HF and BrF$_5$ solvents was not attempted owing to the strongly oxidizing character of the KrF$^+$ cation towards HC≡N and BrF$_5$ as well as its tendency to undergo auto-redox reactions in both solvent media. Rather, the interaction of less reactive KrF$_2$ with HC≡NH$^+$AsF$_6^-$ in HF was the preferred synthetic route. Reaction of sparingly soluble HC≡NH$^+$AsF$_6^-$ with KrF$_2$ in HF at –60 °C led to instantaneous deposition of a white solid which, upon warming

Table 2. NMR Chemical Shifts and Spin-Spin Coupling Constants for the HC≡N-XeF[+] Cation[a]

Chemical Shifts (ppm)[b]

$\delta(^{129}Xe)$	$\delta(^{19}F)$	$\delta(^{14}N/^{15}N)$	$\delta(^{13}C)$	$\delta(^{1}H)$
-1555	-199.0	-234.5	104.1	4.70
(-1570)	(-193.1)	(-230.2)		(6.01)

Coupling Constants (Hz)

$^{1}J(^{129}Xe-^{19}F)$	6171 (6165)		
$^{1}J(^{129}Xe-^{14}N)$	334	$^{1}J(^{129}Xe-^{15}N)$,	471 (483)
$^{1}J(^{14}N-^{13}C)$,	22	$^{1}J(^{13}C-^{1}H)$,	308
$^{2}J(^{129}Xe-^{13}C)$,	84	$^{2}J(^{15}N-^{19}F)$,	23.9 (23.9)
$^{2}J(^{15}N-^{1}H)$,	(13.0)	$^{3}J(^{129}Xe-^{1}H)$,	24.7 (26.8)
$^{3}J(^{19}F-^{13}C)$,	18	$^{4}J(^{19}F-^{1}H)$,	2.6 (2.7)

(a) References (34) and (35). Spectra were recorded in anhydrous HF at -10 °C or at -58 °C on BrF_5 solvent (values in parentheses).

(b) Samples were referenced externally at 24 °C with respect to the neat liquid references standards $XeOF_4$ (^{129}Xe), $CFCl_3$ (^{19}F), CH_3NO_2 (^{14}N and ^{15}N), $(CH_3)_4Si$ (^{13}C and ^{1}H) where a positive chemical shift denotes a resonance occurring to high frequency of the reference compound.

16

Table 3. A Comparison of Xenon-Nitrogen Reduced Coupling Constants in F-Xe-L Type Systems[a]

Species	Hybridization at Nitrogen	^1K(Xe-N) 10^{22} $NA^{-2}m^{-3}$	$\delta(^{129}Xe)$ ppm	T, °C	Ref.
HC≡N-XeF⁺	sp	1.381[b]	-1555 (-1570)	-10 (-58)	34,35
RC≡N-XeF⁺	sp	1.297-1.393	-1541 to -1721	-10 to -50	34,37
F₃S≡N-XeF⁺	sp	1.435	(-1661)	(-60)	38
s-C₃F₃N₂N-XeF⁺	sp²	1.013	-1808 (-1863)	-5 (-50)	9
C₅F₅N-XeF⁺	sp²	0.983	-1872 (-1922)	-30 (-30)	39
4-CF₃C₅F₄N-XeF⁺	sp²	0.991	-1803 (-1853)	-15 (-50)	39
(FO₂S)₂N-XeF	sp²	0.913[c]	-2009	-40	6
F₄S=N(H)-XeF⁺	sp²		-2672	-20	38
F₅S-N(H₂)-XeF⁺	sp³		-2886	-20	38
F₅Te-N(H₂)-XeF⁺	sp³		-2841 (-2903)	-45 (-50)	40

(a) Values, unless otherwise indicated, were determined in HF and in BrF₅ (in parentheses) solvent;

$$^1K(Xe-N) = [4\pi^2 \cdot {}^1J(^{129}Xe-^{19}F)] / [h\gamma(^{14/15}N)\gamma(^{129}Xe)].$$

(b) Recorded for the ¹⁵N enriched cation. (c) Measured in SO₂ClF solvent.

17

above -50 °C, rapidly evolved Kr, NF_3 and CF_4 gases and was usually followed by a violent detonation and accompanying emission of white light. When these reactions were allowed to proceed at approximately -60 °C, the mixtures were periodically quenched to -196 °C in order to study the development of the Raman spectrum of the product (see Bonding Considerations). The interaction of $HC\equiv NH^+AsF_6^-$ and KrF_2 in BrF_5 led to a soluble product which was stable to at least -55 °C in BrF_5 with only slight decomposition. The ^{19}F NMR spectra of these solutions at -58 °C and in HF at -60 °C are consistent with equation (3)

$$KrF_2 \quad + \quad HC\equiv NH^+AsF_6^- \quad \longrightarrow \quad HC\equiv N-KrF^+AsF_6^- \quad + \quad HF \qquad (3)$$
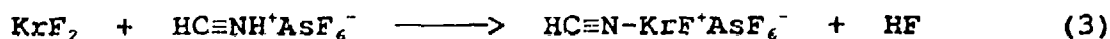
The structure of the $HC\equiv N-KrF^+$ cation in solution has been confirmed by reaction with 99.5% ^{15}N enriched $HC\equiv NH^+AsF_6^-$ in BrF_5 solvent. The ^{19}F and ^1H resonances exhibit new doublet splittings attributed to ^{15}N coupling (Figure 2a). The new splitting (26 Hz) on the ^{19}F resonance was assigned to the two-bond spin-spin coupling $^2J(^{19}F-^{15}N)$ and compares favorably in magnitude with previously reported values for $F-Xe-N(SO_2F)_2$ ($^2J(^{19}F-^{15}N) = 39.2$ Hz) and $CH_3C\equiv N-XeF^+$ ($^2J(^{19}F-^{15}N) = 25$ Hz, calculated from $^2J(^{19}F-^{14}N) = 18$ Hz). Krypton isotopic shifts arising from ^{82}Kr (11.56%), ^{84}Kr (56.90%) and ^{86}Kr (17.37%) were resolved on the ^{19}F resonance (0.0138 ppm/amu) and served as an added confirmation that the fluorine resonance arose from fluorine directly bonded to krypton. The doublet fine structure (12.2 Hz) on the ^1H resonance of the ^{15}N enriched cation (Figure 2b) was assigned to $^2J(^{15}N-^1H)$ (cf. $^2J(^{15}N-^1H) = 19.0$ Hz for $HC\equiv NH^+$ in HF solvent). The ^{15}N NMR spectrum comprised well-resolved doublet of doublets (Figure 2c) arising from $^2J(^{19}F-^{15}N)$ and $^2J(^{15}N-^1H)$ which simplified to a doublet (26 Hz) upon broad band ^1H decoupling, confirming the aforementioned coupling

18
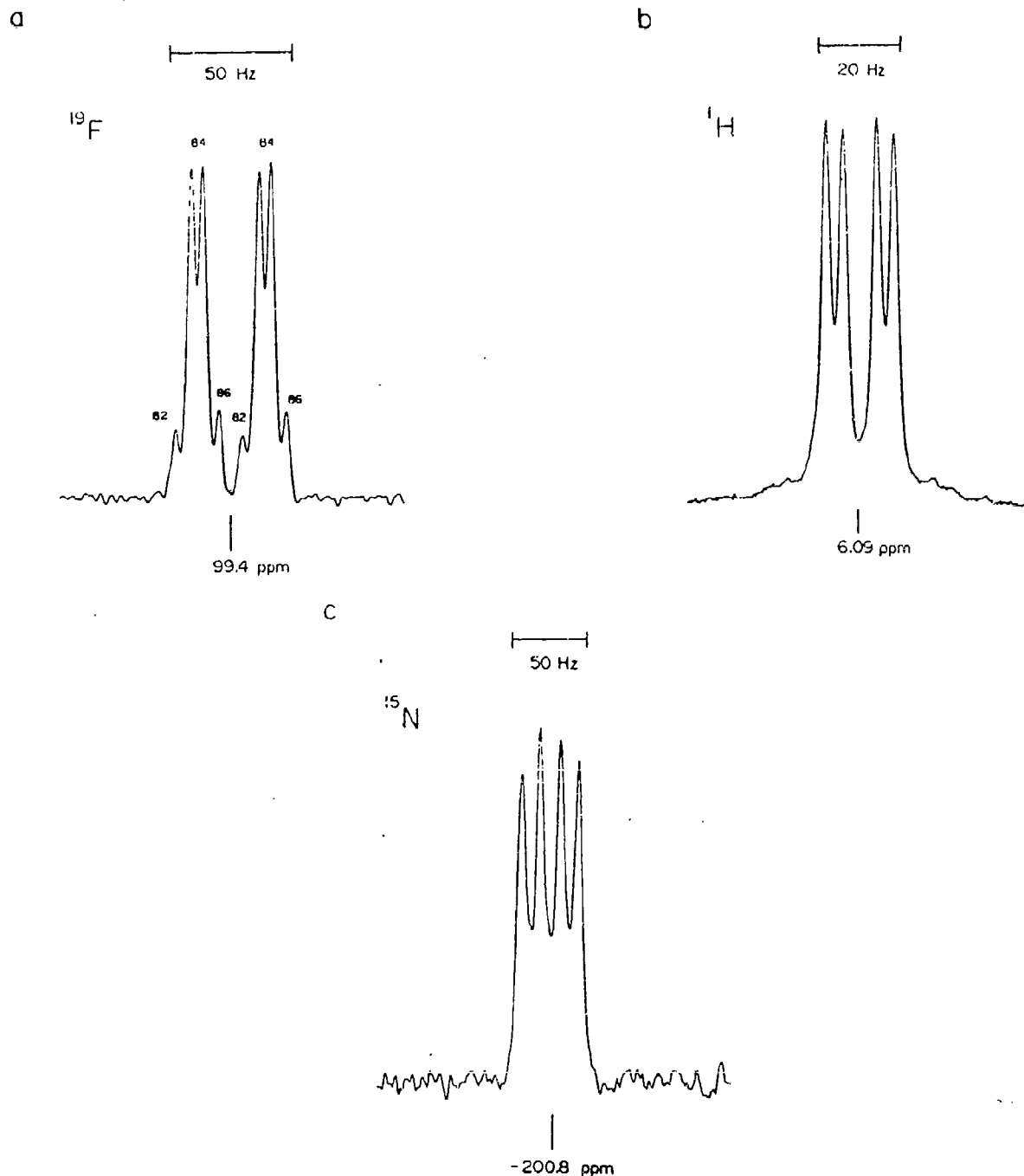
Figure 2.

NMR spectra of the HC≡N-KrF⁺ cation enriched to 99.5% with ¹⁵N, in BrF₅ as solvent at −57°C. (a) ¹⁹F Spectrum (235.36 MHz) depicting $^2J(^{19}F-^{15}N)$ and $^4J(^{19}F-^1H)$ and krypton isotope shifts. Lines assigned to fluorine bonded to ⁸²Kr (11.56%) ⁸⁴Kr (56.90%), and ⁸⁶Kr (17.37%) are denoted by the krypton mass number. The innermost lines of the ⁸²Kr and ⁸⁴Kr doublets overlap their corresponding ⁸⁶Kr doublets. The isotopic shift arising from ⁸³Kr (11.53%) is not resolved; those of ⁷⁸Kr (0.35%) and ⁸⁰Kr (2.27%) are too weak to be observed. (b) ¹H Spectrum (80.02 MHz) depicting $^2J(^{15}N-^1H)$ and $^4J(^{19}F-^1H)$. (c) ¹⁵N Spectrum (50.70 MHz) depicting $^2J(^{19}F-^{15}N)$ and $^2J(^{15}N-^1H)$. (Reprinted with permission from ref. (6)).

19

constant assignments.

Perfluoroalkyl- and Alkylnitrile Adducts of XeF$^+$. The measured value of the
first adiabatic IP of CF$_3$C≡N (13.90 eV) (15) suggests that this base should
be even more resistant to oxidative attack by KrF$^+$ and XeF$^+$ than HC≡N.
Moreover, CF$_3$C≡N would be expected to possess a more weakly basic nitrogen
that would be conducive to the formation of a correspondingly more ionic Ng-N
bond (see section on Theoretical Calculations). The perfluoroalkyl nitrile
adduct cations of XeF$^+$ have been prepared by the interaction of equimolar
amounts of XeF$^+$AsF$_6^-$ or Xe$_2$F$_3^+$AsF$_6^-$ and R$_f$C≡N (R$_f$ = CF$_3$, C$_2$F$_5$, n-C$_3$F$_7$) in BrF$_5$
solvent (9) according to equation (4)

$$R_fC≡N \ + \ XeF^+AsF_6^- \ (Xe_2F_3^+AsF_6^-) \ \longrightarrow \ R_fC≡N-XeF^+AsF_6^- \ (+ \ XeF_2) \quad (4)$$
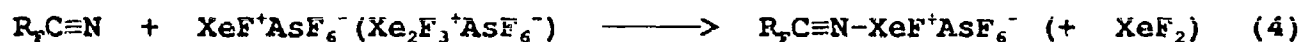
The syntheses of the krypton(II) analogs have also been reported and were
undertaken at low temperatures in BrF$_5$ solvent using the general synthetic
approach given in equation (5)

$$R_fC≡N-AsF_5 \ + \ KrF_2 \ \longrightarrow \ R_fC≡N-KrF^+AsF_6^- \quad (5)$$

The R$_f$C≡N-NgF$^+$ cations have been characterized in BrF$_5$ by low-temperature
(-57 to -61 °C) ^{19}F and ^{129}Xe NMR spectroscopy and consisted of two sets of new
signals: a singlet in the F-on-Kr(II) and in the F-on-Xe(II) regions, and
resonances in the F-on-C region with characteristic $^3J(^{19}F-^{19}F)$ and $^1J(^{19}F-^{13}C)$
couplings having chemical shifts to high frequency of the parent base
molecules (Table 4). In each case, the singlet assigned to F-on-Xe(II) was

20

Table 4. Correlation of Physical Properties for Representative Ng-F Bonds

Species[a]	r(Ng-F)[b] Å	ν(Ng-F) cm^{-1}	NMR Parameters[c]			T, °C	Ref.
			$^1J(^{129}Xe-^{19}F)$[d] Hz	$\delta(^{129}Xe)$[d,e] ppm	$\delta(^{19}F)$[d,e] ppm		
KrF^+	(1.740)						
$KrF^+Sb_2F_{11}^-$		624					42
$KrF^+AsF_6^-$		609					42
$(FKr)_2F^{+f}$		605			73.6	-65	42
$HC{\equiv}N-KrF^+$	(1.748)	560			99.4	-58	8
$CF_3C{\equiv}N-KrF^+$					93.1	-59	9
$C_2F_5C{\equiv}N-KrF^+$					91.1	-59	9
$C_3F_7C{\equiv}N-KrF^+$					91.9	-59	9
KrF_2	1.875 (1.843)	462			68.0	-56	43,44
XeF^+	(1.886)						
$XeF^+Sb_2F_{11}^-$	1.82(3)	619	7230	-574	-290.2	23[g]	31,42,45,46
$XeF^+AsF_6^-$	1.873(6)	610	6892	-869		-47	9,42,47,48
$(FXe)_2F^{+f}$	1.90(3)	593	6740	-1051	-252.0	-62	31,42,46,49
$HC{\equiv}N-XeF^+$	(1.904)	564	6181	-1569	-198.4[h]	-58	34
$F_3S{\equiv}N-XeF^+$		554	6248	-1661	-180.5	-60	38
$CF_3C{\equiv}N-XeF^+$			6397	-1337	-210.4	-63	9
$C_2F_5C{\equiv}N-XeF^+$			6437	-1294	-212.9	-63	9
$C_3F_7C{\equiv}N-XeF^+$			6430	-1294	-213.2	-63	9
$CH_3C{\equiv}N-XeF^{+h}$		560	6020	-1708	-185.5	-10	34
$s-C_3F_3N_2N-XeF^+$		548	5932	-1862	-145.6	-50	9
			5909	-1808	-154.9	-5	
$FO_2SO-XeF$	1.940(8)	528	5830	-1666		-40	31,46,50,51
cis/trans- $F_4OIO-XeF$			5803/	-1824/	-161.7[i]	0	52
			5910	-1720	-170.1[i]	0	
$C_5F_5N-XeF^+$		528	5926	-1922	-139.6	-30	39
$4-CF_3C_5F_4N-XeF^+$		524	5963	-1853	-144.6	-50	39
$F_5TeO-XeF^j$		520		-2051	-151.0[k]	26	53,54
$(FO_2S)_2N-XeF$	1.967(3)	506	5586	-1977	-126.1[j]	-58	3,4
			5664[j]	-2009[j]	-126.0	-40	
$F_4S{=}N(H)-XeF^+$			[l]	-2672[m]	[l]	-20	38
$F_5S-N(H_2)-XeF^+$			[l]	-2886[m]	[l]	-20	38
$F_5Te-N(H_2)-XeF^+$			[l]	-2903	[l]	-50	40
				-2841[m]	[l]	-45	
XeF_2	1.977 (1.984)	496	5621	-1685	-184.3	-52	9,55,56

Table 4 (continued)

(a) Unless otherwise indicated, all cations have AsF_6^- as the counterion.

(b) Values in parentheses are calculated values determined in Ref. (41).

(c) Spectra were obtained in BrF_5 solvent unless otherwise indicated.

(d) The NMR parameters of KrF and XeF groups are very sensitive to solvent and temperature conditions; it is therefore important to make comparisons in the same solvent medium at the same or nearly the same temperatures.

(e) Referenced with respect to the neat liquids $XeOF_4$ (^{129}Xe) and $CFCl_3$ (^{19}F) at 24 °C; a positive sign denotes the chemical shift of the resonance in question occurs to higher frequency of (is more deshielded than) the resonance of the reference substance.

(f) Table entries refer to the terminal fluorine on the noble-gas atom.

(g) Recorded in SbF_5 solvent.

(h) $\delta(^{19}F)$ measured in anhydrous HF solvent at -10 °C.

(i) $\delta(^{19}F)$ measured in SO_2ClF solvent at -40 °C.

(j) NMR parameters measured in SO_2ClF solvent.

(k) NMR parameters measured in SO_2ClF solvent at -50 °C.

(l) Not observed; Xe-F is relatively ionic and readily undergoes exchange in HF solvent.

(m) $\delta(^{129}Xe)$ measured in HF solvent.

22

flanked by natural abundance (26.44%) ^{129}Xe satellites arising from $^1J(^{129}$Xe-^{19}F). The integrated relative intensities of the fluorine-on-noble gas environments and perfluoroalkyl group are consistent with the proposed formulations. Furthermore, the F-on-Kr(II) resonance of $CF_3C\equiv N-KrF^+$ could be resolved to show the ^{82}Kr, ^{84}Kr and ^{86}Kr isotopic shifts (0.0105 ppm/amu), which compare favorably with previously measured values for $HC\equiv N-KrF^+$ (0.0138 ppm/amu) (7) and KrF_2 (0.0104 ppm/amu) (54). In addition, the F-on-Kr(II) resonances occur to high frequency of KrF_2 while the F-on-Xe(II) resonances occur to low frequency of XeF_2 (Table 4). Similar, but slightly more positive ^{19}F chemical shifts have been observed for $HC\equiv N-KrF^+$ ($\delta(^{19}$F) 99.4 ppm; -57 °C; BrF_5 solvent)^3 with respect to KrF_2 ($\delta(^{19}$F) 68.0 ppm; -56 °C; BrF_5 solvent) (8). This is in contrast to the $R_fC\equiv N-XeF^+$ series of cations which display significantly more positive ^{19}F (F-on-Xe(II)) and ^{129}Xe chemical shifts when compared with $HC\equiv N-XeF^+$ ($\delta(^{19}$F) -198.4 ppm; $\delta(^{129}$Xe) -1552 ppm; $^1J(^{129}$Xe-^{19}F) 6150 Hz; -10 °C; HF solvent) (34) and XeF_2 ($\delta(^{19}$F) -184.3 ppm; $\delta(^{129}$Xe) -1685.2 ppm; $^1J(^{129}$Xe-^{19}F) 5621 Hz; -52 °C; BrF_5). The ^{129}Xe and ^{19}F complexation shifts indicate the Xe-N bonds of the $R_fC\equiv N-XeF^+$ cations are significantly more ionic than in $HC\equiv N-XeF^+$ or $RC\equiv N-XeF^+$ (9) and is further supported by significantly larger $^1J(^{129}$Xe-^{19}F) values measured for the $R_fC\equiv N-XeF^+$ cations, which are known to increase with ionic character of the Xe-L bond in F-Xe-L type compounds (see Table 4) (31-33). The $R_fC\equiv N-XeF^+$ cations represent the most ionic Xe-N bonded species presently known. In contrast, the analogous comparison of ^{19}F chemical shifts for $R_fC\equiv N-KrF^+$ cations suggests that the Kr-N bonds of these cations may be slightly more covalent than in $HC\equiv N-KrF^+$.

All three fluoro(perfluoroalkylnitrile)krypton(II) cations are thermally less stable with respect to redox decomposition than $HC\equiv N-KrF^+$ or their

23

xenon(II) analogs, preventing their isolation and characterization in the solid state. Decompositions monitored by ^{19}F NMR spectroscopy occurred over periods of approximately 1 to 2 hours at -57 to -61 °C. The major decomposition products consisted of Kr and the fluorinated products (^{19}F NMR parameters listed in parentheses): CF_4 (-63.1 ppm), C_2F_6 (-88.6 ppm) and NF_4^+ (219.4 ppm, $^1J(^{19}F-^{14}N)$ 229 Hz) for all three $R_fC\equiv N-KrF^+$ cations studied, and $n-C_3F_8$ (-83.8 ppm, F_3C-; -132.8 ppm, $-CF_2-$) for $C_2F_5C\equiv N-KrF^+$ and $n-C_3F_8$, $n-C_4F_{10}$ (-82.8 ppm, F_3C-; -129.2 ppm, $-CF_2-$) for $n-C_3F_7C\equiv N-KrF^+$ (9).

Reactions of $XeF^+AsF_6^-$ with alkyl nitriles, $RC\equiv N$, and C_6F_5CN have also been carried out by combining stoichiometric amounts of the reactants in anhydrous HF and warming to -50 to -10 °C to effect reaction and dissolution in the solvent (34,37). The reactions proceed by analogy with equation (1). In the case of the alkyl nitriles and $HC\equiv N$, equilibrium (6) is significant so that equilibrium amounts of XeF_2, $RC\equiv NH^+$ and $HC\equiv NH^+$ are observed in the ^{129}Xe, ^{19}F, $^{14/15}N$, ^{13}C and ^1H NMR spectra but XeF_2 frequently is not observed in the ^{19}F and ^{129}Xe NMR spectra. The apparent absence of XeF_2 in the NMR spectra is attributed to chemical exchange involving free XeF^+ arising from equilibrium (7) and $Xe_2F_3^+$ as an exchange intermediate (equilibrium (8)).

$$RC\equiv N-XeF^+ \ + \ HF \ \rightleftharpoons \ RC\equiv NH^+ \ + \ XeF_2 \qquad (6)$$

$$RC\equiv N-XeF^+ \ \rightleftharpoons \ RC\equiv NH \ + \ XeF^+ \qquad (7)$$

$$XeF^+ \ + \ XeF_2 \ \rightleftharpoons \ Xe_2F_3^+ \qquad (8)$$

Multi-NMR spectra (^{129}Xe, ^{19}F, ^{14}N, ^{15}N, ^{13}C and ^1H) have provided

unambiguous proof for the structures of the $RC\equiv N-XeF^+$ cations in HF solution (Table 5). Several alkyl nitrile adducts of the XeF^+ cation have also been isolated and characterized in the solid state by low-temperature Raman spectroscopy. The Xe-F stretching frequencies are consistent with weak covalent bonding between xenon and nitrogen (see Bonding Considerations): CH_3 (560), CH_2F (565), CH_2Cl (564), C_2H_5 (541), $(CH_3)_2CH$ (556), $(CH_3)_3C$ (560); values in parentheses are the Xe-F stretching frequencies, cm^{-1}.

The decompositions of the nitrile adduct cations $CH_3(CH_2)_nC\equiv N-XeF^+$ (n = 0 - 3) have been monitored in HF solution by multi-NMR spectroscopy. The rate of fluorination of the alkyl chain increases with increasing chain length with degree of fluorination increasing at the alkyl carbons in the order $\beta <$ $\gamma < \delta$, where no fluorination is observed at the α-carbon.

Perfluoropyridine and s-Trifluorotriazine Adducts of XeF^+. The fluoro-(perfluoropyridine)xenon(II) cations, $4-RC_5F_4N-XeF^+$ (R = F or CF_3), have been observed in HF and BrF_5 solutions and are stable in both media up to -30 °C. The salts $4-RC_5F_4N-XeF^+AsF_6^-$ have been isolated at -30 °C from BrF_5 solutions initially containing equimolar amounts of $4-RC_5F_4NH^+AsF_6^-$ and XeF_2. The resulting white solids were stable to -25 °C. Low-temperature Raman and ^{129}Xe, ^{19}F and ^{14}N NMR spectroscopic results are consistent with planar cations (Structure I) in which the xenon atom is coordinated to the aromatic ring

I

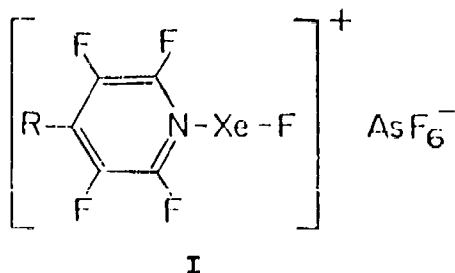Table 5. Selected NMR Chemical Shifts and Coupling Constants for RC≡N-XeF⁺ Cations[a]

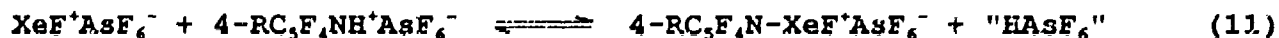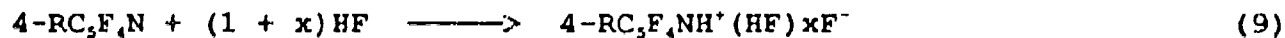| Cation	Chemical Shifts (ppm)[b]			Spin-Spin Couplings (Hz)	
	$\delta(^{129}Xe)$	$\delta(^{19}F)$	$\delta(^{14}N)$	$J(^{129}Xe-^{19}F)$	$J(^{129}Xe-^{14}N)$
CH₃C≡N-XeF⁺	-1707	-185.5	-251.1	6020	313
CH₂FC≡N-XeF⁺	-1541	-198.2 (XeF)	-229.2	6164	333
		-241.7 (CF)			
CH₂ClC≡N-XeF⁺	-1583	-195.5	-236.6	6147	331
CH₃CH₂C≡N-XeF⁺	-1717	-184.6	-251.9	6016	312
CH₂FCH₂C≡N-XeF⁺	-1662	-182.8 (XeF)		6063	322
		-218.8 (CF)			
CH₃CH₂CH₂C≡N-XeF⁺	-1718	-189.1	-249.7	6020	309
CH₂FCH₂CH₂C≡N-XeF⁺	-1663	-187.7 (XeF)		6065	321
		-222.7 (CF)			
CH₃CHFCH₂C≡N-XeF⁺	-1700	-186.1 (XeF)	-257.8	6038	315
		-172.1 (CF)			
CHF₂CH₂CH₂C≡N-XeF⁺		-120.9 (CF)			
CH₃CH₂CH₂CH₂C≡N-XeF⁺	-1720	-183.2	-247.1	6022	309
CH₂FCH₂CH₂CH₂C≡N-XeF⁺	-1703	-184.6 (XeF)		6027	311
CH₃CHFCH₂CH₂C≡N-XeF⁺	-1705[c]	-185.1 (XeF)		6015	[c]
		-175.9 (CF)			
(CH₃)₂CHC≡N-XeF⁺	-1721	-184.5	-251.4	6016	309
(CH₃)₃CC≡N-XeF⁺	-1721	-184.3	-251.4	6024	309
CH₂ClC(CH₃)HC≡N-XeF⁺	-1703	-198.7		6027	314
CH₂FC(CH₃)HC≡N-XeF⁺	-1669	-187.9 (XeF)	-243.8	6027	301
		-235.3 (CF)			
C₆F₅C≡N-XeF⁺	-1424	-201.8		6610	

(a) References (34) and (37).

(b) Recorded at -10 to -30 °C and referenced externally at 24 °C with respect to neat liquid references: XeOF₄ (¹²⁹Xe), CFCl₃(¹⁹F), CH₃NO₂(¹⁴N) and TMS(¹³C) and (¹H).

(c) Resonance overlaps with that of CH₂FCH₂CH₂CH₂C≡N-XeF⁺.

through the lone pair of electrons on the nitrogen (ref. (39) and Tables 3 and 4).

Equimolar amounts of $XeF^+AsF_6^-$ and the perfluoropyridine, $4\text{-}RC_5F_4N$ ($R = F$ or CF_3), react in anhydrous HF at -30 to -20 °C according to equation (9) and equilibria (10) and (11) to give the novel Xe-N bonded cations, $4\text{-}RC_5F_4N\text{-}XeF^+$, as the AsF_6^- salts in solution.

$$4\text{-}RC_5F_4N + (1 + x)HF \longrightarrow 4\text{-}RC_5F_4NH^+(HF)xF^- \qquad (9)$$

$$4\text{-}RC_5F_4NH^+(HF)xF^- + XeF^+AsF_6^- \rightleftharpoons 4\text{-}RC_5F_4NH^+AsF_6^- + XeF_2 + xHF \qquad (10)$$

$$XeF^+AsF_6^- + 4\text{-}RC_5F_4NH^+AsF_6^- \rightleftharpoons 4\text{-}RC_5F_4N\text{-}XeF^+AsF_6^- + "HAsF_6" \qquad (11)$$

At -30 °C these solutions consisted of equilibrium mixtures of XeF_2, $4\text{-}RC_5F_4NH^+AsF_6^-$ and $4\text{-}RC_5F_4N\text{-}XeF^+AsF_6^-$ as determined by NMR spectroscopy (Table 3). Removal of HF solvent by pumping at -50 °C resulted in white solids which Raman spectroscopy at -196 °C also showed to be mixtures of $4\text{-}RC_5F_4N\text{-}XeF^+AsF_6^-$, XeF_2 and $4\text{-}RC_5F_4NH^+AsF_6^-$.

An alternative approach, which led to isolation of the Xe-N bonded cations, allowed stoichiometric amounts of XeF_2 and the perfluoropyridinium cations, as their AsF_6^- salts, to react in HF and BrF_5 solvents at -30 °C according to equilibrium (12).

$$XeF_2 + 4\text{-}RC_5F_4NH^+AsF_6^- \rightleftharpoons 4\text{-}RC_5F_4N\text{-}XeF^+AsF_6^- + HF \qquad (12)$$
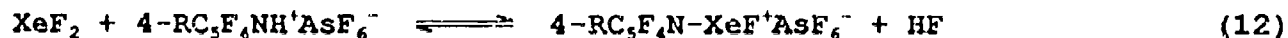
The equilibria in both solvents were monitored by ^{129}Xe, ^{19}F and ^{14}N NMR

27

spectroscopy. In the case of BrF_5, formation of $4-RC_5F_4N-XeF^+AsF_6^-$ was strongly favored over that in HF solvent; the equilibrium ratio $[4-RC_5F_4N-XeF^+]/[4-RC_5F_4NH^+]$ being 0.25 and 2.1 in HF and BrF_5 solvents, respectively, at -30 °C for R = F and 3.7 for R = CF_3 in BrF_5 at -50 °C (K_F = 4.5 at -30 °C and K_{CF} = 13.6 at -50 °C in BrF_5 for equilibrium (8)). Consequently, removal of BrF_5 solvent under vacuum at -30 °C yielded white solids corresponding to the salts $4-RC_5F_4N-XeF^+AsF_6^-$. The CF_3-derivatives substituted at the 2- and 3- positions have also been synthesized from the their perfluoropyridinium salts in BrF_5 solvent and characterized by NMR spectroscopy ($\delta(^{129}Xe)$, -1899 and -1877, respectively) (37).

The interaction of liquid s-trifluorotriazine, $s-C_3N_3F_3$, with $XeF^+AsF_6^-$ at room temperature for three hours followed by removal of excess s-trifluorotriazine under vacuum resulted in a white powder which is stable indefinitely at room temperature (9). The combining ratio $XeF^+AsF_6^-$: $s-C_3N_3F_3$ = 1.00 : 1.00 is consistent with equation (13)

$$XeF^+AsF_6^- + s-C_3F_3N_3 \longrightarrow s-C_3F_3N_2N-XeF^+ \qquad (13)$$
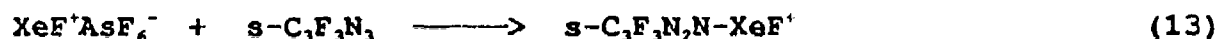
Both the ^{19}F and ^{129}Xe NMR findings (Tables 3 and 4) for the salt dissolved in BrF_5 and HF solvents are consistent with the cation formulation given by Structure II. The ^{129}Xe NMR spectrum recorded in BrF_5 at -50 °C consists of a
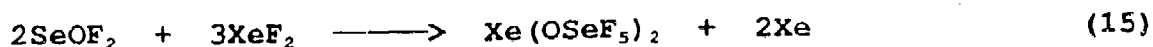

II
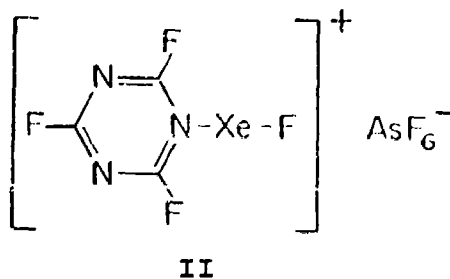
doublet arising from $^1J(^{129}Xe-^{19}F)$ = 5932 Hz. The $^{129}Xe-^{14}N$ coupling is quadrupole collapsed, as has been observed previously for 4-CF_3-C_5F_4N-XeF$^+$AsF$_6^-$ and C_5F_5-XeF$^+$AsF$_6^-$ in BrF$_5$ at low temperatures (39). In HF solvent, however, $^1J(^{129}Xe-^{14}N)$ = 245 Hz was observed at -5 °C and compares favorably in magnitude with those reported previously for the related perfluoropyridine cations (235 - 238 Hz). The ^{19}F NMR spectrum shows two F-on-C environments in the ratio of 1:2 and a F-on-Xe(II) environment with accompanying ^{129}Xe natural abundance (26.44%) satellites arising from $^1J(^{129}Xe-^{19}F)$ and a 1:2:1 triplet arising from $^4J(F_1-F_2)$ = 10.9 Hz. The latter coupling has also been observed for the perfluoropyridine cations 4-CF_3-C_5F_4N-XeF$^+$ (25.8 Hz) and C_5F_5N-XeF$^+$ (25.0 Hz) (39).

The reaction of XeF$_3^+$SbF$_6^-$ with s-$C_3F_3N_3$ in BrF$_5$ solvent at 20 °C fails to give $C_3F_3N_2$N-XeF$_3^+$ (57). Rather, reduction of Xe(IV) to Xe(II) occurs according to equation (14)

$$2XeF_3^+SbF_6^- \ + \ 3s\text{-}C_3F_3N_3 \ \longrightarrow \ s\text{-}C_3F_3N_2\text{N-XeF}^+ \ +$$

 (14)
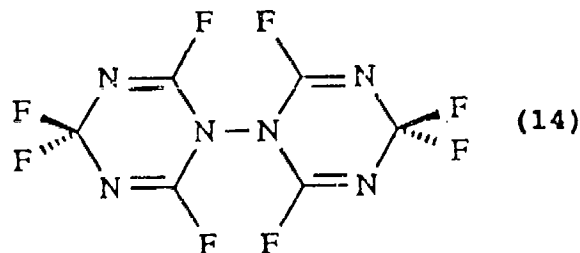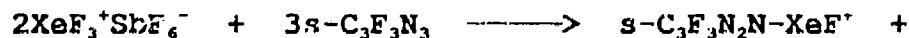
The Lewis Acid Properties of the XeOTeF$_5^+$ and XeOSeF$_5^+$ Cations. More recently, this work has been extended to the Lewis acid properties of the noble-gas cations XeOTeF$_5^+$ and XeOSeF$_5^+$ (38,57). The XeOSeF$_5^+$ cation, which was previously unknown, was prepared according to equations (15) - (17)

$$2SeOF_2 + 3XeF_2 \longrightarrow Xe(OSeF_5)_2 + 2Xe \qquad (15)$$

$$Xe(OSeF_5)_2 + XeF_2 \longrightarrow 2FXeOSeF_5 \qquad (16)$$

$$AsF_5 + FXeOSeF_5 \longrightarrow XeOSeF_5^+AsF_6^- \qquad (17)$$

While the $XeOMF_5^+$ cations (M = Se, Te) are expected to be weaker Lewis acids, they are expected to be less strongly oxidizing than NgF^+ cations, and have been shown to form stable adducts at low temperature with several organic and inorganic nitrogen bases leading to the first examples of O-Xe-N linkages (Table 6).

Although the $s-C_3F_3N_2N-XeOMF_5^+AsF_6^-$ salts were successfully prepared near room temperature by reaction of the neat compounds (equation (18)), other potential organic ligands such as nitriles and pyridines are vigorously oxidized by $XeOMF_5^+$ cations when these reactions are attempted in the absence of a solvent under similar conditions.

$$XeOMF_5^+AsF_6^- + s-C_3F_3N_3 \longrightarrow F_5MO-Xe-NN_2C_3F_3^+AsF_6^- \qquad (18)$$

To partially address this problem, $XeOTeF_5^+Sb(OTeF_5)_6^-$ was synthesized and is the first fully substituted $OTeF_5$ salt prepared to date (57). The salt was prepared in SO_2ClF using the redox synthesis described by equation (19).

$$2Xe(OTeF_5)_2 + Sb(OTeF_5)_3 \longrightarrow XeOTeF_5^+Sb(OTeF_5)_6^- + Xe \qquad (19)$$

It was shown that the decreased polarity of the $Sb(OTeF_5)_6^-$ anion relative to

Table 6. Selected NMR Parameters for XeOMF$_5^+$ (M = Se or Te) Adducts Cations With Nitrogen Bases

Cation	Chemical Shifts, ppm		Coupling Constants, Hz	Solvent (T, °C)
	$\delta(^{129}\text{Xe})$	$\delta(^{19}\text{F})$	$^2J(\text{F}_A\text{-}\text{F}_B)$	
CH$_3$C≡N-Xe-OTeF$_5^+$ [a]	-2061	-45.8 F$_A$ -44.0 F$_B$	181	SO$_2$ClF (-50)
C$_5$F$_5$N-Xe-OTeF$_5^+$ [a]	-2246	-46.3 F$_A$ -42.8 F$_B$	~180	SO$_2$ClF (-70)
s-C$_3$F$_3$N$_2$N-Xe-OTeF$_5^+$ [a]	-2192	-47.1 F$_A$ ~ -42.3 F$_B$	~187	SO$_2$ClF (-50)
F$_3$S≡N-Xe-OSeF$_5$ [b]	-1979	67.9 F$_A$ 70.4 F$_B$	219	BrF$_5$ (-60)

(a) Prepared as the Sb(OTeF$_5$)$_6^-$ salt; ref. (57).   (b) Prepared as the AsF$_6^-$ salt; ref. (38).

31

AsF_6^- anion facilitated solubility in SO_2ClF at low-temperatures and was found to be soluble in high concentrations down to the freezing point of the solvent (-124 °C). This synthetic approach allowed the formation of adduct species with $XeOTeF_5^+$ and representative members of the series of nitrogen bases, i.e., acetonitrile and pentafluoropyridine, at low temperatures and under non-solvolytic conditions in a low-polarity solvent (Table 6 and ref. (57)). Low-temperature ^{19}F NMR studies show that the $XeOTeF_5^+$ cation possesses sufficient Lewis acid strength to coordinate to SO_2ClF (57). The only other known examples of adduct formation with the weakly basic SO_2ClF molecule have been reported for SbF_5 and AsF_5 at low temperatures (58), suggesting that the ability of the $XeOTeF_5^+$ cation to coordinate with the weak electron donor, SO_2ClF, is a consequence of the weak coordinating ability of the $Sb(OTeF_5)_6^-$ anion. Removal of excess SO_2ClF from these solutions under vacuum at 25 °C results in the 1:1 adduct salt, $F_5TeOXe-OSOClF^+Sb(OTeF_5)_6^-$ which slowly dissociates upon further pumping at room temperature (57). In addition, $Bi(OTeF_5)_5$ and $Et_4N^+M'(OTeF_5)_6^-$ (M' = Sb or Bi) were also synthesized and characterized by ^{121}Sb, ^{209}Bi, ^{19}F and ^{125}Te NMR (57). Prior to these studies only the $As(OTeF_5)_5$ and $As(OTeF_5)_6^-$ had been reported (59).

Noble-Gas Cation Adducts with Inorganic Bases. The synthesis of $N\equiv SF_3$ Lewis acid-base adducts with the noble-gas cations XeF^+, $XeOSeF_5^+$, and $XeOTeF_5^+$ have also been investigated (38). Several synthetic approaches have been used (equation (19)).


$$XeL^+AsF_6^- + N\equiv SF_3 \longrightarrow L-Xe-N\equiv SF_3^+AsF_6^- \qquad (20)$$

32
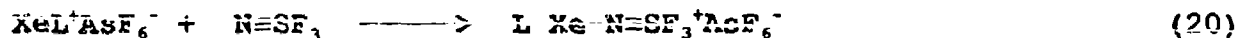
where $L = XeF^+$, $OSeF_5^+$ and the solvent was BrF_5 at $-50\ °C$. In addition, solid $F-Xe-N{\equiv}SF_3^+AsF_6^-$ has been synthesized by the direct interaction of liquid $N{\equiv}SF_3$ with solid $XeF^+AsF_6^-$. Structures have been characterized using primarily ^{19}F and ^{129}Xe NMR spectroscopy (Tables 3, 4 and 6) in solution and by low-temperature Raman spectroscopy in tne solid state (Table 4).

The solvolytic behavior of the $F_3S{\equiv}N-XeF^+$ cation has been monitored in anhydrous HF (38). Two successive additions of HF occur across the sulfur-nitrogen bond to give the $F_4S{=}N(H)-XeF^+$ (Structure III) and $F_5S-N(H_2)-XeF^+$ (Structure IV) cations. The ^{129}Xe NMR spectrum of the SF_5 derivative shows that this xenon is the most shielded ^{129}Xe environment (most covalent Xe-N bond) observed for a xenon-nitrogen bonded species (Tables 3 and 4). Moreover, the $F_5S-N(H_2)-XeF^+$ cation represents the first example of a bond between xenon and an sp^3-hybridized nitrogen. More recently, the tellurium analog has been prepared in HF and BrF_5 solvent at -45 and $-50\ °C$, respectively, (40) according to equation (21).

$$F_5TeNH_3^+AsF_6^-\ +\ XeF_2\ \longrightarrow\ F_5Te-N(H_2)-XeF^+AsF_6^- \qquad (21)$$
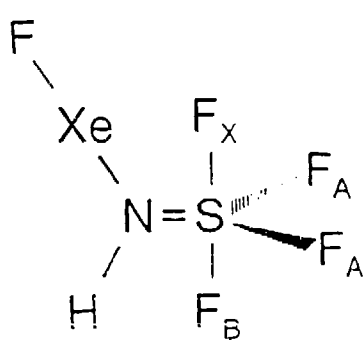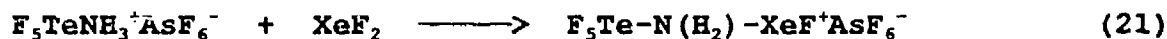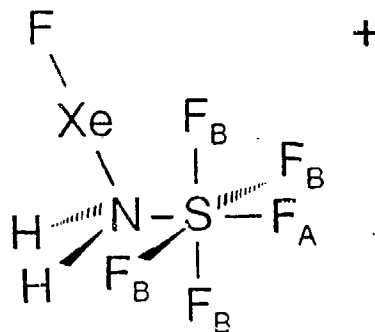
III IV

BONDING CONSIDERATIONS

The Ng-N bonds described in this Review may be thought of as classical Lewis acid-base donor acceptor bonds. Implicit in this description is a considerable degree of ionic character for these weak covalent bonds, which is a dominant feature of their stability. This premise has been supported and further illuminated by several theoretical calculations on $HC \equiv N-NgF^+$ cations (Ng = Ne, Ar, Kr, Xe) and spectroscopic measurements on a wide range of XeF^+, KrF^+ and $XeOMF_5^+$ adducts of nitrogen bases in which the formal hybridization of nitrogen ranges from sp, sp^2 to sp^3.

Spectroscopic Findings. The reaction of the gas phase NgF^+ ions with F^- to yield the difluorides results in increases in the calculated Ng-F bond lengths of 0.1 Å, while their reaction with $HC \equiv N$ causes the same bond lengths (calculated) to increase on average by only 0.016 Å (41). There is a correlation of Ng-F bond length and the Ng-F vibrational frequency with the base strength of the ligand attached to NgF^+. This is illustrated by the examples shown in Table 4. The NgF^+ species are only weakly coordinated by a fluorine bridge to the $Sb_2F_{11}^-$ anion, providing the highest Ng-F stretching frequencies (Xe, 619; Kr, 624 cm^{-1}) while the interaction of XeF^+ with $N(SO_2F)_2^-$ is representative of a much stronger covalent interaction and provides the lowest Xe-F stretching frequency observed to date for a covalent derivative of XeF_2 (506 cm^{-1}) (3). The C-N bond of $HC \equiv N$ is calculated to shorten by ~0.05 Å on forming the adduct, while the C-H bond is calculated to lengthen by 0.008 Å (41). These predicted changes in bond length also correlate with the

34

shielding (more negative chemical shift) with a transfer of negative charge to Xe and, hence, with increased covalent character of the Ng-L interaction (increased ionic character of the Ng-F bond) (31-33). The $F_4S=N(H)-XeF^+$, $F_5S-N(H_2)-XeF^+$ and $F_5Te-N(H_2)-XeF^+$ cations are characterized by the high shieldings of their ^{129}Xe nuclei and the absence of $^1J(^{129}Xe-^{19}F)$ arising from fluorine exchange with the solvent (Tables 3 and 4). The NMR findings are consistent with a strong covalent bonding interaction between xenon and nitrogen with a commensurate increase in Xe-F bond lability and ionic character and may be conveniently represented by an increased contribution from valence bond Structure VIII and/or by deprotonation upon adduct formation to give the neutral derivatives $F_4S=N-XeF$, $F_5S-N(H)-XeF$ and $F_5Te-N(H)-XeF$, which may be in equilibrium with the cations in HF and BrF_5 solvents. Whatever the precise nature of the nitrogen bonded ligand may be in solution, these Xe-N bonded derivatives represent the most covalent Xe-N bonds synthesized to date.

Quadrupolar nuclei in noncubic environments generally yield poorly resolved one-bond coupling patterns in their NMR spectra due to quadrupolar relaxation effects (36). In spite of the low symmetries about the nitrogen atoms in the cations investigated to date, the ^{14}N NMR spectra frequently show well resolved and only partially quadrupole collapsed scalar couplings, $^1J(^{129}Xe-^{14}N)$ (and $^1J(^{14}N-^{13}C)$ in the case of $HC\equiv N-XeF^+$; Tables 2, 3 and 5). In prior studies of the imidodisulfurylfluoride derivatives of xenon(II) (3,4,6), the lack of cubic symmetry and the small electric field gradient at ^{14}N in the trigonal planar $-N(SO_2F)_2$ group necessitated ^{15}N enrichment in order to observe xenon-nitrogen scalar couplings and nitrogen chemical shifts in $FXeN(SO_2F)_2$ (3), $XeN(SO_2F)_2^+$ (6), $Xe[N(SO_2F)_2]_2$ (4) and $F[XeN(SO_2F)_2]_2^+$ (4) cations in SbF_5, BrF_5 and SO_2ClF solvents. The extent of minimal quadrupolar

relaxation via a reduced electric field gradient has been examined theoretically for $HC\equiv N-NgF^+$ (Ng = Kr, Xe) by calculating the field gradient at the nitrogen nucleus and comparing it to that in isolated $HC\equiv N$ (41). Relative to free $HC\equiv N$, the principal component of the electric field gradient tensor in the H $\rightarrow$ N direction, is halved upon formation of both $HC\equiv N-XeF^+$ and $HC\equiv N-KrF^+$ and is in agreement with the fact that $^1J(^{129}Xe-^{14}N)$ can be readily observed under conditions favoring low molecular correlation times. The electric field gradients at the Xe nucleus in XeF^+ and $HC\equiv N-XeF^+$ have also been calculated (41), and differ by less than 7%, a result in agreement with the experimental observation that the quadrupolar splitting observed in the ^{129}Xe Mössbauer spectrum of $HC\equiv N-XeF^+$ (40.2 $\pm$ 0.3 mm/s) is, within experimental error, the same as that obtained for the salt $XeF^+AsF_6^-$ (40.5 $\pm$ 0.1 mm/s) (60).

The difference in the magnitudes of $^1J(^{129}Xe-^{15}N)$ in $HC\equiv N-XeF^+$ (471 Hz) (34) and $FXeN(SO_2F)_2$ (307 Hz) (3) may be discussed using a previous assessment of the nature of bonding to xenon in solution for $FXeN(SO_2F)_2$ where the Xe-N bond of $FXeN(SO_2F)_2$ is regarded as a σ-bond having sp^2 hybrid character (3,4,6). In high-resolution NMR spectroscopy spin-spin coupling involving heavy nuclides is, with few exceptions, dominated by the Fermi contact mechanism (61). For Xe-N spin-spin couplings dominated by the Fermi contact mechanism, one-bond coupling constants can be discussed on the basis of the formalism developed by Pople and Santry (62). In discussions of xenon-nitrogen scalar couplings in xenon(II) imidodisulfurylfluoride compounds (6), the s-electron density at the xenon nucleus was assumed constant and a change in the hybridization at nitrogen accounted for changes in xenon-nitrogen spin-spin coupling. Even though the Xe-N bond is markedly less covalent in the hydrocyano cation than in $FXeN(SO_2F)_2$, the $^1J(^{129}Xe-^{15}N)$ values observed for

HC≡N-XeF⁺ are substantially larger than for xenon bonded to the trigonal planar nitrogen in FXeN(SO$_2$F)$_2$ (Table 3). The dependence of xenon-nitrogen spin-spin coupling on nitrogen s-character in the xenon-nitrogen bonds may also be invoked to account for the relative magnitudes of the scalar couplings. A comparison of $^1J(^{129}Xe-^{15}N)$ for HC≡N-XeF⁺ with that of the trigonal planar sp^2 hybridized nitrogen atom in FXeN(SO$_2$F)$_2$ illustrates this point and allows assessment of the relative degrees of hybridization of the nitrogen orbitals used in σ-bonding to xenon. The ratio, $[^1J(^{129}Xe-^{15}N)_{sp}]/[^1J(^{129}Xe-^{15}N)_{sp}2]$ = 1.53, for the HC≡N-XeF⁺ cation and FXeN(SO$_2$F)$_2$ is in excellent agreement with the theoretical ratio, 1.50, calculated from the predicted fractional s-characters of the nitrogen orbitals used in bonding to xenon in both compounds.

The formal s-character in the Xe-N bond of other adduct cations, for which either $^1J(^{129}Xe-^{14}N)$ or $^1J(^{129}Xe-^{15}N)$ are known, can be related to the reduced coupling constant, $^1K(Xe-N)$, thus eliminating the effect of the different gyromagnetic ratios of ^{14}N and ^{15}N on the magnitude of the scalar coupling (6,62). A comparison of $^1K(Xe-N)$ of XeF⁺ adduct cations with nitrogen bases and of xenon(II) derivatives containing the N(SO$_2$F)$_2$ group is given in Table 3. In general, $^1K(Xe-N)$ values occur in two discreet ranges corresponding to the formal hybridization of nitrogen, sp or sp^2. There are presently no measured values for xenon coordinated to an sp^3 example, even though the F$_5$S-N(H$_2$)-XeF⁺ and F$_5$Te-N(H$_2$)-XeF⁺ cations are known (see Structure IV), owing to quadrupole relaxation of their $^1J(^{129}Xe-^{14}N)$ scalar couplings.

Theoretical Calculations. In order to better characterize the nature of the Ng-N bonds in HC≡N-KrF⁺ and HC≡N-XeF⁺, their syntheses and spectroscopic

measurements have been complemented by several theoretical calculations on the $HC\equiv N-NgF^+$ (Ng = Ne, Ar, Kr or Xe) cations (41,63-66).

Theoretical investigation of $HC\equiv N-KrF^+$ and $HC\equiv N-KrF^+$ at the SCF level using the theory of atoms in molecules (41) has shown that the ability of KrF^+ and XeF^+ cations to act as Lewis acids is related to the presence of holes in the valence shell (... concentrations of the noble-gas atoms that expose their cores. The mechanism of formation of the Ng-N bonds in the adducts of KrF^+ and XeF with $HC\equiv N$ is similar to the formation of a hydrogen bond, i.e., the mutual penetration of the outer diffuse non-bonded densities of the Ng and N atoms is facilitated by their dipolar and quadrupolar polarizations, which remove density along their axis of approach, to yield a final density in the interatomic surface that is only slightly greater than the sum of the unperturbed densities (Figures 3 and 4). Thus, not surprisingly, the KrF^+ and XeF^+ cations are best described as hard acids. The energies of formation of these adducts are dominated by the large stabilizations of the Ng atoms that result from the increase in the concentration of charge in their inner quantum shells. The Ng-N bonds that result from the interaction of the closed-shell reactants KrF^+/XeF^+ and $HC\equiv N$ lie closer to the closed shell limit than do bonds formed in the reaction of KrF^+/XeF^+ with F^-. The calculated gas phase energies of the reaction between the closed-shell species are -136.0 and -144.3 kJ mol^{-1} for Ng = Kr and Xe, respectively, for

$$NgF^+ + HC\equiv N \longrightarrow HC\equiv N-NgF^+ \qquad (22)$$

38
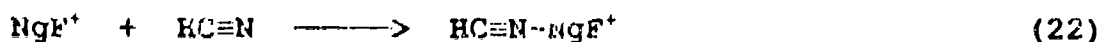
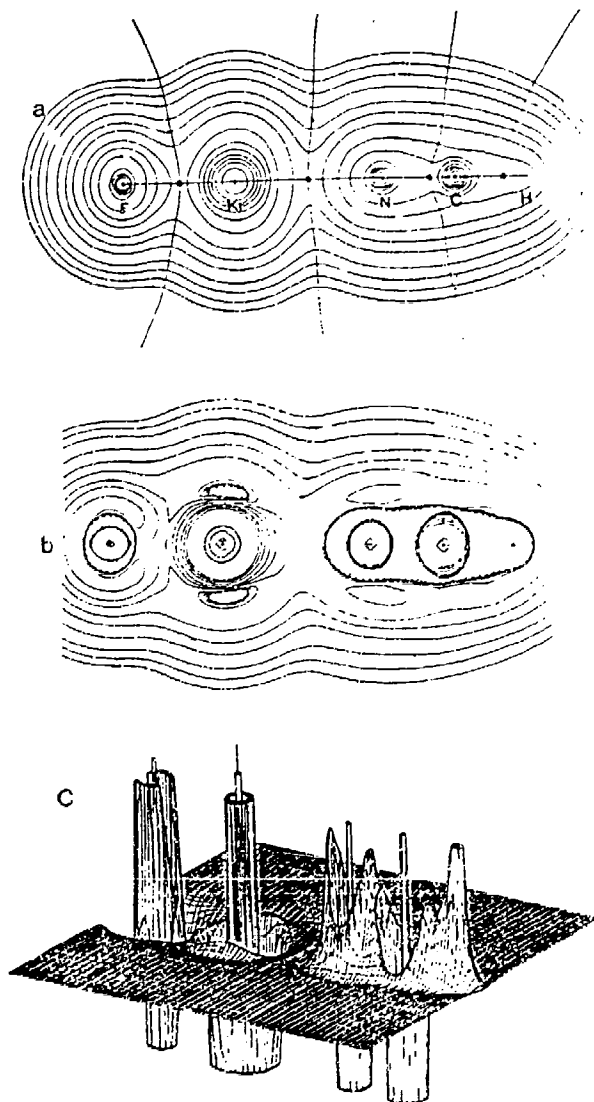**Figure 3.**

(a) Contour map of the charge density in the adduct $HC\equiv N-KrF^+$ showing the bond paths and the interaction of the interatomic surfaces. Bond critical points are denoted by black circles. Note the near planarity of the Kr-N interatomic surface, which is also a characteristic of a hydrogen bond. The outer contour value is 0.001 au. The remaining contours increase in value in the order 2×10^n, 4×10^n, 8×10^n with n starting at -3 and increasing in steps of 1 to give a maximum contour value of 20. (b) Contour map of the Laplacian distribution for $HC\equiv N-KrF^+$. The positions of the nuclei are the same as in part (a). Solid contours denote positive and dashed lines denote negative values of $\nabla^2\rho$. The magnitudes of the contour values are as in part (a), without the initial value of 0.001 au. (c) A relief map of $-\nabla^2\rho$. A maximum in the relief map is a maximum in charge concentration. If the inner spikelike feature at its nucleus is counted, the Kr atom exhibits four alternating regions of charge concentration and charge depletion corresponding to the presence of four quantum shells. Note the absence of a lip on the N side of the Kr VSCC demonstrating the presence of a hole in its outer sphere of charge concentration. Contrast the localized, atomic-like nature of the Laplacian distribution for the F and Kr atoms with the continuous valence shell of charge concentration enveloping all three of the nuclei in $HC\equiv N$. (Reprinted with permission from ref. (41))
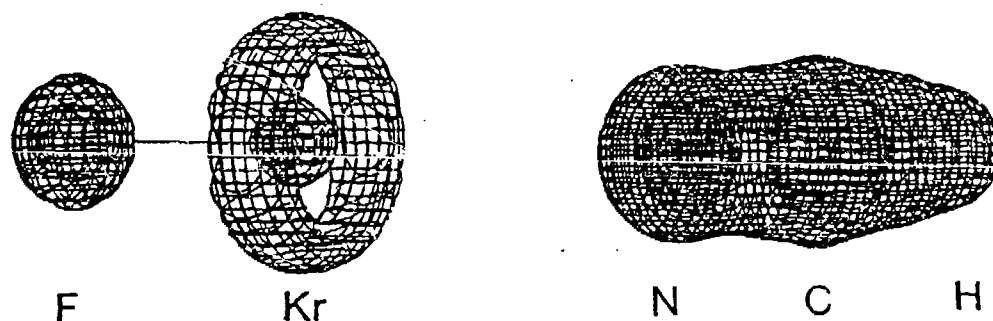
F   Kr   N   C   H

Figure 4.

Zero envelopes of the Laplacian distributions ($\nabla^2\rho = 0$ for all points on the surface) for isolated KrF^+ and $HC\equiv N$ shown aligned for adduct formation and shown to the same scale. The separation between the Kr and N nuclei is 5.0 Å. All that remains of the VSCC of the Kr atom is a belt of charge concentration, and the diagram clearly illustrates the exposure of its penultimate spherical shell of charge concentration--the core of the krypton atom. The diagram also contrasts the interatomic nature of the charge concentration in HCN with its pronounced intraatomic form in KrF^+. (Reprinted with permission from ref. (41)).
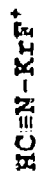
and -874.5 and -886.6 kJ mol^{-1} for

$$NgF^+ \;+\; F^- \;\longrightarrow\; F\text{-}Ng\text{-}F \qquad\qquad (23)$$

The molecular structure and force field of $HC\equiv N\text{-}KrF^+$ have also been calculated at higher levels of theory (Tables 7 and 8 and ref. (63-66)). The incorporation of electron correlation is necessary to describe satisfactorily the structures, stabilities and vibrational frequencies. The force field has been calculated, and the cation is predicted to be linear. Reasonable agreement with the two observed vibrational Raman bands in the solid has been found in all four sets of calculations. The stretching mode leading to dissociation into KrF^+ and $HC\equiv N$ was calculated to be near 200 cm^{-1} (66). The KrF and $HC\equiv N$ fragments in the complex have geometries similar to those for the isolated molecules (Table 8): the Kr-N bond distance is predicted to be relatively long, 2.18 - 2.32 Å (cf. sum of Kr and N van der Waals radii; 3.4 Å), the Kr-F distance in the adduct is predicted to increase by only 0.0 - 0.13 Å relative to that of KrF^+. The $HC\equiv N\text{-}KrF^+$ cation is predicted to be bound by 130.1 - 176.1 kJ mol^{-1} with respect to KrF^+ and $HC\equiv N$ at higher levels of theory (cf. 126.4 - 136.0 kJ mol^{-1} at SCF level) with zero-point energy corrections (63-66).

All four of the calculated results are consistent with an ionic and a covalent component in the bonding of KrF^+ with $HC\equiv N$, i.e., the fragments are σ-bonded with a high degree of ionic character. The Kr-N bond is the result of a donor-acceptor interaction between the sp-lone pair on N and the empty σ^* orbital on KrF^+. In the study by Dixon and Arduengo (66), the molecular orbitals and bonding are analyzed in terms of hypervalent bonds. Their

41

Table 7. Bond Distances (Å) for Optimized Geometries for KrF⁺, HC≡N   and
HC≡N-KrF⁺

Species	r(C-H)	r(C≡N)	r(Kr-F)	r(Kr-N)	Ref.
KrF⁺			1.697		66
			1.752		72
HC≡N	1.057	1.126			66
	1.064	1.156			73
HC≡N-KrF⁺	1.065	1.122	1.709	2.320	66
	1.068	1.128	1.748	2 307	41
	1.067	1.168	1.707	2.313	64
	1.073	1.129	1.772	2.183	64
	1.076	1.175	1.83	2.281	63

Table 8. Calculated Vibrational Frequencies (cm^{-1}) and Infrared Intensities (km/mol) for

HC≡N-KrF$^+$

Vibrational Assignment	v(calc) HF[a]	v(scaled) HF[a]	v(calc) HF[b]	v(calc) MP-2d[b]	v(calc) MP-2[c]	v(expt)[d]	I(calc)[a]
C-H str.	3556	3253	3588	3467	3446		133
C≡N str.	2446	2128	2461	2130	2100	2158	221
H-C≡N bend	935	760	940	762	752		43
Kr-F str.	782	620	782	644	562	560	66
F-Kr-N≡C bend	253	228	256	271	244		63
Kr-N str.	217	195	222	287	267		72
F-Kr-N≡C bend	115	104	120	116	117		28

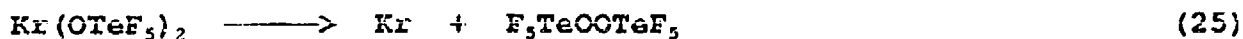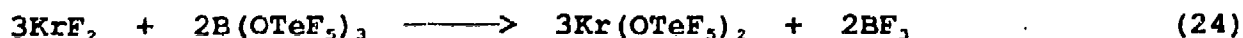(a) Reference (66). (b) Reference (64). (c) Reference (63). (d) Reference (8).

43

results indicate that the bonding between Kr and N is not a simple covalent σ-bond but is best described in terms of three-center and four-center hypervalent bonds, where both types of hypervalent bonds are needed to describe the covalent σ-bonding in $HC\equiv N-KrF^+$. The charge distribution for $HC\equiv N-KrF^+$ shows some transfer of electronic charge from the carbon to the KrF^+ region, consistent with a contribution from the resonance structure $H-^+C=N-Kr-F$.

High-level $\underline{ab}$ $\underline{initio}$ calculations (65) also predict that the $HC\equiv N-ArF^+$ cation is a stable argon-nitrogen bonded species with a heat of association, -160 kJ mol^{-1}, corresponding to equation (22), which is comparable to that of the observed krypton analog (-157 kJ mol^{-1}). These results, together with another recent high-level theoretical calculation which estimates the electron affinity for ArF^+ to be 13.66 eV (11) suggest that $HC\equiv N$, with its high first ionization potential (13.59 eV) (13), may be oxidatively resistant enough to withstand the formidable electron affinity of the ArF^+ cation. The synthesis of the $HC\equiv N-ArF^+$ cation is likely to require the ArF^+ cation, which is expected to be an oxidizer of unprecedented strength, if and when it is synthesized. Reactions analogous to those given in equations (3) and (5) involving ArF_2 are not feasible, as ArF_2 is predicted to be unbound (11). The synthesis of ArF^+ is in itself, formidable and will entail the use of a counter anion which is capable of withstanding its high electron affinity (11).

At the correlated level, the $HC\equiv N-NeF^+$ cation (65) is found to be an unstable species, dissociating spontaneously to $HC\equiv N-Ne^+ + F$, where the $HC\equiv N-Ne^+$ fragment is itself a weakly bound species having a binding energy of only 6 kJ mol^{-1}.

44

The gap resulting from the syntheses of the first examples of Kr-N bonds (8,9) and the previous existence of several examples of Kr-F bonds (KrF_2), KrF^+ and $F(KrF)_2^+$ (42)) has prompted the reinvestigation of the possibility of forming the first Kr-O bonded species (67). Using ^{19}F and ^{17}O NMR spectroscopy of ^{17}O enriched samples, it has been possible to document the formation of the first Kr-O bonds by the synthesis and decomposition of thermally unstable $Kr(OTeF_5)_2$ according to equations (24) and (25).

$$3KrF_2 \ + \ 2B(OTeF_5)_3 \ \longrightarrow \ 3Kr(OTeF_5)_2 \ + \ 2BF_3 \qquad (24)$$

$$Kr(OTeF_5)_2 \ \longrightarrow \ Kr \ + \ F_5TeOOTeF_5 \qquad (25)$$

The syntheses of the first examples of xenon bonded to aromatic rings; $n\text{-}CF_3C_5F_4N\text{-}XeF^+$ (n = 2, 3, 4) (37,39), $C_5F_5N\text{-}XeF^+$ (39), $C_5F_5N\text{-}Xe\text{-}OTeF_5^+$ (57), $s\text{-}C_3F_3N_2N\text{-}XeF^+$ (9) and $s\text{-}C_3F_3N_2N\text{-}Xe\text{-}OTeF_5^+$ (57) have recently been complemented by the first documented case of xenon bonded to an aromatic ring through carbon, namely, the $C_5F_5Xe^+$ cation (70-72). While the aryl group of the $C_5F_5Xe^+$ cation serves to reduce the electron density at Xe(II), as evidenced from the extreme low-frequency position of the ^{129}Xe chemical shift (-3769 ppm relative to $XeOF_4$ in $CH_3C\equiv N$ solvent), the ^{129}Xe shieldings in the s-trifluorotriazine and perfluoropyridine derivatives are less than in the carbon analog and may in large part be associated with the electron-withdrawing character of the fluorine on xenon. The electron donating character of the nitrogen heterocycles relative to $HC\equiv N$ and $RC\equiv N$ in the $XeOTeF_5^+$ and XeF^+ adducts is,

45

however, apparent from the higher ^{129}Xe shieldings in the former (Tables 3 and 4). The crystal structure of the $C_5F_5Xe^+$ $(C_6F_5)_2BF_2^-$ shows the Xe-C distance (2.092(8) Å) (72) is comparable to the I-C distance in $C_6F_5I(O_2CC_6F_5)_2$ (2.072(4) Å) (73). Coordination of $CH_3C{\equiv}N$ with the $C_5F_5Xe^+$ cation serves to lower the effective positive charge at xenon by corrdination to the nitrogen of $CH_3C{\equiv}N$, to give an Xe$\cdots$N contact of 2.681 Å, that is significantly shorter than the sum of the van der Waals radii for Xe and N (3.6 Å) and substantially longer than in the Xe-N$(SO_2F)_2^+$ (2.02(1) Å) (6) and FXe-N$(SO_2F)_2$ (2.200(3) Å) (3). The Xe-N bond in C_5F_5Xe-N${\equiv}CCH_3^+$ is clearly weakly covalent and can be described in terms very similar to those used to describe the XeL$^+$ adducts considered in this Review.

REFERENCES

1. N. Bartlett and F.O. Sladky, "Comprehensive Inorganic Chemistry," Pergamon, New York, 1973, Vol. 1, Chapt. 6, pp. 213 - 330.

2. R.D. LeBlond and D.D. DesMarteau, J. Chem. Soc., Chem. Commun., 1974, 555.

3. J. F. Sawyer, G.J. Schrobilgen and S.J. Sutherland, Inorg. Chem., 1982, 21, 4064.

4. G.A. Schumacher and G.J. Schrobilgen, Inorg. Chem., 1983, 22, 2178.

5. D.D. DesMarteau, R.D. LeBlond, S.F. Hossain and D. Nöthe, J. Am. Chem. Soc., 1981, 103, 7734.

6. R. Faggiani, D.K. Kennepohl, C.J.L. Lock and G.J. Schrobilgen, Inorg. Chem., 1986, 25, 563.

7. J. Foropoulos, Jr. and D.D. DesMarteau, J. Am. Chem. Soc., 1982, 104, 4260.

8. G.J. Schrobilgen, J. Am. Chem. Soc., Chem. Commun., 1988, 863.

9. G.J. Schrobilgen, J. Am. Chem. Soc., Chem. Commun., 1988, 1506.

10. H. Selig and J.H. Holloway, Top. Curr. Chem., 1984, 124, 33.

11. G. Frenking, W. Koch, C.A. Deakyne, J.F. Liebman and N. Bartlett, J. Am. Chem. Soc., 1989, 111, 31.

12. $EA(KrF^+) \approx IP(Kr) + BE(KrF\cdot) - BE(KrF^+) = 14.0 + 0.8 - 1.6 = 13.2$ eV.

13. $EA(XeF^+) \approx IP(Xe) + BE(XeF\cdot) - BE(XeF^+) = 12.1 + 0.86 - 2.1 = 10.9$ eV.

14. V.H. Dibeler and S.K. Liston, J. Chem. Phys., 1968, 48, 4765.

15. H. Bock, R. Dammel and D. Lentz, Inorg. Chem., 1984, 23, 1535.

16. F.H. Field and J.L. Franklin, "Electron Impact Phenomena and the Properties of Gaseous Ions", Academic Press: New York, 1957, Chapt. 4,

p. 113.

17. J.T. Herron and V.H. Dibeler, J. Res. Nat. Bur. Standards, 1961, 65 A, 405.

18. G.P. van der Kelen and P.J. DeBièvre, Bull. Soc. Chim. Belg., 1960, 69, 379.

19. D.B. Beach, W.L. Jolly, R. Mews and A. Waterfeld, Inorg Chem., 1984, 23, 4080.

20. J.T. Herron and V.H. Dibeler, J. Am. Chem. Soc., 1960, 82, 1555.

21. D.M. Rider, G.W. Ray, E.J. Darland and G.E. Leroi, J. Chem. Phys., 1981, 74, 1652.

22. J.T. Herron and V.H. Dibeler, J. Chem. Phys., 1960, 33, 1595.

23. B.W. Levitt, H.F. Widing and L.S. Levitt, Chem. and Ind., 1973, 793.

24. H. Neuert, Z. Naturforsch., 1952, 7 A, 293.

25. C.R. Brundle, M.B. Robin and N.A. Kuebler, J. Am. Chem. Soc., 1972, 94, 1466.

26. V.H. Dibeler, R.M. Reese and J.L. Franklin, J. Am. Chem. Soc., 1961, 83, 1813.

27. P. Rosmus, H. Stafast and H. Bock, Chem. Phys. Lett., 1975, 34, 275.

28. S.R. Prasad and A.N. Singh, Indian J. Phys., 1985, 59 B, 1.

29. J. Collin, Can. J. Chem., 1959, 37, 1053.

30. I. Omura, H. Baba, K. Higasi and Y Kanaoka, Bull. Chem. Soc. Japan, 1957, 30, 633.

31. G.J. Schrobilgen, J.H. Holloway, P. Granger and C. Brevard, Inorg. Chem., 1978, 17, 980.

32. G.J. Schrobilgen in "NMR and the Periodic Table, "R.K. Harris and B.E. Mann, Eds.; Academic Press: London, 1978, Chapt. 14, pp. 439-454.

33. C.J. Jameson in "Multinuclear NMR," J. Mason, Ed.; Plenum Press: New York, 1987, Chapt. 18, pp. 463-475.

34. A.A.A. Emara and G.J. Schrobilgen, J. Chem. Soc., Chem. Commun., 1987, 1646.

35. A.A.A. Emara and G.J. Schrobilgen, Inorg. Chem., submitted for publication.

36. J.C.P. Sanders and G.J. Schrobilgen, in "A Methodological Approach to Multinuclear in Liquids and Solids-Chemical Applications"; NATO Advanced Study Institute, Magnetic Resonance; P. Granger and R.K. Harris, Eds., Kluwer Academic Publishers, Dordrecht, pp. 157-186.

37. A.A.A. Emara and G.J. Schrobilgen, unpublished work.

38. N.T. Arner, J.C.P. Sanders, G.J. Schrobilgen and J.S. Thrasher, Proceedings of the Fourth United States Air Force High-Energy Density Matter (HEDM) Conference, Long Beach, California, February 25-28, 1990.

39. A.A.A. Emara and G.J. Schrobilgen, J.C.S. Chem. Commun., 1988, 257.

40. J.C.P. Sanders, G.J. Schrobilgen and J.M. Whalen, Proceedings of the Fifth United States Air Force High-Energy Density Matter (HEDM) Conference, Albuquerque, New Mexico, February 24-27, 1991.

41. P.J. MacDougall, G.J. Schrobilgen and R.F.W. Bader, Inorg. Chem., 1989, 28, 763.

42. R.J. Gillespie and G.J. Schrobilgen, Inorg. Chem., 1976, 15, 22.

43. C. Murchison, S. Reichman, D. Anderson, J. Overend and F. Schreiner, J. Am. Chem. Soc., 1968, 90, 5680.

44. H.H. Claassen, G.L. Goodman, J.G. Malm and F. Schreiner, J. Chem. Phys., 1965, 42, 1229.

45. J. Burgess C.J.W. Fraser, V.M. McRae, R.D. Peacock and D.R. Russell, J.

Inorg. Nucl. Chem., Suppl., 1976, 183.

46. R.J. Gillespie, A. Netzer and G.J. Schrobilgen, Inorg. Chem., 1974, 13, 1455.

47. G.J. Schrobilgen, unpublished work.

48. A. Zalkin, D.L. Ward, R.N. Biagioni and D.H. Templeton, Inorg. Chem., 1978, 17, 1318.

49. N. Bartlett, B.G. DeBoer, F.J. Hollander, F.O. Sladky, D.H. Templeton, A. Zalkin, Inorg. Chem., 1974, 12, 780.

50. N. Bartlett, M. Wechsberg, G.R. Jones, R.D. Burbank, Inorg. Chem., 1972, 11, 1124.

51. B. Landa and R.J. Gillespie, Inorg. Chem., 1973, 12, 1383.

52. R. G. Syvret and G.J. Schrobilgen, Inorg. Chem., 1989, 28 , 1564.

53. T. Birchall, R.D. Myers, H. deWaard and G.J. Schrobilgen, Inorg. Chem., 1982, 21, 1068.

54. J.C.P. Sanders and G.J. Schrobilgen, unpublished work.

55. S. Reichman and F. Schreiner, J. Chem. Phys., 1969, 51, 2355.

56. P.A. Agron, G.M. Begun, H.A. Levy, A.A. Mason, G. Jones and D.F. Smith, Science, 1963, 139, 842.

57. A.A.A. Emara, D. Hutchinson, A. Paprica, J.C.P. Sanders and G.J. Schrobilgen, Proceedings of the Third United States Air Force High-Energy Density Materials (HEDM) Conference, New Orleans, Louisiana, March 12 - 15, 1989.

58. (a) P.A.W. Dean and R.J. Gillespie, J. Am. Chem. Soc., 1969, 91, 7260.
    (b) M. Brownstein and R.J. Gillespie, J. Am. Chem. Soc., 1970, 92, 2718.

59. M. J. Collins and G. J. Schrobilgen, Inorg. Chem., 1985, 24, 2608.

60. J. Valsdóttir, M.Sc. Thesis, McMaster University, 1990.

61.   (a) C.J. Jameson, In "Multinuclear NMR"; J. Mason, J., Ed.; Plenum Press: New York, 1987; Chapter 4, pp. 116-118. (b) C.J. Jameson and H.S. Gutowsky, J. Chem. Phys., 1969, 51, 2790. (c) R.W. Kunz, Helv. Chim. Acta, 1980, 63, 2054. (d) J. Mason, J. Polyhedron, 1989, 8, 1657. (e) B. Wrackmeyer and K. Horchler, In "Annual Reports on NMR Spectroscopy"; G.A. Webb, Ed.; Academic Press: London, 1989; Vol. 22, p. 261.

62.   J.A. Pople and D.P. Santry, Mol. Phys., 1964, 8, 1.

63.   I.H. Hillier and M.A. Vincent, J. Chem. Soc., Chem. Commun., 1989, 30.

64.   W. Koch, J. Chem. Soc., Chem. Commun., 1989, 215.

65.   M.W. Wong and L. Radom, J. Chem. Soc., Chem. Commun., 1989, 719.

66.   D.A. Dixon and A.J. Arduengo, Inorg. Chem., 1990, 29, 970.

67.   J.C.P. Sanders and G.J. Schrobilgen, J. Chem. Soc., Chem. Commun., 1989, 1576.

68.   B. Liu and H.F. Schaefer, III, J. Chem. Phys., 1971, 55, 2369.

69.   M.D. Harmony, V.W. Laurie, R.L. Kuczkowski, R. H. Schwendeman, D.A. Ramsay, F.J. Lovas, W.J. Lafferty and A.J. Maki, J. Phys. Chem. Ref. Data, 1979, 8, 619.

70.   D. Naumann and W. Tyrra, J. Chem. Soc., Chem. Commun., 1989, 47.

71.   H.J. Frohn and S. Jakobs, J. Chem. Soc., Chem. Commun., 1989, 625.

72.   H.J. Frohn, S. Jakobs and G. Henkel, Angew. Chem. Int. Ed. Engl., 1989, 28, 1506.

73.   H.J. Frohn, J. Helber and A. Richter, Chem. Ztg., 1983, 107, 169.

Fluoro(nitrile)xenon(II) Cations, RC≡N–XeF+ AsF6− (R = H, CH3, CH2F, C2H5, C2F5, C3F7, or C6F5); Novel Examples of Xenon–Nitrogen Bonds and ^{129}Xe–^{13}C, ^{129}Xe–^{1}H, and ^{129}Xe–^{14}N Nuclear Spin–Spin Couplings
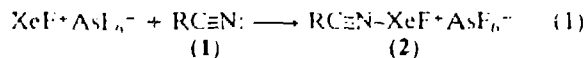
Adel A. A. Emara and Gary J. Schrobilgen*

*Department of Chemistry, McMaster University, Hamilton, Ontario L8S 4M1, Canada*

A new class of Xe–N bonded compound results from the interaction of the electron lone pair of a nitrile with the Lewis acid, XeF+; the cationic adducts, RC≡N–XeF+, have been derived from the interaction of the appropriate nitrile with either XeF+AsF6− or Xe2F3+AsF6− in anhydrous HF at low temperature and characterized in the solid state by Raman spectroscopy (for R = H and Me) and in HF solution by ^{129}Xe, ^{19}F, ^{14}N, ^{13}C, and ^{1}H n.m.r. spectroscopy.

Herein we report a new ligand group for xenon which is bonded to the noble gas atom through nitrogen. In choosing a likely ligand precursor for a Xe–C or Xe–N bond, the very weak protonic acid HCN was considered and initially found to be unreactive towards XeF2 in SO2ClF at room temperature by the usual HF displacement to give the Xe–C and Xe–N bonded compounds, FXe(CN) and Xe(CN)2. Although the conventional HF displacement is not a viable route to xenon(II) cyanides and isocyanides, we have found that HCN, and nitriles in general, behave as nitrogen bases towards the XeF+ cation.

The reactions of XeF+AsF6− and Xe2F1+AsF6− with HCN, CH3CN, CH2FCN, C2H5CN, C2F5CN, C3F7CN, and C6F5CN were carried out by combining stoicheiometric amounts of the reactants in anhydrous HF and warming to −20 to −10 °C to effect reaction and dissolution in the solvent (HCN reactions were also conducted in SO2ClF solvent). The reactions proceed according to equations (1) and (2).
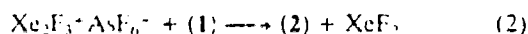
Multinuclear magnetic resonance spectra were recorded for the nitrile cations in HF solvent, and in the case of the ^{1}H and ^{129}Xe n.m.r. spectra of the HC≡N–XeF+ cation, in BrF5 solvent. As every element in the RC≡N–XeF+ cations studied possesses at least one nuclide which is suitable for observation by n.m.r. spectroscopy, n.m.r. studies using both naturally abundant and ^{13}C enriched compounds were undertaken and have provided unambiguous proof for the structures of a majority of the cations in solution (Table 1). In the case of HC≡N–XeF+, the chemical shifts of all five nuclei and eight of the ten possible spin–spin couplings that have been observed are listed in Table 1. The ^{129}Xe, ^{14}N, ^{13}C, and ^{1}H spectra are illustrated in Figures 1 and 2. The couplings, $^{1}J(^{129}$Xe–^{14}N), $^{2}J(^{129}$Xe–^{13}C), and $^{3}J(^{129}$Xe–^{1}H), represent the first examples of nuclear spin–spin couplings observed between these nuclides. Owing to the cylindrical symmetry of the C≡N–Xe–F moiety in the new cation series, low viscosity of the HF solvent medium, and the small quadrupole moment of ^{14}N, quadrupole relaxation of the ^{129}Xe–^{14}N coupling is found to be minimal giving rise to slightly quadrupole collapsed 1:1:1 triplets in the ^{129}Xe spectra and ^{129}Xe satellites in the ^{14}N spectra (Figures 1 and 2). The similarities of $^{1}J(^{129}$Xe–^{14}N) and $^{1}J(^{129}$Xe–^{19}F) values to those the HC≡N–XeF+ cation

$$XeF^+AsF_6^- + RC≡N: \longrightarrow RC≡N–XeF^+AsF_6^- \quad (1)$$
$$\qquad\quad (1) \qquad\qquad\qquad (2)$$
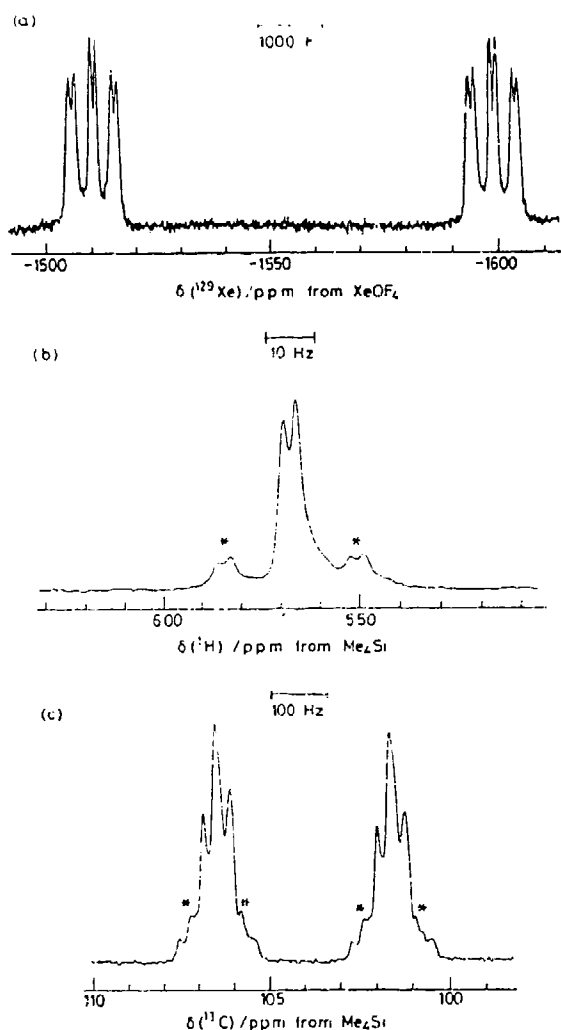
$$Xe_2F_3^+AsF_6^- + (1) \longrightarrow (2) + XeF_2 \quad (2)$$

1645

Figure 1. N.m.r. spectra of $HC\equiv N-XeF^+AsF_6^-$: (a) ^{129}Xe spectrum for a 99.2% ^{13}C enriched sample recorded in HF solvent at $-10\,°C$; (b) ^1H spectrum for a natural abundance sample recorded in BrF_5 solvent at $-58\,°C$ at 1.8790 T; (c) ^{13}C spectrum for a 99.2% ^{13}C enriched sample recorded in HF at $-10\,°C$. Asterisks (*) denote ^{129}Xe satellites.

Figure 2. N.m.r. spectra of $CH_3C\equiv N-XeF^+AsF_6^-$ recorded in HF solvent at $-10\,°C$: (a) and (b) are ^{129}Xe spectra, where (a) is natural abundance and (b) is 99.7% ^{13}C enriched at the 2-carbon; (c) natural abundance ^{14}N spectrum. Asterisks (*) denote ^{129}Xe satellites.

also allow analogous structures to be assigned to the alkyl-, fluoroalkyl- and pentafluorobenzonitrile cations.

The observation of $^1J(^{129}Xe-^{14}N)$ in both the ^{14}N and ^{129}Xe spectra is particularly noteworthy and provides conclusive proof that in each case the nitrogen atom is directly bonded to xenon. This is confirmed by comparing their respective reduced coupling constants, $^1K(Xe-N)$ (calculated using the expression given in refs. 1—3; (see Table 1), with that of $FXeN(SO_2F)_2$ [$^1J(^{129}Xe-^{15}N)$ 307 Hz; $^1K(Xe-N)$ 0.913 × 10^{22} $NA^{-2}\,m^{-3}$].[1] In addition, the small value of the J-coupling, $^{129}Xe-^{13}C$, observed for the ^{13}C enriched sample of $H-C\equiv N-XeF^+$, and a one-bond $^{13}C-^1H$ coupling, also confirm that the xenon atom is not bonded to carbon in this species.

Assuming that the Xe–N spin–spin couplings in xenon–nitrogen compounds are dominated by the Fermi contact term, a comparison of $^1K(Xe-N)$ values for $R-C\equiv N-XeF^+$ with that of the trigonal planar sp^2-hybridised nitrogen atom in $FXeN(SO_2F)_2$[1] allows assessment of the relative degrees of hybridisation for the nitrogen orbitals used in bonding to

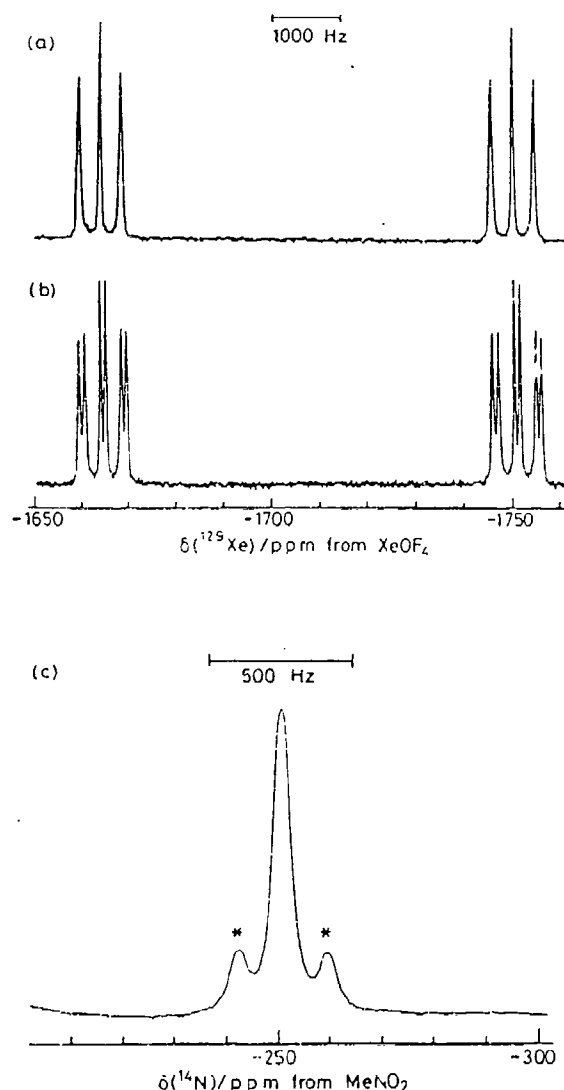xenon. The ratios of $[^1K(Xe-N)]_{sp}$ to $[^1K(Xe-N)]_{sp^2}$ are 1.42—1.53 for the cations listed in Table 1, in excellent agreement with the theoretical ratio, 1.50, calculated from the predicted fractional s-characters of the nitrogen orbitals used in bonding to xenon.

In the case of the perfluoroalkyl derivatives ($R = C_2F_5$ and C_3F_7), the Xe–N bonds are found to be labile on the n.m.r. time scale in HF solvent at temperatures down to $-30\,°C$ as a result of a decrease in base strength for $RC\equiv N$: with increasing fluorine substitution at C-2.

The salts $HC\equiv N-XeF^+AsF_6^-$ and $CH_3C\equiv N-XeF^+AsF_6^-$ were isolated from HF solvent by pumping the solutions under vacuum at -50 to $-30\,°C$ to give white solids whose Raman spectra were recorded at $-196\,°C$ (514.5 nm excitation). The Raman spectrum of $HC\equiv N-XeF^+AsF_6^-$ was assigned in detail while only key frequencies of $CH_3C\equiv N-XeF^+AsF_6^-$ have presently been assigned. In addition to the three Raman active

Table 1. N.m.r. parameters[a] for RC≡N–XeF[+] cations

Chemical shifts[b]

R	δ(^{129}Xe)	δ(^{19}F)[c]	δ(^{14}N)	δ(^{13}C)	δ(^{1}H)
H[d]	−1552	−198.4	−235.4	104.1	6.01
	−1569[e]				5.67[f]
CH₂F	−1541	−198.4 (XeF)	−229.2		5.44
		−241.7 (CF)			
CH₃	−1708	−185.5	−251.1	115.3 (CN)[g]	2.41
				0.6 (CH₃)[h]	
C₂H₅	−1717	−184.6	−251.9		1.29 (CH₃)
					2.80 (CH₂)
C₆F₅[i]	−1426				

Coupling Constants[j]

	HC≡N–XeF[e]	CH₂FC≡N–XeF[+]	CH₃C≡N–XeF[+]	[k]C₂H₅C≡N–XeF[+]	C₆F₅C≡N–XeF[+]
^1J(^{129}Xe–^{14}N)	334	333	313	311	
^1J(^{129}Xe–^{19}F)	6150 (6181)[e]	6163	6020	6017	6610
^1J(^{14}N–^{13}C)	22				
^1J(^{13}C–^{1}H)	308		141		
^2J(^{129}Xe–^{13}C)	84		79		
^2J(^{19}F–^{1}H)		44			
^2J(^{19}F–^{14}N)			18		
^3J(^{129}Xe–^{1}H)	26.8				
^3J(^{19}F–^{13}C)	18		19		
^3J(^{1}H–^{1}H)				7.5	
^4J(^{19}F–^{1}H)	2.6				
^1K(Xe–N)	1.393 × 10²²	1.389 × 10²²	1.305 × 10²²	1.297 × 10²²	

[a] Spectra were recorded in anhydrous HF at −10 °C using 9 mm o.d. FEP sample tubes at 5.8719 T, and spectrometer frequencies (MHz): ^{129}Xe 69.563, ^{19}F 235.361, ^{14}N 18.075, ^{13}C 62.915, ^{1}H 250.132. [b] Samples were referenced externally at 24 °C with respect to the neat liquid references: XeOF₄ (^{129}Xe), CFCl₃ (^{19}F), CH₃NO₂ (^{14}N), SiMe₄ (^{13}C and ^{1}H). A positive chemical shift denotes a resonance occurring to high frequency of the reference compound. [c] All ^{19}F spectra displayed a broad saddle-shaped feature at ca. −68 p.p.m. arising from the partially quadrupole collapsed ^{75}As–^{19}F coupling of the octahedral AsF₆^{–} anion. [d] Sample prepared from 99.2% ^{13}C enriched H^{13}CN [e] Measured in BrF₅ solvent at −58 °C; the ^1J(^{129}Xe–^{14}N) coupling was found to be completely quadrupole collapsed under these conditions. The sample was prepared by redissolving solid HC≡N–XeF⁺AsF₆^{–}, prepared in HF solvent, in BrF₅ at −50 °C. [f] Measured in a 5 mm o.d. precision glass tube in BrF₅ solvent at −58 °C. at 80.022 MHz (1.8790 T) for ^{1}H. The sample was prepared by redissolving solid HC≡N–XeF⁺AsF₆^{–}, prepared in HF solvent, in BrF₅ at −50 °C. [g] Sample prepared from 99% ^{13}C enriched CH₃^{13}CN. [h] Sample prepared from 99.7% ^{13}C enriched ^{13}CH₃CN. [i] Decomposition occurred at −10 to −20 °C, preventing fuller characterisation. [j] J values in Hz; K values in NA⁻²m⁻³.

modes consistent with an octahedral AsF₆^{–} anion at 679(50), v_1(a$_{1g}$); 581(13), v_2(e$_g$); 371(15), v_5(t$_{2g}$) cm⁻¹; and the formally Raman inactive modes v_3(t$_{1u}$) at 692(12) and v_4(t$_{1u}$) at 244(1), 269(6), 280(14) cm⁻¹; the most prominent features of the linear HC≡N–XeF⁺ cation spectrum are the factor-group-split C≡N stretch at 2159(41) and 2163(18) cm⁻¹ and a pair of intense lines at 559(100) and 569(94) cm⁻¹ assigned to the factor-group-split Xe–F stretch. ^{13}C enrichment (99.2%) confirms the assignment of v(C≡N) (isotopic shift, 31.6 cm⁻¹) and the split, doubly degenerate bend δ(C≡N–Xe) at 327(4), 334(2) cm⁻¹ (isotopic shift, 5.5 cm⁻¹; also cf. the N≡C–I bend in ICN at 304 cm⁻¹).[4] A low-frequency shoulder on v_5 of the anion at 368 cm⁻¹ was tentatively assigned to the Xe–N stretch (cf. v(Xe–N) of FXeN(SO₂F)₂ at 422 cm⁻¹)[1] and a weak band at 3141(4) cm⁻¹ was assigned to v(C–H) (cf. the C–H stretching frequency of gaseous HC≡N, 3311 cm⁻¹).[5] The remaining features were assigned to the doubly degenerate bends δ(F–Xe–N) [116(33), 133(10), 157(5), 180(2) cm⁻¹] and δ(H–C≡N) [706(1) cm⁻¹]. Preliminary assignments of some key frequencies for the CH₃C≡N–XeF⁺ cation spectrum were made by comparison with those of CH₃C≡N⁶ and HC≡N–XeF⁺: v_{asym}(CH₃), 3013(6), 3021(7), 3027(4) cm⁻¹; v_{sym}(CH₃), 2944(19), 2940(19) cm⁻¹; $v_{i,sym}$(CH₃), 2335(16) cm⁻¹; v(XeF), 559(100), 5.0(74), 571(34) cm⁻¹; δ(F–Xe–N), 160(7), 170(6) cm⁻¹.

Additional examples of nitriles and other inorganic and organic nitrogen bases are under active investigation as potential electron-pair donors towards noble gas-cations, as well as representative X-ray crystal structures containing the RC≡N–XeF⁺ cations.

References

1 J. F. Sawyer, G. J. Schrobilgen, and S. J. Sutherland, Inorg Chem., 1982, 21, 4064.
2 G. A. Schumacher and G. J. Schrobilgen, Inorg. Chem., 1983, 22, 2178.
3 R. Faggiani, D. K. Kennepohl, C. J. L. Lock, and G. J. Schrobilgen, Inorg. Chem., 1986, 25, 563.
4 S. Hemple and E. R. Nixon, J. Chem. Phys., 1967, 47, 4273.
5 H. C. Allen, E. D. Tidwell, and E. K. Plyler, J. Chem. Phys., 1956, 25, 302.
6 J. E. Griffiths in 'Vibrational Spectra and Structure,' ed. J. R. Durig, Elsevier, New York, 1977, vol. 6, p. 333.

Contribution from the Department of Chemistry,

McMaster University, Hamilton, Ontario L8S 4M1, Canada

The Fluoro(hydrocyano)xenon(II) Cation; Preparation of HC≡N-XeF$^+$AsF$_6^-$; a Multinuclear Magnetic Resonance and Raman Spectroscopic Study

Adel A.A. Emara and Gary J. Schrobilgen[*]

Abstract

The XeF$^+$ or Xe$_2$F$_3^+$ cations react with HC≡N in anhydrous HF solvent to give the Lewis acid-base adduct cation, HC≡N-XeF$^+$. The HC≡N-XeF$^+$ cation has been characterized in HF and BrF$_5$ solvents by ^{129}Xe, ^{19}F, ^{14,15}N, ^{13}C and ^{1}H NMR spectroscopy and has been characterized as its AsF$_6^-$ salt in the solid state by low-temperature Raman spectroscopy. The scalar couplings, $^1J(^{129}$Xe-^{14}N), $^2J(^{129}$Xe-^{13}C) and $^3J(^{129}$Xe-^{1}H), represent the first examples of couplings observed between these nuclides. The vibrational assignments of the ν(Xe-N) stretching and δ(XeNC) δ(FXeN) bending modes have been aided by obtaining Raman spectra for natural abundance ^{15}N- and ^{13}C-enriched HC≡N-XeF$^+$AsF$_6^-$. The solution NMR and low-temperature Raman spectroscopic studies are consistent with a linear C$_{\infty v}$ structure for the HC≡N-XeF$^+$ cation. The vibrational data together with the NMR chemical shifts indicate that the Xe-N bond is weakly covalent and are in agreement with recent theoretical calculations. NMR spectroscopic studies also show that solutions of HC≡N-XeF$^+$AsF$_6^-$ in HF are extensively solvolyzed to give equilibrium concentrations of the HC≡NH$^+$ cation and XeF$_2$.

INTRODUCTION

While many examples of xenon bonded to oxygen or fluorine and of xenon bonded to other highly electronegative inorganic ligands through oxygen were synthesized immediately following the discovery of noble-gas reactivity,[1] over a decade had elapsed before an example with a ligating atom other than oxygen and fluorine, namely nitrogen, was synthesized[2] and two decades before the Xe-N bond in $FXeN(SO_2F)_2$ was definitively characterized in the solid state by X-ray crystallography and in solution by multinuclear magnetic resonance spectroscopy.[3] Other imidodisulfurylfluoride xenon-nitrogen bonded species have since been definitively characterized using primarily NMR spectroscopy, namely, $Xe[N(SO_2F)_2]_2,[4,5]$ $F[XeN(SO_2F)_2]_2^+,[4,5]$ $XeN(SO_2F)_2^+AsF_6^-$ [6] and $XeN(SO_2F)_2^+Sb_3F_{16}^-$ [6] and the latter salt has also been characterized by single crystal X-ray diffraction. The compound, $Xe[N(SO_2CF_3)_2]_2,$[7] has also been prepared and characterized, and is the most thermally stable of the imido derivatives of xenon.
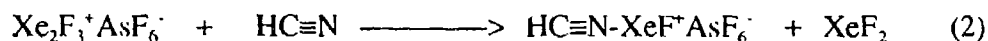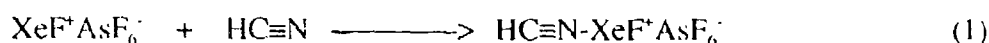
Recently, a significant extension of noble-gas chemistry, and in particular compounds containing noble-gas nitrogen bonds, has been achieved by taking advantage of the Lewis acid properties of noble-gas cations.[8] In view of the propensity of the XeF^+ cation to form strong fluorine bridges to counter anions in the solid state,[9] the XeF^+ cation may be regarded as having a significant Lewis acid strength. Based on photoionization studies, $HC\equiv N$ is one of the most oxidatively resistant ligands among the perfluoropyridines and nitriles we have investigated thus far (first adiabatic ionization potential, 13.59 eV[10]). The estimated electron affinity of XeF^+ (10.9 eV)[11] suggested that $HC\equiv N$ would be resistant to oxidative attack by the XeF^+ cation and that the $HC\equiv N-XeF^+$ cation might have sufficient thermal stability to permit its spectroscopic

characterization in solution and in the solid state. The reaction of XeF^+ with $HC\equiv N$ and the subsequent isolation and characterization of $HC\equiv N\text{-}XeF^+AsF_6^-$ have been reported in our previous communication.[12] We subsequently reported that a large number of oxidatively resistant Lewis nitrogen bases can interact with XeF^+ to form Lewis acid-base cations with XeF^+. Included among these bases are alkyl nitriles and pentfluorophenylnitrile,[12] perfluoroalkyl nitriles,[13] perfluoropyridines[14] and s-trifluorotriazine.[13] The present paper provides a detailed account of the synthesis and structural characterization of the $HC\equiv N\text{-}XeF^+$ cation by low-temperature Raman spectroscopy in the solid state and in solution by ^1H, ^{13}C, $^{14,15}N$, ^{19}F and ^{129}Xe NMR spectroscopy. More recently the krypton(II) analog, $HC\equiv N\text{-}KrF^+$ [15] and $R_FC\equiv N\text{-}KrF^+$ ($R_F = CF_3$, C_2F_5, n-C_3F_7)[13] have also been synthesized and characterized in this laboratory, representing the first examples of krypton-nitrogen bonds.

The present paper and previous communications outlining the syntheses of $HC\equiv N\text{-}XeF^+AsF_6^-$ [12] and $HC\equiv N\text{-}KrF^+AsF_6^-$ [15] have been complemented by a recent theoretical investigation of $HC\equiv N\text{-}NgF^+$ (Ng = Kr, Xe) at the SCF level by determination of the properties of the atoms and bonds in these molecules using the theory of atoms in molecules.[16]

RESULTS AND DISCUSSION

The reactions of $XeF^+AsF_6^-$ and $Xe_2F_3^+AsF_6^-$ with $HC\equiv N$ were carried out according to equations (1) and (2) by combining stoichiometric amounts of the reactants in anhydrous HF and warming to -20 to -10 °C to effect reaction and dissolution.

$$XeF^+AsF_6^- + HC\equiv N \longrightarrow HC\equiv N\text{-}XeF^+AsF_6^- \qquad (1)$$

$$Xe_2F_3^+AsF_6^- + HC\equiv N \longrightarrow HC\equiv N\text{-}XeF^+AsF_6^- + XeF_2 \qquad (2)$$

The compound, $HC\equiv N\text{-}XeF^+AsF_6^-$, was isolated as a colorless microcrystalline solid upon removal of HF solvent under vacuum at -30 °C and was stable for up to 6 hrs. at 0 °C. After HF removal at -30 °C following reaction (2), XeF_2 was observed in the Raman spectrum of the solid sample prior to pumping off XeF_2 at 0 °C ($v_1(\Sigma_g^+)$, 495 cm^{-1}). Solutions of $HC\equiv N\text{-}XeF^+AsF_6^-$ in HF at ambient temperature slowly decompose over a period of 14 hrs. The solvolytic behavior of $HC\equiv N\text{-}XeF^+AsF_6^-$ in anhydrous HF at room temperature has been compared with that of $HC\equiv N$ in the accompanying paper.[17] The reactions were also conducted in SO_2ClF solvent at 0 °C, but owing to the low solubility of the reactants and product in this solvent, the reactions did not go to completion.[12]

NMR Spectroscopy

Structure of the $HC\equiv N\text{-}XeF^+$ Cation in Solution. Every element in the $HC\equiv N\text{-}XeF^+$ cation possesses at least one nuclide which is suitable for observation by NMR spectroscopy, namely, the spin-½ nuclei ^1H, ^{13}C, ^{15}N, ^{129}Xe and ^{19}F, and the spin-1 nucleus ^{14}N. Multinuclear magnetic resonance spectra were recorded for $HC\equiv N\text{-}XeF^+AsF_6^-$ in HF and BrF_5 solvents for all six nuclei using natural abundance and ^{13}C and ^{15}N enriched compounds. All possible nuclear spin-spin couplings have been observed (Structure I and Table 1), establishing the solution structure of the

$HC\equiv N$-XeF^+ cation. In the course of the present NMR study, the couplings, $^1J(^{129}Xe$-$^{14}N)$, $^2J(^{129}Xe$-$^{13}C)$ and $^3J(^{129}Xe$-$^1H)$ were observed, representing the first examples of scalar couplings between these nuclides.

$$^1H\text{-}^{13}C\equiv\overset{\oplus}{^{14/15}N}\text{-}^{129}Xe\text{-}^{19}F$$
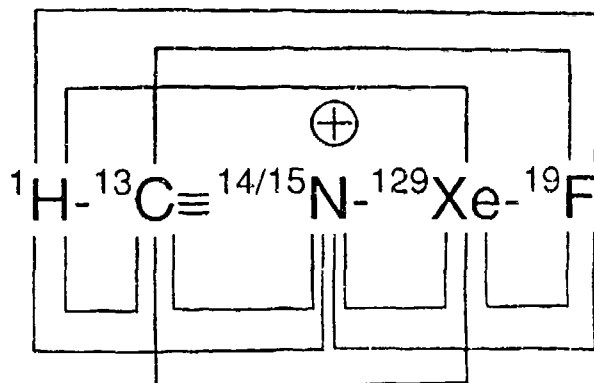
Structure I

In prior studies of the imidodisulfurylfluoride derivatives of xenon(II), the low symmetry and resulting large electric field gradient (efg) at the ^{14}N nucleus in the trigonal planar -$N(SO_2F)_2$ group necessitated ^{15}N enrichment in order to observe xenon-nitrogen scalar couplings and nitrogen chemical shifts in $FXeN(SO_2F)_2$,[3] $XeN(SO_2F)_2^+$,[6] $Xe[N(SO_2F)_2]_2$[4] and $F[XeN(SO_2F)_2]_2^+$ [6] cations in SbF_5, BrF_5 and SO_2ClF solvents. In contrast, the axial symmetry of the $HC\equiv N$-XeF^+ cation and resulting low efg at the ^{14}N nucleus, low viscosity of the HF solvent at -10 °C and small quadrupole moment of ^{14}N serve to minimize quadrupole relaxation of the ^{129}Xe-^{14}N and ^{14}N-^{13}C couplings (see Nature of Bonding in $HC\equiv N$-XeF^+), allowing ready observation of the directly bonded ^{129}Xe-^{14}N and ^{14}N-^{13}C scalar couplings. However, in the higher viscosity solvent, BrF_5 (-58 °C), the ^{129}Xe-^{14}N and ^{14}N-^{13}C couplings are quadrupole collapsed into single lines. Because they are generally obscured owing to quadrupolar relaxation caused by the ^{14}N nucleus,

^{15}N enrichment was required for the observation of scalar couplings between nitrogen and non-directly bonded nuclei when the magnitudes of the couplings were small.

The ^{129}Xe NMR spectrum of natural abundance HC≡N-XeF$^+$ consists of a doublet arising from $^1J(^{129}$Xe-^{19}F) in the Xe(II) region of the spectrum and is centered at -1570 ppm in BrF$_5$ solvent at -50 °C; $^1J(^{129}$Xe-^{19}F), 6176 Hz. The doublet ($^1J(^{129}$Xe-^{19}F), 6161 Hz) is centered at -1552 ppm in HF at -10 °C and each doublet branch is further split into partially quadrupole collapsed 1:1:1 triplets arising from the one-bond scalar coupling $^1J(^{129}$Xe-^{14}N), 332 Hz. The magnitude of $^1J(^{129}$Xe-^{19}F) is comparable to directly bonded ^{129}Xe-^{19}F couplings of other xenon(II) compounds.[18-20] Failure to observe $^1J(^{129}$Xe-^{14}N) in BrF$_5$ at -50 °C is attributed to the increased viscosity of BrF$_5$ relative to HF, leading to a longer molecular correlation time in the former solvent and quadrupole collapse of the ^{129}Xe-^{14}N scalar coupling. Carbon-13 enrichment (99.2%) led to further splitting into a doublet (84 Hz) on each peak in the ^{129}Xe NMR spectrum, and is assigned to $^2J(^{129}$Xe-^{13}C), representing the first reported example of a scalar coupling between ^{13}C and ^{129}Xe (Figure 1a).

Nitrogen-15 enrichment (99.5%) of the HC≡N-XeF$^+$ cation was necessary because $^2J(^{14}$N-^{1}H) and $^2J(^{19}$F-^{14}N) could not be observed in natural abundance HC≡N-XeF$^+$AsF$_6^-$. In addition to observing $^2J(^{15}$N-^{1}H) and $^2J(^{19}$F-^{15}N) in their respective ^{19}F, ^{15}N and ^{1}H NMR spectra (vide infra), a well resolved doublet of doublets on each doublet ($^1J(^{129}$Xe-^{19}F)) branch in the ^{129}Xe NMR spectrum of the ^{15}N-enriched cation was observed in both HF (-10 °C) and BrF$_5$ (-50 °C) solvents (Figure 1b). The fine structure is assigned to $^1J(^{129}$Xe-^{15}N) (471 Hz in HF; 483 Hz in BrF$_5$) and $^3J(^{129}$Xe-^{1}H) ($\leq$ 4.7 Hz in HF; 26.8 Hz in BrF$_5$); the ^{129}Xe-^{1}H coupling was confirmed by a ^{1}H broad band decoupling experiment in the ^{129}Xe spectrum. Because of the smaller size of $^3J(^{129}$Xe-

^{1}H), quadrupolar line broadening by ^{14}N precludes observation of the latter coupling in the ^{129}Xe NMR spectrum of the natural abundance cation. The magnitudes of $^1J(^{129}Xe\text{-}^{14}N)$ in the absence of quadrupole relaxation have been calculated for comparison with their observed values in HF solvent from the measured values of $^1J(^{129}Xe\text{-}^{15}N)$ using equation (3): 334 Hz (BrF$_5$ solvent at -50 °C) and 336 Hz (HF solvent at -10 °C; cf., 332 Hz, measured value) and show the effect of residual quadrupolar relaxation on the measurement of $^1J(^{129}Xe\text{-}^{14}N)$ is negligible.

$$^1J(^{129}Xe\text{-}^{14}N) = {^1J}(^{129}Xe\text{-}^{15}N) \; \frac{\gamma(^{14}N)}{\gamma(^{15}N)} \qquad (3)$$

The ^{19}F NMR spectra for natural abundance and 99.2% ^{13}C-enriched HC≡N-XeF$^+$AsF$_6^-$ in HF solvent at -10 °C and for 99.5% ^{15}N-enriched HC≡N-XeF$^+$AsF$_6^-$ in BrF$_5$ solvent at -50 °C (Figure 2) consist of single ^{19}F environments with accompanying satellites that are attributed to $^1J(^{129}Xe\text{-}^{19}F)$. Under high resolution and in the absence of quadrupolar line broadening arising from ^{14}N, $^4J(^{19}F\text{-}^1H)$, 2.6 (HF), 2.7 (BrF$_5$); $^3J(^{19}F\text{-}^{13}C)$, 24.7 (HF), 26.8 (BrF$_5$) and $^2J(^{19}F\text{-}^{15}N)$, 23.9 Hz were observed in the ^{15}N enriched compounds (Table 1). A broad, saddle-shaped feature (3150 Hz linewidth) also occurs at -68 ppm in these spectra and arises from the partially quadrupole collapsed $^1J(^{75}As\text{-}^{19}F)$ coupling in the AsF$_6^-$ anion.

The ^{14}N and ^{15}N NMR spectra have been recorded for natural abundance and 99.5% ^{15}N-enriched HC≡N-XeF$^+$AsF$_6^-$, respectively. The ^{14}N NMR spectrum recorded in HF solvent at -10 °C consisted of a single line at -235.1 ppm with ^{129}Xe satellites ($^1J(^{129}Xe\text{-}^{14}N)$). The ^{15}N NMR spectrum of a 99.5% enriched sample was also recorded under the same conditions in HF at -10 °C (-234.5 ppm) and in BrF$_5$ at -50 °C (-230.2 ppm) (Figure 3). The splitting pattern in the ^{15}N

spectrum consisted of a doublet of doublets arising from $^2J(^{15}N\text{-}^{19}F)$, 23.9 (HF, BrF$_5$) and $^2J(^{15}N\text{-}$ $^1H)$, 13.0 Hz (BrF$_5$) (also observed in the ^1H and ^{19}F NMR spectra) and were accompanied by ^{129}Xe satellites ($^1J(^{129}Xe\text{-}^{15}N)$).
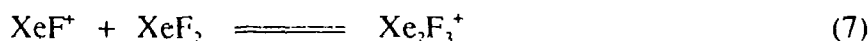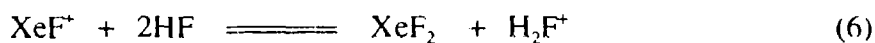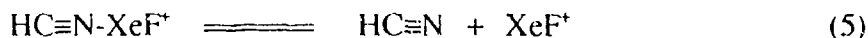
The ^1H NMR resonance of natural abundance HC≡N-XeF$^+$AsF$_6^-$ in BrF$_5$ solvent at -58 °C occurred at 6.01 ppm and consisted of a doublet with ^{129}Xe satellites, $^3J(^{129}Xe\text{-}^1H)$, 2.7 Hz. The doublet is assigned to $^4J(^{19}F\text{-}^1H)$, but the two-bond $^{14}N\text{-}^1H$ coupling was not observed due to quadrupole relaxation by ^{14}N. However, $^4J(^{19}F\text{-}^1H)$ and $^2J(^{15}N\text{-}^1H)$ were both observed in the ^1H NMR spectrum for a 99.5% ^{15}N enriched sample in BrF$_5$ solvent at -50 °C (Figure 4). The ^1H resonance in HF at -10 °C has also been observed for a natural abundance sample and consisted of a single line at 4.70 ppm with ^{129}Xe satellites ($^3J(^{129}Xe\text{-}^1H)$).

The ^{13}C NMR resonance of HC≡N-XeF$^+$ (Figure 5) for a 99.2% ^{13}C enriched sample in HF solvent at -10 °C occurred at 104.1 ppm and consisted of a doublet ($^1J(^{13}C\text{-}^1H)$) of partially quadrupole collapsed 1:1:1 triplets ($^1J(^{14}N\text{-}^{13}C)$, 22 Hz) with ^{129}Xe satellites ($^2J(^{129}Xe\text{-}^{13}C)$) on each doublet branch.

Intense signals assigned to the HC≡NH$^+$ cation were also observed in the ^1H and ^{13}C NMR spectra and are attributed to equilibrium (4). The relative concentrations [HC≡NH$^+$]/[HC≡N-XeF$^+$] measured in the ^1H NMR spectrum $ $ $ $ a HF solution having an initial [HC≡N-XeF$^+$AsF$_6$] of 2.18 M at -10 °C was 4 : 1. The proton chemical shift, δ(^1H), 7.43 ppm and $^2J(^{15}N\text{-}^1H)$, 18.6 Hz for the proton on carbon of a ^{15}N-enriched sample are in excellent agreement with the previously reported values for HC≡NH$^+$ in the FSO$_3$H-SbF$_5$-SO$_2$ solvent system.[21] In contrast to the previous work in FSO$_3$H-SbF$_5$-SO$_2$, the proton on nitrogen environment and $^1J(^{14,15}N\text{-}^1H)$ were not observed, and is presumably the result of proton exchange

62

with HF solvent. Additional NMR parameters for the $HC\equiv NH^+$ cation are reported here for the first time: $\delta(^{13}C)$, 97.1 ppm; $^1J(^{13}C\text{-}^1H)$, 324.6 ; $^1J(^{13}C\text{-}^{14}N)$, 40.7 and $^1J(^{13}C\text{-}^{15}N)$, 59.5 Hz, however, neither the ^{14}N nor ^{15}N spectra of the $HC\equiv NH^+$ cation could be observed, even after a relaxation delay of 30 s was applied in the ^{15}N spectrum. A previous determination of $\delta(^{15}N)$ in $FSO_3H\text{-}SbF_5\text{-}SO_2$ solvent by the INDOR method gave a value of 119.4 ppm relative to external aqueous NH_4^{+} [21] (chemical shift relative to neat external CH_3NO_2 is -240.3 ppm calculated from a $\delta(^{15}N)$ value of -359.7 ppm for aqueous $NH_4^+Cl^-$ relative to CH_3NO_2 [4]).

Although significant equilibrium amounts of $HC\equiv NH^+$ are observed in the ^{13}C and ^1H NMR spectra, XeF_2 is not observed in the ^{19}F and ^{129}Xe NMR spectra even in the presence of a an equimolar amount of XeF_2 as in reaction (2). The apparent absence of XeF_2 in the NMR spectra is presumed to result from chemical exchange involving trace amounts of XeF^+ and $Xe_2F_3^+$ as exchange intermediates arising from equilibria (4) - (7) and XeF_2.

$$HC\equiv N\text{-}XeF^+ \;+\; HF \;=\!=\!=\!=\; HC\equiv NH^+ \;+\; XeF_2 \qquad (4)$$

$$HC\equiv N\text{-}XeF^+ \;=\!=\!=\!=\; HC\equiv N \;+\; XeF^+ \qquad (5)$$

$$XeF^+ \;+\; 2HF \;=\!=\!=\!=\; XeF_2 \;+\; H_2F^+ \qquad (6)$$

$$XeF^+ \;+\; XeF_2 \;=\!=\!=\!=\; Xe_2F_3^+ \qquad (7)$$

The ^{129}Xe NMR spectra of $HC\equiv N\text{-}XeF^+AsF_6^-$ and $CH_3C\equiv N\text{-}XeF^+AsF_6^-$ in HF at -10 °C have been

reported previously[12] and clearly show that the ^{129}Xe linewidth of $HC\equiv N\text{-}XeF^+AsF_6^-$ (84 Hz, center line of the triplet) compared to that of $CH_3C\equiv N\text{-}XeF^+AsF_6^-$ (40 Hz, center line of the triplet) is significantly larger. This observation is consistent with the anticipated lower base strength of $HC\equiv N$ towards XeF^+ relative to that of $CH_3C\equiv N$, resulting in a greater degree of dissociation for $HC\equiv N\text{-}XeF^+$ (equilibrium (5)) and ensuing chemical exchange by means of equilibria (4), (6) and (7).

In the course of this study it has also been shown that XeF_2 displaces HF in its reaction with $HC\equiv NH^+AsF_6^-$ in HF or BrF_5 solvents according to the reverse of equilibrium (4). The ^{129}Xe NMR spectrum was recorded for the molar ratio $XeF_2/HC\equiv NH^+AsF_6^- = 2.47$ at -15 °C in HF solvent (initial $[XeF_2] = 0.230$ M), and gave the relative equilibrium concentrations $[XeF_2]/[HC\equiv N\text{-}XeF^+] = 0.81$. While the XeF_2 1:2:1 triplet (-1555 ppm; $^1J(^{129}Xe\text{-}^{19}F)$, 5530 Hz) could be observed under these conditions, it was significantly exchange broadened (linewidth, 2590 Hz) relative to that of $HC\equiv N\text{-}XeF^+$ (-1555 ppm; $^1J(^{129}Xe\text{-}^{19}F)$, 6156 Hz; $^1J(^{129}Xe\text{-}^{14}N)$, 330 Hz; linewidth, 110 Hz), indicating that XeF_2 was undergoing slow chemical exchange, presumably via equilibria (5) - (7). Because $HC\equiv N\text{-}XeF^+AsF_6^-$ has a low solubility in HF at temperatures approaching -30 °C, an equilibrium mixture of $HC\equiv NH^+AsF_6^-$ and XeF_2 was also studied in BrF_5 solvent at -50 °C for the molar ratio $XeF_2/HC\equiv NH^+AsF_6^- = 2.17$, giving $[XeF_2]/[HC\equiv N\text{-}XeF^+] = 0.72$ at equilibrium (initial $[XeF2] = 0.314$ M). In contrast, the XeF_2 triplet (-1666 ppm; $^1J(^{129}Xe\text{-}^{19}F)$, 5629 Hz) was significantly sharper (linewidth, 250 Hz), which is consistent with a lower degree of dissociation of $HC\equiv N\text{-}XeF^+$ according to equilibrium (5) (-1573 ppm; $^1J(^{129}Xe\text{-}^{14}N)$ was quadrupole collapsed at low temperatures in BrF_5; linewidth, 470 Hz).

Raman Spectroscopy. The low-temperature (-1℃5 °C) Raman spectra of the crystalline product, isolated from the reaction of natural abundance, ^{15}N- and ^{13}C-enriched HC≡N with XeF$^+$AsF$_6^-$ in anhydrous HF solvent are shown in Figures 6 and 7 and the observed frequencies, along with their assignments, are listed in Table 2. The ^{13}C (99.2%) and ^{15}N (99.5%) enriched salts were prepared in order to aid in the assignments of the ν(XeN) stretching and δ(HC≡N), δ(CNXe) and δ(NXeF) bending frequencies. The isotopic shifts are given by the ratios $\Delta\lambda(^{14/15}N)/\lambda(^{14}N)$ and $\Delta\lambda(^{12/13}C)/\lambda(^{12}C)$, as described in reference (24) and are defined and listed in Table 2.

The Raman spectra are consistent with the formation of HC≡N-XeF$^+$AsF$_6^-$ in the solid state. The linear HC≡N-XeF$^+$ cation is expected to give rise to 3N - 5 = 10 normal modes belonging to the irreducible representations 4 Σ^+ + 3 Π under the point symmetry C$_{\infty v}$. All ten modes are predicted to be Raman and infrared active, and consist of four stretching modes, $\nu_1(\Sigma^+)$, ν(H-C); $\nu_2(\Sigma^+)$, ν(C-N); $\nu_3(\Sigma^+)$, ν(Xe-F) and $\nu_4(\Sigma^+)$, ν(Xe-N) and three doubly degenerate bending modes ν_5(Π), δ(HCN); ν_6(Π), δ(CNXe) and ν_7(Π), δ(NXeF). Therefore, seven bands are expected in the Raman and infrared spectra of the HC≡N-XeF$^+$ cation. In addition, the octahedral AsF$_6^-$ anion is expected to give rise to three Raman-active vibrational bands under O$_h$ symmetry, ν_1(a$_{1g}$), ν_2(e$_g$) and ν_5(t$_{2g}$). However, 28 bands as opposed to the predicted 13 from a consideration of free ion symmetries are observed in the Raman spectrum of HC≡N-XeF$^+$AsF$_6^-$ (Table 2). The disparity between the number of observed bands and the number predicted from a consideration of the free species is attributed to vibrational coupling within the unit cell and/or reduction of the free ion symmetries due to site symmetry effects. The removal of all degeneracies by lowering of the cation and anion site symmetries to C$_{2v}$ or lower would result in 25 Raman-active bands, however, in the absence of a crystallographic space group for HC≡N-XeF$^+$AsF$_6^-$, it has not been

65

possible in the ensuing discussion to determine their site symmetries and thereby account for the additional splittings and assign their symmetry species in a rigorous manner.

Vibrational assignments were aided by comparison with the vibrational frequencies of $HC\equiv N$,[22] $FXe-N(SO_2F)_2$,[3] $XeF^+AsF_6^-$,[25] $Xe_2F_3^+AsF_6^-$ [26] and $M^+AsF_6^-$,[23] where M is an alkali metal and by recent theoretical calculations of the harmonic frequencies of the $HC\equiv N-KrF^+$ cation.[27-30] The three fundamental stretching modes $v(Xe-F)$, $v(C-N)$ and $v(C-H)$ are readily assigned by comparison with the Raman spectra of $HC\equiv N$ in the gas phase and $XeF^+AsF_6^-$, which are also listed in Table 2. As the Xe-F and C-N stretching modes belong to the totally symmetric representation, Σ^+, their splittings can only be attributed to coupling of vibrational modes within the unit cell. The C-H stretching mode is also presumed to be factor-group split, but owing to its broadness, the anticipated splitting could not be resolved.

The most intense bands at 561(100) and 569(93) cm^{-1} are assigned to the Xe-F stretching frequency of the $HC\equiv N-XeF^+$ cation and is characteristic of the terminal Xe-F bond in xenon(II) species of the type L-Xe-F (see Table 3). The Xe-F stretching frequency can be used to assess the covalent nature of the Xe-F bond. The XeF^+ cation has been shown to be weakly coordinated to the anion by means of a fluorine bridge, and the Xe-F stretch has been shown to correlate with the degree of covalent character in the Xe---F bridge bond, decreasing with increasing base strength of the anion.[x] Consequently, the Xe-F stretching frequency is expected to increase as the xenon-nitrogen bond becomes more ionic and the terminal XeF bond becomes more covalent. A comparison of the Xe-F stretching frequency of $HC\equiv N-XeF^+$ with other Xe-N bonded species, XeF^+ and $Xe_2F_3^+$ allows one to assess the relative covalency of the Xe-N bond in the $HC\equiv N-XeF^+$ cation. The stretching frequencies of the terminal XeF bond for F-Xe-L type derivatives are listed

66

in Table 3 along with their Xe-F and Xe-L bond lengths when known. The $HC\equiv N$-XeF^+ cation has the most ionic xenon-nitrogen bond when compared to previously reported Xe-N bonded compounds for which vibrational data are available and is also in accord with our NMR findings (see above and Table 3) and theoretical calculations at the SCF level (see Nature of the Bonding in $HC\equiv N$-XeF^+). The latter calculations show that the reaction of the gas phase XeF^+ ion with F^- to yield the difluoride results in an increase in the calculated Xe-F bond length of 0.1 Å, while the reaction of XeF^+ with $HC\equiv N$ causes the same bond length (calculated) to increase on average by only 0.016 Å.[16] Similar conclusions have been reached based on the high-frequency position of the Kr-F stretching frequency of $HC\equiv N$-$KrF^+AsF_6^-$ [15] and theoretical calculations for the $HC\equiv N$-KrF^+ cation.[16,27-30]

The $\nu_1(\Sigma^+)$ C-H stretching vibration is assigned to a broad, weak band at 3142(2) cm^{-1} and occurs at a significantly lower frequency than in gaseous $HC\equiv N$, i.e., 3311 cm^{-1},[22] and is consistent with coordination of the nitrogen lone pair to an electron pair acceptor. Two sharp lines at 2160(41) and 2162(18) cm^{-1} are assigned to the factor-group split $\nu_2(\Sigma^+)$ $C\equiv N$ stretching mode and occur 63 cm^{-1} to higher frequency than the $C\equiv N$ stretch of gaseous $HC\equiv N$. The shift to higher frequency upon coordination to XeF^+ is consistent with cation formation and with $HC\equiv N$ acting as a σ-electron pair donor to XeF^+. The C-H and $C\equiv N$ stretching frequencies also exhibit the expected sensitivities to ^{13}C and ^{15}N substitution (Table 2). The calculated changes in C-H and $C\equiv N$ bond lengths parallel the observed shifts in the stretching frequencies in the $HC\equiv N$-$XeF^+AsF_6^-$ salt (see Nature of the Bonding in $HC\equiv N$-XeF^+).[16]

The assignments of the low-frequency cation bands arising from ν(Xe-N), δ(CNXe) and δ(FXeN) were aided by ^{15}N and ^{13}C isotopic enrichment. The relative order of the corresponding

calculated frequencies for HC≡N-KrF[+],[27,30] which are uniformly lower than in the xenon analog, are consistent with the order arrived at for HC≡N-KrF[+], i.e., v(Xe-N) > δ(CNXe) > δ(FXeN).

The $v_3(\Sigma^+)$ Xe-N stretching vibration of the HC≡N-XeF[+] cation is assigned to the weak, low-frequency lines 328(4) and 335(2) cm^{-1} where the splitting is again attributed to vibrational coupling within the crystallographic unit cell. The assignment of the Xe-N stretch has been confirmed using ^{15}N and ^{13}C enrichment and results in relative shifts $\Delta\lambda$([14/15]N)/λ(^{15}N), -0.027 and -0.024, for the two bands in the spectrum of [^{15}N]HC≡N-XeF[+]AsF$_6^-$, and $\Delta\lambda$([12/13]C)/λ(^{13}C), -0.030 and -0.024 for [^{13}C]HC≡N-XeF[+]AsF$_6^-$ (Figure 7). The similarity between the ^{14}N/^{15}N and ^{12}C/^{13}C isotopic shifts is expected from a consideration of the form of the normal coordinate corresponding to $v_3(\Sigma^+)$. In the case of a heavy atom like Xe, the N and C displacements are expected to essentially equal to one another and in the same but opposite sense to the small Xe displacement (cf. the actual form of the displacements in the normal coordinate corresponding to $v_1(\Sigma^+)$, the C-X stretch in XC≡N, where X = Cl, Br or I [42]). The Xe-N frequency of the HC≡N-XeF[+]AsF$_6^-$ salt occurs at lower frequency than those of FXeN(SO$_2$F)$_2$ (422 cm^{-1})[3] and Xe[N(SO$_2$F)$_2$]$_2$ (386 - 413 cm^{-1}).[4] This is attributed to the greater covalent character of the Xe-N bonds in the imidodisulfurylfluoride derivatives, whereas the Xe-N bond of the HC≡N-XeF[+] cation is among the most ionic Xe-N bonded species presently known (the Xe-N bonds in n-C$_3$F$_7$C≡N-XeF[+], C$_2$F$_5$C≡N-XeF[+] and CF$_3$C≡N-XeF[+] appear to be weaker based on a comparison of their [129]Xe and ^{19}F chemical shifts, however, the vibrational spectra of these cations have not been recorded[11]). This is corroborated by the high-frequency position of the Xe-F stretch, which is among the highest of any F-Xe-L type species known where L is not bonded to the XeF group through fluorine.

The formally doubly degenerate bending mode $\nu_5(\Pi)$, $\delta(HCN)$ was not observed; this band is very weak in the Raman spectrum of gaseous $HC{\equiv}N$.[22] Although the frequency of the weak band at 707(2) is similar to $\delta(HCN)$ of gaseous $HC{\equiv}N$ (712 cm^{-1}), it was found to be insensitive to either ^{13}C or ^{15}N isotopic substitution and was accordingly assigned to an anion mode (vide infra). The assignments of the remaining doubly degenerate bending modes have been made with the aid of their relative $^{12}C/^{13}C$ and $^{14}N/^{15}N$ isotopic shift data. The presence of more than a single band for the $\delta(CNXe)$ and $\delta(FXeN)$ bending modes is ascribed to factor-group splitting and/or removal of the degeneracy by a cation site symmetry lower than $C_{\infty v}$.

The bending mode, $\nu_6(\Pi)$, $\delta(CNXe)$ is assigned to lines at 271(6), and 281(14) cm^{-1} and exhibits the anticipated low-frequency shifts in the Raman spectra of $[^{13}C]HC{\equiv}N-XeF^+AsF_6^-$ and $[^{15}N]HC{\equiv}N-XeF^+AsF_6^-$, i.e., $\Delta\lambda(^{14/15}N)/\lambda(^{15}N)$, -0.038 and -0.032 and $\Delta\lambda(^{12/13}C)/\lambda(^{12}C)$, -0.005 and -0.008 (Figure 7). The $^{14}N/^{15}N$ dependence is large, and is in fact similar to $\nu_1(\Sigma^+)$, the Xe-N stretching mode. The displacement of nitrogen from the molecular axis is expected to be large when bonded to a heavy atom while that of carbon is expected to be considerably less than the nitrogen displacement and in the opposite sense (cf. displacements for the normal modes in $XC{\equiv}N^{42}$). The relatively small $^{12}C/^{13}C$ isotopic dependence for this mode is also supported by this qualitative description and is consistent with a smaller carbon displacement.

The bending mode $\nu_7(\Pi)$, $\delta(FXeN)$ is expected at lower frequencies than $\delta(CNXe)$, and is assigned to the moderately intense bands at 118(20) and 135(10), 158(6) and 181(3) cm^{-1} by comparison with $XeF^+AsF_6^-$ [25] and $Xe_2F_3^+AsF_6^-$,[26] where $\delta(FXe{-}{-}{-}F)$ are 155 (average) and 161 cm^{-1} (average), respectively, and $FXe-N(SO_2F)_2$,[1] where $\delta(FXeN)$ is 200 cm^{-1} (average). The FXeN bend of $HC{\equiv}N-XeF^+$ is expected to be significantly lower than that of $FXe-N(SO_2F)_2$.

69

These modes also exhibit $^{14}N/^{15}N$ and $^{12}C/^{13}C$ isotopic dependences (Table 2 and Figure 7); however, no simple explanation for the relative magnitudes of each shift for each component of this doubly degenerate bend is presently available.

Although the AsF_6^- anion is not expected to be fluorine bridged to the $HC\equiv N\text{-}XeF^+$ cation, the AsF_6^- anion exhibits 14 bands compared to the three Raman-active bands that are expected under O_h symmetry. Because the totally symmetric mode of AsF_6^-, $\nu_1(a_{1g})$, is not split, additional Raman-active bands are largely attributed to site symmetry lowering (15 Raman-active bands are expected for a site symmetry of C_{2v} or lower), although vibrational coupling in the unit cell may also contribute to the number of observed bands. The modes have been assigned under C_s symmetry by analogy with $XeF^+AsF_6^-$ (Table 2) in which the O_h symmetry of the anion is reduced to C_s or lower symmetry by formation of a fluorine bridge to the anion. The vibrational frequencies for AsF_6^- under O_h symmetry have also been listed for comparison.

Lines occurring below 112 cm^{-1} exhibit no measurable shifts upon ^{13}C or ^{15}N substitution and have been assigned to lattice modes.

Nature of the Bonding in HC≡N-XeF$^+$. Previous NMR studies of xenon(II) derivatives containing XeF groups bonded to oxygen or fluorine have shown that the NMR parameters measured in the ^{19}F and ^{129}Xe spectra can generally be used to assess relative covalent characters of the Xe-O, Xe--F bridge and Xe-F terminal bonds.[18-20] In general, as the ionic character of the Xe-L (L = ligand atom) bond increases, the covalent character of the terminal Xe-F bond increases, increasing the formal charge on xenon. These trends are paralleled by decreases in $\delta(^{129}Xe)$ and increases in

both $^1J(^{129}Xe-^{19}F)$ and $\delta(^{19}F)$ for the terminal XeF group. Table 3 provides the $\delta(^{129}Xe)$ and $\delta(^{19}F)$ chemical shifts and $^1J(^{129}Xe-^{19}F)$ for a number of xenon(II) compounds containing terminal Xe-F bonds for comparison with HC≡N-XeF$^+$, showing that the Xe-F bond of HC≡N-XeF$^+$ is second only to R$_f$C≡N-XeF$^+$ (R$_f$ = CF$_3$, C$_2$F$_5$, n-C$_3$F$_7$), Xe$_2$F$_3^+$ and XeF$^+$ in covalent character. Excluding fluorine bridging to xenon and the R$_f$C≡N-XeF$^+$ cations,[11] the Xe-N bond of HC≡N-XeF$^+$ is then among the weakest xenon-ligand bonds observed thus far. The XeF$^+$ character of the XeF group in HC≡N-XeF$^+$ is supported by theoretical calculations of the efgs at the Xe nuclei in XeF$^+$ and HC≡N-XeF$^+$,[16] which are found to differ by only 7%, in agreement with the experimental observation that the quadrupolar splitting in the ^{129}Xe Mössbauer spectra of HC≡N-XeF$^+$ (40.2 ± 0.3 mm s^{-1}) is the same, within experimental error, as that obtained for the salt XeF$^+$AsF$_6^-$ (40.5 ± 0.1 mm s^{-1}).[43]

The observation of a well resolved $^{129}Xe-^{14}N$ coupling in HF is the combined result of the low viscosity of HF, the axial symmetry and accompanying low efg at the ^{14}N nucleus.[44] The axial symmetry of the cation results in an asymmetry parameter η= 0 so that the efg at the ^{14}N nucleus is dominated by q$_{zz}$, the efg component along the C$_\infty$ axis of the cation. Consequently, the effect of the efg on quadrupolar relaxation of ^{14}N will only depend on q$_{zz}$ and the molecular correlation time, τ$_c$. Coordination of XeF$^+$ to the nitrogen sp lone pair of HC≡N is expected to reduce q$_{zz}$ significantly in the adduct cation, leading to a longer spin lattice relaxation time relative to the free base, further enhancing the possibility of observing $^1J(^{129}Xe-^{14}N)$ in the low viscosity solvent, HF. The principal components of the efg tensor (+z is in the direction H → N) at the nitrogen nuclei in HC≡N and HC≡N-XeF$^+$ have been calculated and the corresponding reduction in efg in going from HC≡N to HC≡N-XeF$^+$ is 48%, in accord with our observation of

$^1J(^{129}Xe-^{14}N)$ and $^1J(^{14}N-^{13}C)$ for HC≡N-XeF$^+$ in HF solvent. The axial component of the efg tensor at the nitrogen nucleus is also halved upon the formation of HC≡N-KrF$^+$.

The difference in the magnitudes of the reduced coupling constants $^1K(Xe-N)$ in HC≡N-XeF$^+$ (1.389 x 10^{22} NA^{-2}m^{-3}) and FXeN(SO$_2$F)$_2$ (0.949 x 10^{22} NA^{-2}m^{-3})[3,4,6] may be discussed using a previous assessment of the nature of bonding to xenon in solution for FXeN(SO$_2$F)$_2$. The Xe-N bond of FXeN(SO$_2$F)$_2$ is regarded as a σ-bond having sp^2 hybrid character. In high-resolution NMR spectroscopy spin-spin coupling involving heavy nuclides is generally dominated by the Fermi contact mechanism.[6] For Xe-N spin-spin couplings dominated by the Fermi contact mechanism, one-bond coupling constants can be discussed on the basis of the formalism developed by Pople and Santry.[45] In discussions of xenon-nitrogen scalar couplings in xenon(II) imidodisulfurylfluoride compounds,[46] the s-electron density at the xenon nucleus was assumed constant and a change in the hybridization at nitrogen accounted for changes in xenon-nitrogen spin-spin coupling. The dependence of xenon-nitrogen spin-spin coupling on nitrogen s-character in the xenon-nitrogen bond may also be invoked to account for the substantially larger $^1K(Xe-N)$ value observed for HC≡N-XeF$^+$ than for xenon bonded to the trigonal planar nitrogen in FXeN(SO$_2$F)$_2$. A comparison of $^1K(Xe-N)$ for HC≡N-XeF$^+$ with that of the trigonal planar sp^2 hybridized nitrogen atom in FXeN(SO$_2$F)$_2$ allows assessment of the relative degrees of hybridization of the nitrogen orbitals used in σ-bonding to xenon. The ratio, [$^1K(Xe-N)_{sp}$]/[$^1K(Xe-N)_{sp}2$] = 1.46, for the HC≡N-XeF$^+$ cation and FXeN(SO$_2$F)$_2$ is in excellent agreement with the theoretical ratio, 1.50, calculated from the predicted fractional s-characters of the formally sp- and sp^2-hybridized nitrogen orbitals used in bonding to xenon in these compounds.

The Xe-N bond of the HC≡N-XeF$^+$ cation may be thought of as a classical Lewis acid-

base donor acceptor bond. Implicit in this description of the Xe-N bond is a considerable degree of ionic character, which appears to be a dominant feature of the stability of the $HC\equiv N\text{-}XeF^+$ cation. This premise has been supported and further illuminated by theoretical calculations on the $HC\equiv N\text{-}NgF^+$ cations.[16,27-30] The ability of NgF^+ (Ng = Kr, Xe) cations to act as Lewis acids was shown to be related to the presence of holes in the valence shell charge concentrations of the Ng atoms that expose their cores.[16] The mechanism of formation of the Ng-N bonds in the adducts of NgF^+ with $HC\equiv N$ is similar to the formation of a hydrogen bond, i.e., the mutual penetration of the outer diffuse nonbonded densities of the Ng and N atoms is facilitated by their dipolar and quadrupolar polarizations, which remove density along their axis of approach, to yield a final density in the interatomic surface that is only slightly greater than the sum of the unperturbed densities. Thus, not surprisingly, the KrF^+ and XeF^+ cations are best described as hard acids, which form weak covalent Ng-N adduct bonds as already noted in the context of the present NMR and Raman spectroscopic studies. The energies of formation of these adducts are dominated by the large stabilizations of the Ng atoms that result from the increase in the concentration of charge in their inner quantum shells. The Ng-N bonds that result from the interaction of the closed-shell reactants NgF^+ and $HC\equiv N$ actually lie closer to the closed shell limit than do bonds formed in the reaction of NgF^+ with F^-. The calculated gas phase energies of the reactions between the closed-shell species are -32.5 and -34.5 kcal mol^{-1} for Ng = Kr and Xe,[16] respectively, for

$$NgF^+ \;+\; HC\equiv N \;\longrightarrow\; HC\equiv N\text{-}NgF^+ \qquad (8)$$

73
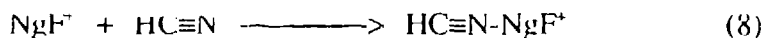
and -209.0 and -211.9 kcal mol^{-1} for

$$NgF^+ \; + \; F^- \; \longrightarrow \; F\text{-}Ng\text{-}F \qquad\qquad (9)$$

The reaction of the gas phase NgF^+ ions with F^- to yield the difluorides results in increases in the calculated Ng-F bond lengths of 0.1 Å, while their reaction with HC≡N causes the same bond lengths (calculated) to increase on average by only 0.016 Å.[16] The C-N bond of HC≡N is calculated to shorten by -0.005 Å on forming the adduct, while the C-H bond is calculated to lengthen by 0.008 Å.[16] These predicted changes in bond length also correlate with the observed shifts in their corresponding stretching frequencies, ν(C≡N), increasing by 63 cm^{-1} and ν(C-H) decreasing by 169 cm^{-1} for HC≡N-XeF$^+$.

A simple valence bond description may also be used to satisfactorily account for qualitative trends in bond lengths and associated spectroscopic parameters. The bonding in XeF$_2$ and HC≡N-XeF$^+$ may be represented by valence bond Structures II-VII, where Structures IV and VII are the least important contributing structures. The XeF$_2$ molecule has a formal bond order of ½ and the Xe-F bond of HC≡N-XeF$^+$ has a formal bond order of ½ ≤ b.o. < 1; b.o. = 1 is approached only in the most weakly coordinated case of FXe$^+$---F-Sb$_2$F$_{10}^-$.

$$\text{F-Xe}^+ \; \text{F}^- \; \longleftrightarrow \; \text{F}^- \; ^+\text{Xe-F} \; \longleftrightarrow \; \text{F}^- \; \text{Xe}^{2+} \; \text{F}^-$$

II III IV

$$\text{HC≡N-Xe}^{2+} \; \text{F}^- \; \longleftrightarrow \; \text{HC≡N} \; ^+\text{Xe-F} \; \longleftrightarrow \; \text{HC≡N} \; \text{Xe}^{2+} \; \text{F}^-$$

V VI VII

74
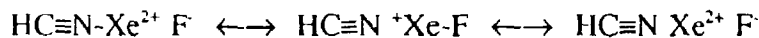
Unlike valence bond Structures II and III of XeF_2 the analogous structures for $HC{\equiv}N\text{-}XeF^+$, namely, Structures V and VI, do not have equal weighting owing to the large build up of formal positive charge on the Xe atom of Structure V, consequently, Structure VI dominates, resulting in an Xe-F bond having considerable covalent (XeF^+) character and a weak covalent Xe-N bond.

EXPERIMENTAL SECTION

Apparatus and Materials. All manipulations involving air-sensitive materials were carried out under anhydrous conditions on vacuum lines or in a dry box. Bromine pentafluoride and hydrogen fluoride were transferred on vacuum lines constructed largely from 316 stainless steel and nickel. Glass vacuum lines equipped with glass/Teflon grease-free stopcocks (J. Young) were used for the transfer of dry $HC{\equiv}N$ and $H^{13}C{\equiv}N$.

Air-sensitive substances of low volatility and/or low thermal stability were transferred in a dry box equipped with cryogenic wells. Dry box moisture levels were routinely maintained at <0.1 ppm in a Vacuum Atmospheres Model DLX dry box.

Bromine pentafluoride (Ozark Mahoning Co.) was distilled into a ¾" Kel-F tube fitted with a Kel-F valve containing dry KF and purified by maintaining F_2 (2 atm.) above the liquid for 5 to 7 days or until all the Br_2 and BrF_3 had reacted. The solvent was stored at room temperature under 1 atm. of F_2 until used.

Anhydrous hydrogen fluoride (Harshaw Chemical Co.) was purified by treatment with 5 atm. of F_2 gas in a nickel can for a period of at least 1 month, converting residual water to HF and O_2 gas. After the specified time period, anhydrous HF was vacuum distilled into a dry Kel-F storage vessel equipped with a Kel-F valve and stored at room temperature until used.

Hydrogen cyanide, $HC\equiv N$ and $H^{13}C\equiv N$, was prepared by dropwise addition of H_2O to an equimolar mixture of $KC\equiv N$ (British Drug Houses) or $K^{13}C\equiv N$ (Merck) and P_2O_5 (British Drug Houses).[47] The $HC\equiv N/H^{13}C\equiv N$ gas evolved was condensed into a glass U-tube at -196 °C, and finally vacuum distilled into a glass vessel for drying over P_2O_5. In a typical reaction, 10.00 g, 154 mmol, of $KC\equiv N$ (1.0098 g, 15.272 mmol, of $K^{13}C\equiv N$) was allowed to react to give 4.150 g of $HC\equiv N$ and (0.428 g of $H^{13}C\equiv N$). The purities of the products were checked by recording the ^1H and ^{13}C NMR spectra of the neat liquids.

The salts, $XeF^+AsF_6^-$ and $Xe_2F_3^+AsF_6^-$ were prepared as previously described.[33]

$\underline{HC\equiv NXeF^+AsF_6^-,\ [^{15}N]HC\equiv NXeF^+AsF_6^-,\ and\ [^{13}C]HC\equiv NXeF^+AsF_6^-}$. The salt, $HC\equiv N\text{-}XeF^+AsF_6^-$, was prepared according to equations (1) and (2). In typical preparations, two equal portions totalling 0.452 mmol of anhydrous $HC\equiv N$ gas were condensed from a 54.41 mL bulb onto 0.1176 g (0.347 mmol) of $XeF^+AsF_6^-$ in 1.0 - 1.5 mL of HF solvent in a ¼" o.d. FEP tube outfitted with a Kel-F valve and previously cooled to -196 °C. The ambient pressure of anhydrous $HC\equiv N$ gas that was condensed was 100 - 200 Torr to minimize dimer formation.[47] After the additions were complete, the mixture was warmed to -20 °C to effect dissolution and complete reaction. The product, $HC\equiv N\text{-}XeF^+AsF_6^-$, was only sparingly soluble in HF at -30 °C and by increasing the

temperature gradually to -10 °C, the product dissolved. Slow cooling of the solution to -35 °C resulted in colorless needle-shaped crystals. The product was isolated by removal of HF solvent and excess HC≡N under vacuum at -30 °C. In the case of $Xe_2F_3^+AsF_6^-$, two equal portions of anhydrous HC≡N totaling 1.365 mmol were condensed onto 0.4722 g (0.9285 mmol) of $Xe_2F_3^+AsF_6^-$ in ca. 1.0 - 1.5 mL of anhydrous HF at -196 °C. The remainder of the procedure was identical to that used in the $XeF^+AsF_6^-$/HC≡N reaction except the product was pumped on for 6 hrs. at 0 °C to remove XeF_2.

Nitrogen-15 (99.5%) and carbon-13 enriched (99.2%) HC≡N-$XeF^+AsF_6^-$ were prepared according to the equation (1). In typical preparations, anhydrous hydrogen fluoride (1 mL) was condensed at -196 °C onto 0.1124 g (1.700 mmol) of [^{15}N]KC≡N in a 9 mm FEP tube fitted with a Kel-F valve. The sample was agitated until all the [^{15}N]KC≡N had dissolved. The resulting [^{15}N]HC≡N was vacuum distilled, along with the HF solvent, onto 0.4631 g (1.365 mmol) of $XeF^+AsF_6^-$ in an ¼" o.d. FEP reaction tube/Kel-F valve assembly, followed by warming to -10 °C. A colorless solution resulted, which was rapidly cooled to -40 °C, whereupon HF and excess [^{15}N]HC≡N were removed under vacuum. In a typical preparation of [^{13}C]HC≡N-$XeF^+AsF_6^-$, 0.1498 g (2.266 mmol) of [^{13}C]KC≡N and 0.5480 g (1.630 mmol) of $XeF^+AsF_6^-$ were used. The procedure was then the same as for the preparation of [^{15}N]HC≡N$XeF^+AsF_6^-$.

After HF removal, Raman spectra were obtained by running the spectra directly on the ¼" FEP reaction tube under 2 atm. (ambient temperature) of dry N_2 gas. The ^{15}N- and ^{13}C-enriched samples were subsequently divided and transferred into 4 mm, 9 mm (FEP) and/or 5 mm glass sample tubes for NMR spectroscopy. During transfers, samples were maintained at low temperature by placing the sample tubes inside drilled copper blocks previously cooled to -196

77

°C in a cryogenic well inside the dry box. Natural abundance samples for NMR spectroscopy were prepared by condensing a 30 - 35% molar excess of HC≡N onto the appropriate amount of $XeF^+AsF_6^-$ or $Xe_2F_3^+AsF_6^-$ in HF contained in the FEP NMR sample tube. In cases where the exact stoichiometry was desired, the sample was isolated as described above and redissolved in the appropriate solvent. All samples were dissolved at low temperature in either HF (-20 to -10 °C) or BrF_5 (-60 to -50 °C) and heat sealed off from their Kel-F valves and stored at -196 °C until their NMR spectra could be recorded.

Nuclear Magnetic Resonance Spectroscopy

All NMR spectra were recorded unlocked (field drift < 0.1 Hz h⁻¹) with the use of Bruker AC-200 (4.6975 T) and WM-250 (5.8719 T) spectrometers.

Spectra were recorded on natural abundance, 99.2% ^{13}C and 99.5% ^{15}N enriched samples in heat sealed 9 mm o.d. or 4 mm o.d. FEP NMR tubes (HF and BrF_5 solvents) or in 5 mm precision Pyrex tubes (BrF_5 solvent; Wilmad Glass Co.) as described below. The FEP sample tubes were placed inside precision 10 mm o.d. or 5 mm o.d. glass NMR tubes before being placed in the probe.

The ^{129}Xe, ^{14}N, ^{15}N, and ^{13}C spectra were recorded at 5.8719 T in 9 mm FEP sample tubes (HF and BrF_5 solvent) on the same 10 mm probe (broad-banded over the frequency range 23 - 103 MHz) tuned to 69.563 (^{129}Xe), 18.075 (^{14}N), 25.347 (^{15}N) or 62.915 (^{13}C) MHz, respectively. Fluorine-19 spectra (235.361 MHz) were obtained on a 5 mm dual $^1H/^{19}F$ probe. Proton spectra (200.133 MHz) were recorded at 4.6975 T in HF solvent in 4 mm FEP sample tubes and in BrF_5 solvent in medium or thin wall 5 mm o.d. precision glass sample tubes.

Xenon-129 NMR spectra of natural abundance $HC\equiv N-XeF^+AsF_6^-$ samples were recorded for spectral widths of 25 and 100 kHz with acquisition times of 0.164 and 0.082 s (17,000 and 150,000 scans), respectively, and a data point resolution of 6.10 Hz/pt. The ^{129}Xe NMR spectra of ^{13}C- and ^{15}N-enriched samples were recorded for spectral widths of 50 and 25 kHz (50,000 and 1200 - 2500 scans), respectively, with acquisition times of 0.328 and 0.655 s and data point resolutions of 3.05 and 1.53 Hz/pt., respectively. Fluorine-19 NMR spectra were recorded for spectral widths of 50 and 100 kHz with acquisition times of 0.082 and 0.164 s and data point resolutions of 3.05 and 6.10 Hz/pt. (4500 and 7500 scans), respectively. Nitrogen-15 and -14 NMR spectra were recorded for spectral widths of 25 and 10 kHz with acquisition times of 0.655 and 0.410 s and data point resolutions of 1.53 and 2.44 Hz/pt. (1400 and 26,000 scans), respectively. Carbon-13 NMR spectra were recorded for a spectral width of 15 kHz with an acquisition time of 0.541 s and data point resolution of 1.85 Hz/pt. (3000 scans). Proton spectra were recorded for spectral widths of 800 Hz and 3 kHz with acquisition times of 5.12 and 2.80 s and data point resolutions of 0.098 and 0.357 Hz/pt. (64 and 172 scans), respectively.

Pulse widths corresponding to bulk magnetization tip angles of ~90 ° were 22 (^{129}Xe), 2 (^{19}F), 49 (^{14}N), 35 (^{15}N), 7 (^{13}C) and 0.5 µs (^1H). No relaxation delays were applied except in the case of ^{15}N, where a relaxation delay of 10 s was applied. Line broadening parameters used in exponential multiplication of the free induction decays were set equal to or less than their respective data point resolutions. All line shape functions were Lorentzian with the exception of the ^1H spectra and the ^{129}Xe NMR spectrum of $[^{13}C]HC\equiv N-XeF^+AsF_6^-$, in these cases Gaussian line shapes were applied for resolution enhancement.

The respective nuclei were referenced externally to neat samples of $XeOF_4$ (^{129}Xe), $CFCl_3$

(^{19}F), CH$_3$NO$_2$ (^{14}N and ^{15}N) and (CH$_3$)$_4$Si (^{13}C and ^{1}H) at 24 °C. Positive chemical shifts were assigned to resonances occurring to high frequency of the reference substance.[48]

For variable temperature measurements, samples were kept cold (-196 or -78 °C) until immediately prior to their placement in the probe. They were generally warmed only enough to liquify and solubilize the contents and were then quickly placed in the precooled probe. Prior to data accumulation, the tubes were allowed to equilibrate in the probe for periods of several minutes while spinning. Temperatures were periodically checked by placing a copper constantan thermocouple into the sampling region of the probe. Temperatures were considered to be accurate to within ±1 °C.

Raman Spectroscopy. A Coherent Model Innova 90 argon ion laser giving up to 3.5 W of power at 5145 Å was used to excite the Raman spectra. The spectrometer was a Spex Industries Model 14018 double monochromator equipped with 1800 grooves/mm holographic gratings. Slit widths depended on the scattering efficiency of the sample, laser power, etc., and were set at 100 - 150 μm. An RCA C31034 phototube detector in conjunction with a pulse count system consisting of pulse amplifier, analyzer and rate meter (Hamner NA-11, NC-11, and N-780 A, respectively) and a Texas Instruments Model FSOZWBA strip-chart recorder were used to record the spectra. The scanning rates used were 0.2 and 0.5 cm^{-1}s^{-1}. The typical power range used was between 0.7 and 1 W. The spectrometer was periodically calibrated by recording the discharge lines from an argon lamp over the spectral range of interest; all the Raman shifts quoted are estimated to be accurate to at least ±2 cm^{-1} while the precision of each Raman shift measurement is estimated to be ±0.2 cm^{-1}.

Cylindrical ¼" FEP sample tubes were mounted vertically. The angle between the incident laser beam and sample tube was 45°, and Raman scattered radiation was observed at 45° to the laser beam (90° to the sample tube axis). Low-temperature spectra were recorded at -196 °C by mounting the sample vertically in an unsilvered Pyrex glass dewar filled with liquid nitrogen. All spectra were obtained directly in ¼" FEP reaction vessels. The spectrum of the FEP sample tube was nearly always observed, however, their prominence in the overall spectrum depended on the efficiency of the sample as a Raman scatterer, and could be minimized by focusing the laser beam on the sample surface. Lines arising from FEP have been subtracted out of the spectra reported in the Tables but not in the Figures.

Figure 1. ^{129}Xe NMR spectra (69.563 MHz) of HC≡N-XeF$^+$AsF$_6^-$ recorded in HF solvent at

-10 °C (a) 99.2% ^{13}C enriched sample. (b) 99.5% ^{15}N enriched sample; expansion

(A) with proton coupling and expansion (B) {^{1}H}-decoupled.

Figure 2. ^{19}F NMR spectrum (235.361 MHz) of 99.5% ^{15}N-enriched HC≡N-XeF$^+$AsF$_6$

recorded in BrF$_5$ solvent at -50 °C. Asterisks (*) denote ^{129}Xe satellites.

Figure 3. ^{15}N NMR spectrum (25.347 MHz) of HC≡N-XeF$^+$AsF$_6^-$ for a 99.5% ^{15}N-enriched

sample recorded in BrF$_5$ solvent at -50 °C. Asterisks (*) denote ^{129}Xe satellites.

Figure 4. ^{1}H NMR spectrum (200.133 MHz) of 99.5% ^{15}N-enriched HC≡N-XeF$^+$AsF$_6^-$

recorded in BrF$_5$ solvent at -50 °C. Asterisks (*) denote ^{129}Xe satellites.

Figure 5. ^{13}C NMR spectrum (62.915 MHz) of HC≡N-XeF$^+$AsF$_6^-$ for a 99.2% ^{13}C-enriched

sample recorded in HF solvent at -10 °C. Asterisks (*) denote ^{129}Xe satellites.

Figure 6.   Raman spectrum of natural abundance HC≡N-XeF$^+$AsF$_6^-$ recorded at -196 °C

Asterisks (*) denote FEP sample tube lines.

Figure 7.   Raman spectra of natural abundance, 99.2% ^{13}C-enriched and 99.5% ^{15}N-enriched HC≡N-XeF$^+$AsF$_6^-$, recorded at -196 °C; (a) 3200 - 2100 cm^{-1} region and (b) 400 - 100 cm^{-1} region. Asterisks (*) denote FEP sample tube lines.

Table 1.   NMR Chemical Shifts and Spin-Spin Coupling Constants for the HC≡N-XeF$^+$ Cation

Chemical Shifts[a]		Coupling Constants, Hz	
$\delta(^{129}Xe)$	-1552 (-1570)	$^1J(^{129}Xe-^{19}F)$	6161 (6176)
$\delta(^{19}F)^{[b]}$	-198.7 (-193.1)	$^1J(^{129}Xe-^{14}N)$	332
$\delta(^{14}N)$	-235.1	$^1J(^{129}Xe-^{15}N)$	471 (483)
$\delta(^{15}N)^{[c]}$	-234.5 (230.2)[d]	$^1J(^{14}N-^{13}C)$	22
$\delta(^{13}C)^{[c]}$	104.1	$^1J(^{13}C-^1H)$	308
$\delta(^1H)$	4.70 (6.01)[f]	$^2J(^{129}Xe-^{13}C)$	84
		$^2J(^{15}N-^{19}F)$	23.9 (23.9)
		$^2J(^{15}N-^1H)$	(13.0)
		$^3J(^{19}F-^{13}C)$	18
		$^3J(^{129}Xe-^1H)$	24.7 (26.8)
		$^4J(^{19}F-^1H)$	2.6 (2.7)[f]

84

a Samples were referenced externally at 24 °C with respect to the neat liquid references; $XeOF_4$ (^{129}Xe), $CFCl_3$ (^{19}F), CH_3NO_2 (^{14}N and ^{15}N), $(CH_3)_4Si$ (^{13}C and ^1H). A positive chemical shift denotes a resonance occurring to high frequency of the reference compound. The values in parentheses have been measured in BrF_5 solvent.

b All ^{19}F spectra displayed a broad saddle-shaped feature at ca. -68 ppm. arising from the partially quadrupole collapsed $^1J(^{75}As-^{19}F)$ of the octahedral AsF_6^- anion.

c Obtained from a 99.5% ^{15}N enriched sample of $HC\equiv N-XeF^+AsF_6^-$.

d The sample was prepared and run at -50 °C in BrF_5 solvent by redissolving a solid sample of 99.5% ^{15}N-enriched $HC\equiv N-XeF^+AsF_6^-$ that had been prepared in HF solvent.

e Obtained form a 99.2% ^{13}C enriched sample of $HC\equiv N-XeF^+AsF_6^-$.

f The sample was prepared and run at -50 °C in BrF_5 solvent by redissolving a solid sample of natural abundance $HC\equiv N-XeF^+AsF_6^-$ that had been prepared in HF solvent.

Table 2.   Raman Frequencies and Assignments for HC≡N-XeF⁺AsF₆⁻, [¹⁵N]HC≡N-XeF⁺AsF₆⁻ and [¹³C]HC≡N-XeF⁺AsF₆⁻ and Related Compounds

		Frequency (cm⁻¹)ᵃ					$\Delta\lambda(^{14/15}N)^f$	$\Delta\lambda(^{12/13}C)^f$	
HCN ᵇ	XeF⁺AsF₆⁻ ᶜ	HC≡N-XeF⁺ AsF₆⁻	[¹⁵N]HC≡N-XeF⁺ AsF₆⁻	[¹³C]HC≡N-XeF⁺ AsF₆⁻	$\Delta\nu(^{14/15}N)^{d,e}$	$\Delta\nu(^{12/13}C)^{d,e}$	$\lambda(^{14}N)$	$\lambda(^{12}C)$	Assignment
3311		3141.9(2)	3139.3(3)	3121.0(4)	-2.6	-20.9	-0.0016	-0.0133	$\nu_1(\Sigma^+)$, ν(CH)
2097		2162.1(18)	2129.0(17)	2130.8(23)	-33.1	-31.3	-0.0304	-0.0287	$\nu_2(\Sigma^+)$, ν(CN)
		2160.0(41)	2126.9(47)	2128.7(64)	-33.1	-31.3	-0.0304	-0.0288	
712									$\nu_5(\Pi)$, δ(HCN)
	612(61)	569.4(93)	569.4(97)	569.4(97)	0.0	0.0	0.000	0.000	$\nu_3(\Sigma^+)$, ν(XeF)
	610(80)	561.2(100)	561.2(100)	561.2(100)	0.0	0.0	0.000	0.000	
	608(100)								
	602(8)								
	347 sh								ν(F---XeF)
	345(58)								
		-	-	334.3(1)					?
		334.7(2)	330.6(1)	330.6(3)	-4.1	-4.1	-0.024	-0.024	$\nu_4(\Sigma^+)$, ν(XeN)
		327.9(4)	323.4(3)	322.9(5)	-4.5	-5.0	-0.027	-0.030	
		280.9(14)	276.3(11)	279.7(14)	-4.6	-1.2	-0.032	-0.008	$\nu_6(\Pi)$, δ(CNXe)
		270.6(6)	265.4(6)	269.9(6)	-5.2	-0.7	-0.038	-0.005	
	167(2)								δ(F---XeF)
	164(5)								
	160(7)								
	150(9)								
	147(6)								
	142(3)								
		181.2(3)	181.2(2)	177.8(2)	0.0	-3.4	0.000	-0.037	$\nu_7(\Pi)$, δ(FXeN)
		163.0 sh	163 sh	163.3 sh	0.0	-1.7	0.00	-0.021	
		157.6(6)	156.9(5)	156.2(7)	-0.7	-1.4	-0.009	-0.018	
		134.6(10)	133.6(9)	132.1(11)	-0.8	-2.5	-0.015	-0.037	
		118.0(20)	117.1(18)	117.0(24)	-0.9	-1.0	-0.015	-0.017	

Table 2 (continued)

Frequency (cm^{-1})[a]			Assignment	
AsF$_6$[a]	XeF$^+$AsF$_6$[c]	HC≡N–XeF$^+$AsF$_6$	O$_h$ (AsF$_6$)	C$_s$ (AsF$_6$)
700	735(20)		$v_3(t_{1u})$ ———— A"	
	730(5)			
	723(13)	707(2)	A'	
		693(11)	A'	
689	681(56)	680(49)	$v_1(a_{1g})$ ———— A'	
573		582(12)	$v_2(e_g)$ ———— A'	
		577(5)	A'	
	465(3)		v(As···F)	
384	421(11)	419(<1), 415(1)	$v_4(t_{1u})$ ———— A'	
		406(1)	A'	
		401(2)	A"	
375	386(14)	397(1), 392(<1)	$v_5(t_{2g})$ ———— A'	
	378(5)	372(15), 370(10)	A"	
			A"	
252		244(1)	$v_6(t_{2u})$ ———— A'	
			A"	
			A"	
	73(9)	111(sh), 77(2),	Lattice modes	
		71(1), 65(6), 62(8),		
		54(5), 44(2), 43(3)		

87

a   Raman spectra of all of the HC≡N-XeF⁺AsF₆⁻ salts were recorded with FEP sample tubes at -196 °C using 514.5 nm excitation. Lines due to FEP have been deleted from the spectra. Values in parentheses denote intensities; sh denotes a shoulder. Data given are for the spectra depicted in Figures 6 and 7.

b   Reference (22).

c   Recorded at -196 °C; this work.

d $\Delta v(^{14/15}N) = v(^{15}N) - v(^{14}N)$; $\Delta v(^{12/13}C) = v(^{13}C) - v(^{12}C)$.

e   The estimated precision of each value is ± 0.4 cm⁻¹.

f $\Delta\lambda(^{14/15}N) = \lambda(^{15}N) - \lambda(^{14}N)$; $\Delta\lambda(^{12/13}C) = \lambda(^{13}C) - \lambda(^{12}C)$; where $\lambda = 4\pi^2 c^2 v^2$, c is the velocity of light and v the observed frequency (in cm⁻¹).

g   Reference (23).

Table 3.   Comparison of Xe-F Stretching Frequencies, Chemical Shifts and Coupling Constants in F-Xe-L Derivatives

Species[a]	XeF/XeL[b] Bond Lengths Å	v(Xe-F) cm⁻¹	NMR Parameters[c]			T. °C	Ref.
			$^1J(^{129}Xe\text{-}^{19}F)$[d] Hz	$\delta(^{129}Xe)$[e,f] ppm	$\delta(^{19}F)$[d,e] ppm		
$XeF^+...FSb_2F_{10}^-$[f]	1.82(3)/2.34(3)	619	7230	-574	-290.2	23[g]	18,31,32,33
$XeF^+...FAsF_5^-$[f]	1.873(6)/2.212(5)	610	6892	-869		-47	13,25,31,34,26
$(FXe)_2F^+$[f]	1.90(3)/2.14(3)	593	6740	-1051	-252.0	-62	18,31,33,35
$CF_3C{\equiv}N\text{-}XeF^+$			6397	-1337	-210.4	-63	13
$C_2F_5C{\equiv}N\text{-}XeF^+$			6437	-1294	-212.9	-63	13
$C_3F_7C{\equiv}N\text{-}XeF^+$			6430	-1294	-213.2	-63	13
$HC{\equiv}N\text{-}XeF^+$	(1.904)/(2.421)	564	6181	-1569	-198.4[h]	-58	12
$CH_3C{\equiv}N\text{-}XeF^+$[i]		560	6020	-1708	-185.5	-10	12
$s\text{-}C_3F_3N_2N\text{-}XeF^+$		548	5932	-1862	-145.6	-50	13
			5909	-1808	-154.9	-5	
$FO_2SO\text{-}XeF$ cis/trans-	1.940(8)/2.155(8)	528	5830	-1666		-40	18,33,36,37
$F_4OIO\text{-}XeF$		527	5803/	-1824/	-161.7[j]	0	38
			5910	-1720	-170.1[j]	0	
$C_5F_5N\text{-}XeF^+$		528	5926	-1922	-139.6	-30	14
$4\text{-}CF_3C_5F_4N\text{-}XeF^+$		524	5963	-1853	-144.6	-50	14
$F_5TeO\text{-}XeF$[k]		520		-2051	-151.0[j]	26	39,40
$(FO_2S)_2N\text{-}XeF$	1.967(3)/2.200(3)	506	5586	-1977	-126.1	-58	3,4
			5664[l]	-2009[l]	-126.0[l]	-40	
XeF_2	1.977 (1.984)	496	5621	-1685	-184.3	-32	13,5,41

59

a   Unless otherwise indicated, all cations have AsF_6^- as the counterion.

b   Bond lengths obtained from theoretical calculations are indicated in parentheses.

c   Spectra were obtained in BrF_5 solvent unless otherwise indicated.

d   The NMR parameters of XeF group, in particular $\delta(^{129}Xe)$, are very sensitive to solvent and temperature conditions; it is therefore important to make comparisons in the same solvent medium at the same or nearly the same temperature.

e   Referenced with respect to the neat liquids $XeOF_4$ (^{129}Xe) and $CFCl_3$ (^{19}F) at 24 °C; a positive sign denotes the chemical shift of the resonance in question occurs to higher frequency of (is more deshielded than) the resonance of the reference substance.

f   Table entries refer to the terminal fluorine on the xenon atom.

g   Recorded in SbF_5 solvent.

h $\delta(^{19}F)$ measured in anhydrous HF solvent at -10 °C.

i   NMR parameters measured in HF solvent.

j $\delta(^{19}F)$ measured in SO_2ClF solvent at -40 °C.

k   NMR parameters measured in SO_2ClF solvent.

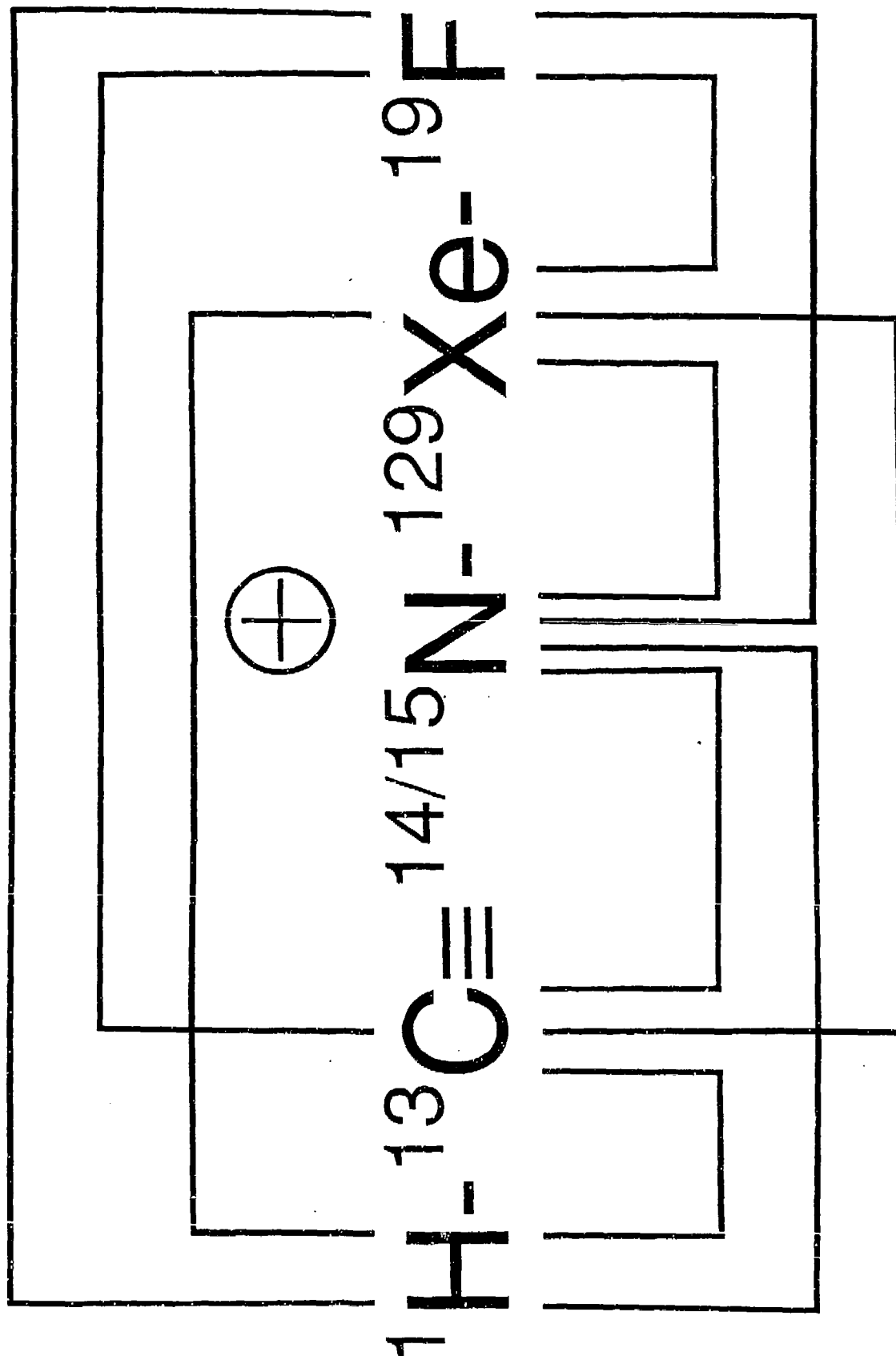l   NMR parameters measured in SO_2ClF solvent at -50 °C.

REFERENCES

1. Bartlett, N.; Sladky, F.O., In Comprehensive Inorganic Chemistry; Bailar, J.C.; Emeleus, H.J.; Nyholm, R; Trotman-Dickenson, A.F., Eds.; Pergamon: New York, 1973, Vol. 1, Chapt. 6.

2. LeBlond, R.D.; DesMarteau, D.D. J. Chem. Soc., Chem. Commun. 1974, 555.

3. Sawyer, J.F.; Schrobilgen, G.J.; Sutherland, S.J. Inorg. Chem. 1982, $\underline{21}$, 4064.

4. Schumacher, G.A.; Schrobilgen, G.J. Inorg. Chem. 1983, $\underline{22}$, 2178.

5. DesMarteau, D.D.; LeBlond, R.D.; Hossain, S.F.; Nöthe, D. J. Am. Chem. Soc. 1981, $\underline{103}$, 7734.

6. Faggiani, R.; Kennepohl, D.K.; Lock, C.J.L.; Schrobilgen, G.J. Inorg. Chem. 1986, $\underline{25}$, 563.

7. Foropoulos, J; DesMarteau, D.D. J. Am. Chem. Soc. 1982, $\underline{104}$, 4260.

8. Schrobilgen, G.J. In Synthetic Fluorine Chemistry; Olah, G.A.; Chambers, R.D.; Prakash, G.K.S., Eds.; Wiley, in press.

9. Selig, H.; Holloway, J.H. Top. Curr. Chem. 1984, $\underline{124}$, 33.

10. Dibeler, V.H.; Liston, S.K. J. Chem. Phys. 1968, $\underline{48}$, 4765.

11. $EA(XeF^+) = IP(Xe) + BE(XeF) - BE(XeF^+) = 12.1 + 0.86 - 2.1 = 10.9$ eV.

12. Emara, A.A.A.; Schrobilgen, G.J. J. Chem. Soc., Chem. Commun. 1987, 1646.

13. Schrobilgen, G.J. J. Am. Chem. Soc., Chem. Commun. 1988, 1506.

14. Emara, A.A.A.; G.J. Schrobilgen, G.J. J.C.S. Chem. Commun. 1988, 257.

15. Schrobilgen, G.J J. Am. Chem. Soc., Chem. Commun. 1988, 863.

16. MacDougall, P.J.; Schrobilgen, G.J.; Bader, R.F.W. Inorg. Chem. 1989, $\underline{28}$, 763.

17. Emara, A.A.A.; Schrobilgen, G.J. Inorg. Chem., to be submitted for publication.

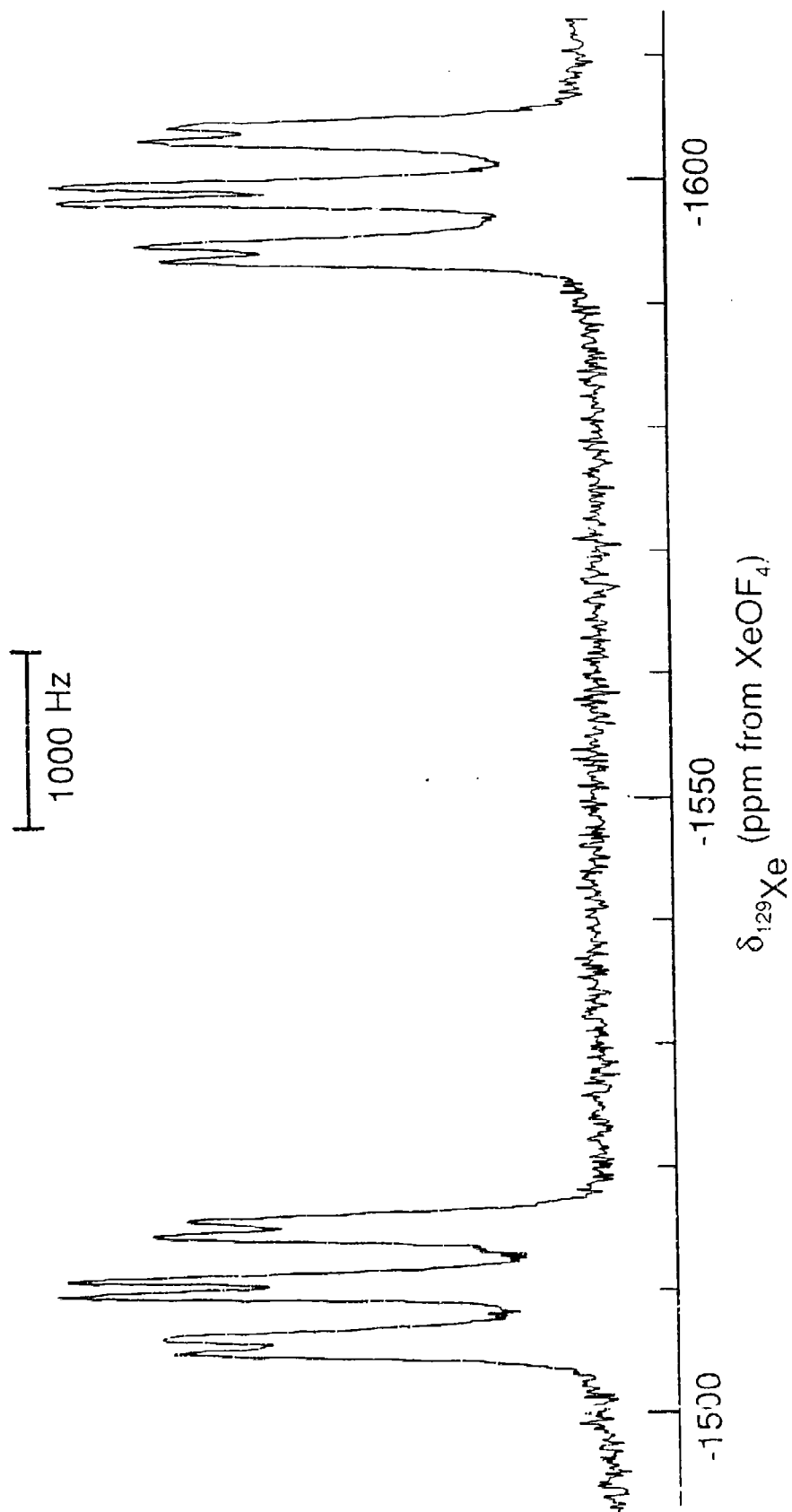18. G.J. Schrobilgen, G.J.; Holloway, J.H.; Granger, P.; Brevard, C. Inorg. Chem. 1978, $\underline{17}$, 980.

19. Schrobilgen, G.J. In NMR and the Periodic Table; Harris, R.K.; Mann, B.E., Eds.; Academic Press: London. 1978, Chapter 14, pp. 439-454.

20. Jameson, C.J. In Multinuclear NMR; Mason, J., Ed.; Plenum Press: New York, 1987, Chapter 18, pp. 463-475.

21. Olah, G.A.; Kiovsky, T.E. J. Am. Chem. Soc. 1968, 90, 4666.

22. Allen, H.C.; Tidwell, E.D.; Plyler, E.K. J. Chem. Phys. 1956, 25, 302.

23. Naulin C.; Bougon R. J. Chem. Phys. 1976, 64, 4155.

24. Tsuboi. M. Spectrochim. Acta 1960, 16, 505.

25. This work.

26. Zalkin, A.; Ward, D.L.; Biagioni, R.N.; Templeton, D.H.; Bartlett, N. Inorg. Chem. 1978, 17, 1318.

27. Hillier, I.H.; Vincent, M.A. J. Chem. Soc., Chem. Commun. 1989, 30.

28. Koch, W. J. Chem. Soc., Chem. Commun. 1989, 215.

29. Wong, M.W.; Radom, L. J. Chem. Soc., Chem. Commun. 1989, 719.

30. Dixon D.A.; Arduengo, A.J. Inorg. Chem. 1990, 29, 970.

31. Gillespie, R.J.; Schrobilgen, G.J. Inorg. Chem. 1976, 15, 22.

32. Burgess, J.; Fraser, C.J.W.; McRae, V.M.; Peacock R.D.; Russell, D.R. J. Inorg. Nucl. Chem., Suppl. 1976, 183.

33. Gillespie, R.J.; Netzer A.; Schrobilgen, G.J. Inorg. Chem. 1974, 13, 1455.

34. Schrobilgen, G.J., unpublished work.

35. Bartlett, N.; DeBoer, B.G.; Hollander, F.J.; Sladky, F.O.; Templeton, D.H.; Zalkin, A. Inorg. Chem. 1974, 12, 780.

36. Bartlett, N.; Wechsberg, M.; Jones, G.R.; Burbank, R.D. Inorg. Chem. 1972, 11, 1124.

37.   Landa, B.; Gillespie, R.J. Inorg. Chem. 1973, 12, 1383.

38.   Syvret, R.G.; Schrobilgen, G.J. Inorg. Chem. 1989, 28, 1564.

39.   Birchall, T.; Myers, R.D.; H. deWaard, H.; Schrobilgen, G.J. Inorg. Chem. 1982, 21, 1068.

40.   Sanders, J.C.P.; Schrobilgen, G.J. unpublished work.

41.   Agron, P.A.; Begun, G.M.; Levy, H.A.; Mason, A.A.; Jones, G.; Smith, D.F. Science 1963, 139, 842.

42.   Herzberg, G. "Infrared and Raman Spectra of Polyatomic Molecules"; Van Nostrand: New York, 1945;
       p 174.

43.   Schrobilgen, G.J.; Valsdóttir, N., unpublished work.

44.   (a) Mason, J. In Multinuclear NMR; Mason, J., Ed.; Plenum Press: New York, 1987; Chapter 2, pp 11-
       13, 19. (b) Howarth, O.; ibid.; Chapter 5, pp 151-152.

45.   Pople, J.A.; Santry, D.P. Mol. Phys. 1964, 8, 1.

46.   (a) Jameson, C. J. In Multinuclear NMR; Mason, J., Ed.; Plenum Press: New York, 1987; Chapter 4, pp.
       116-118. (b) Jameson, C. J.; Gutowsky, H. S. J. Chem. Phys. 1969, 51, 2790. (c) Kunz, R. W. Helv.
       Chim. Acta 1980, 63, 2054. (d) Mason, J. Polyhedron 1989, 8, 1657. (e) Wrackmeyer, B.; Horchler, K.
       In Annual Reports on NMR Spectroscopy; Webb, G. A., Ed.; Academic Press: London, 1989; Vol. 22,
       p 261.

47.   King, C.M.; Nixon, E.R. J. Chem. Phys. 1968, 48, 1685.
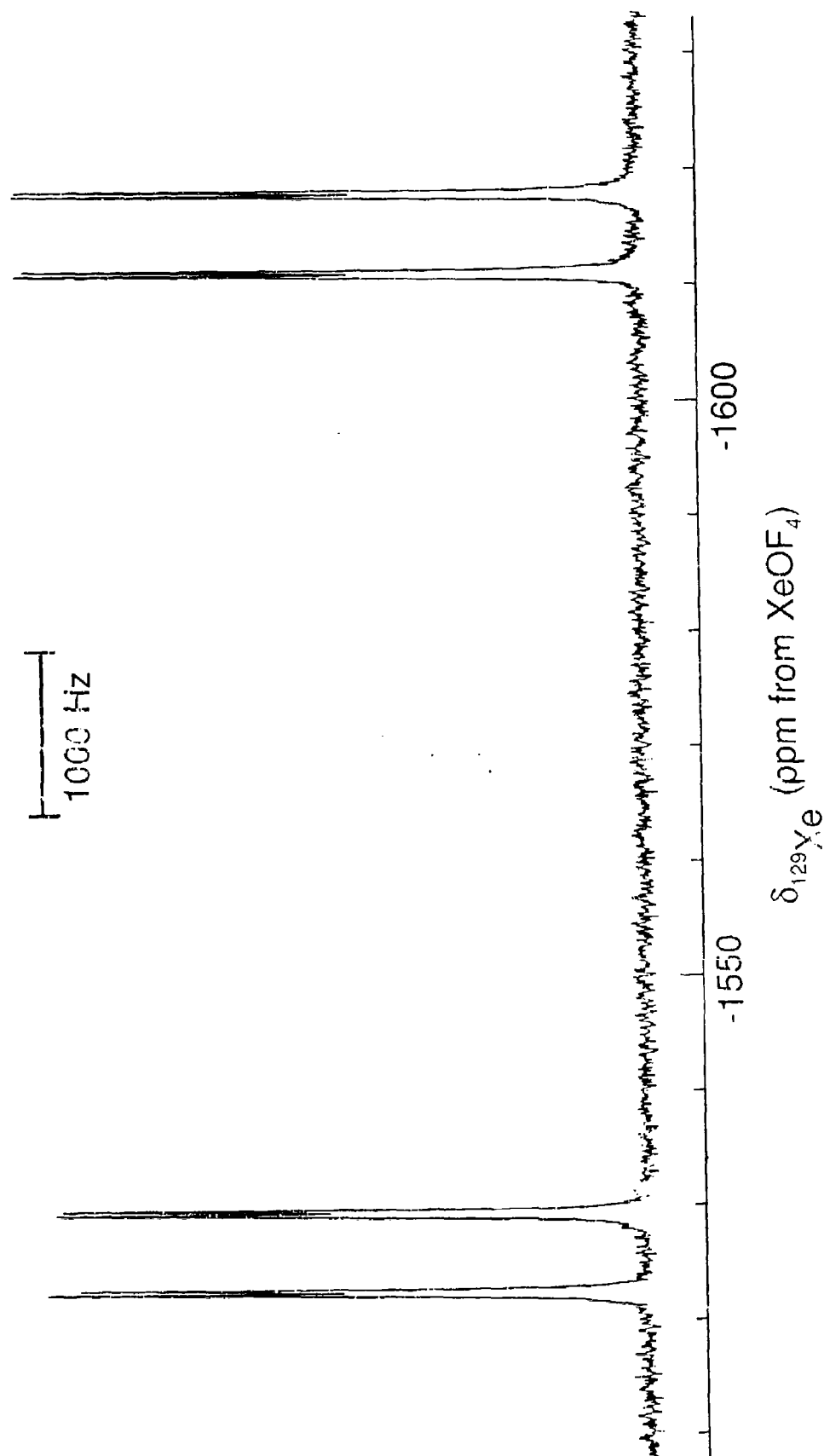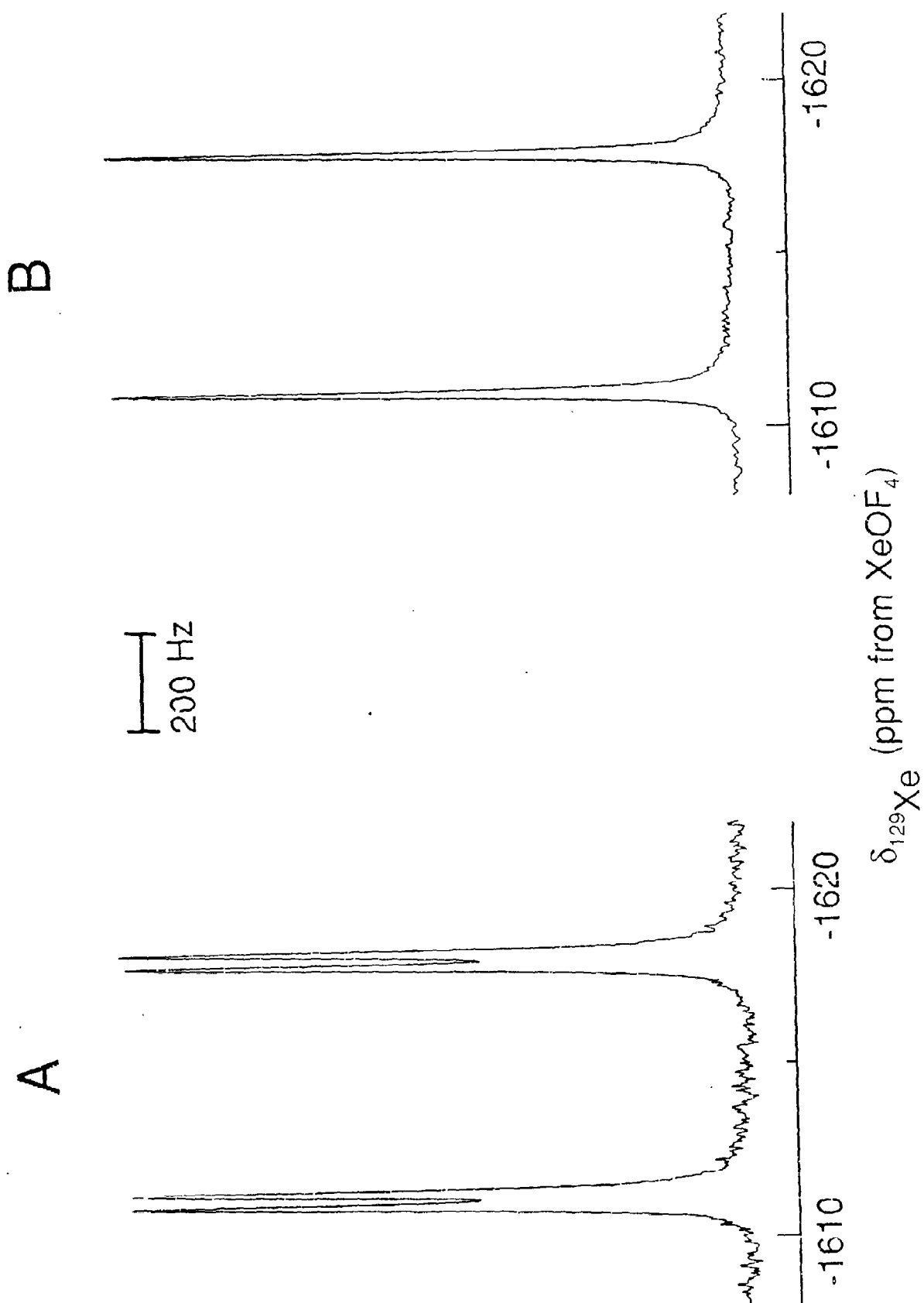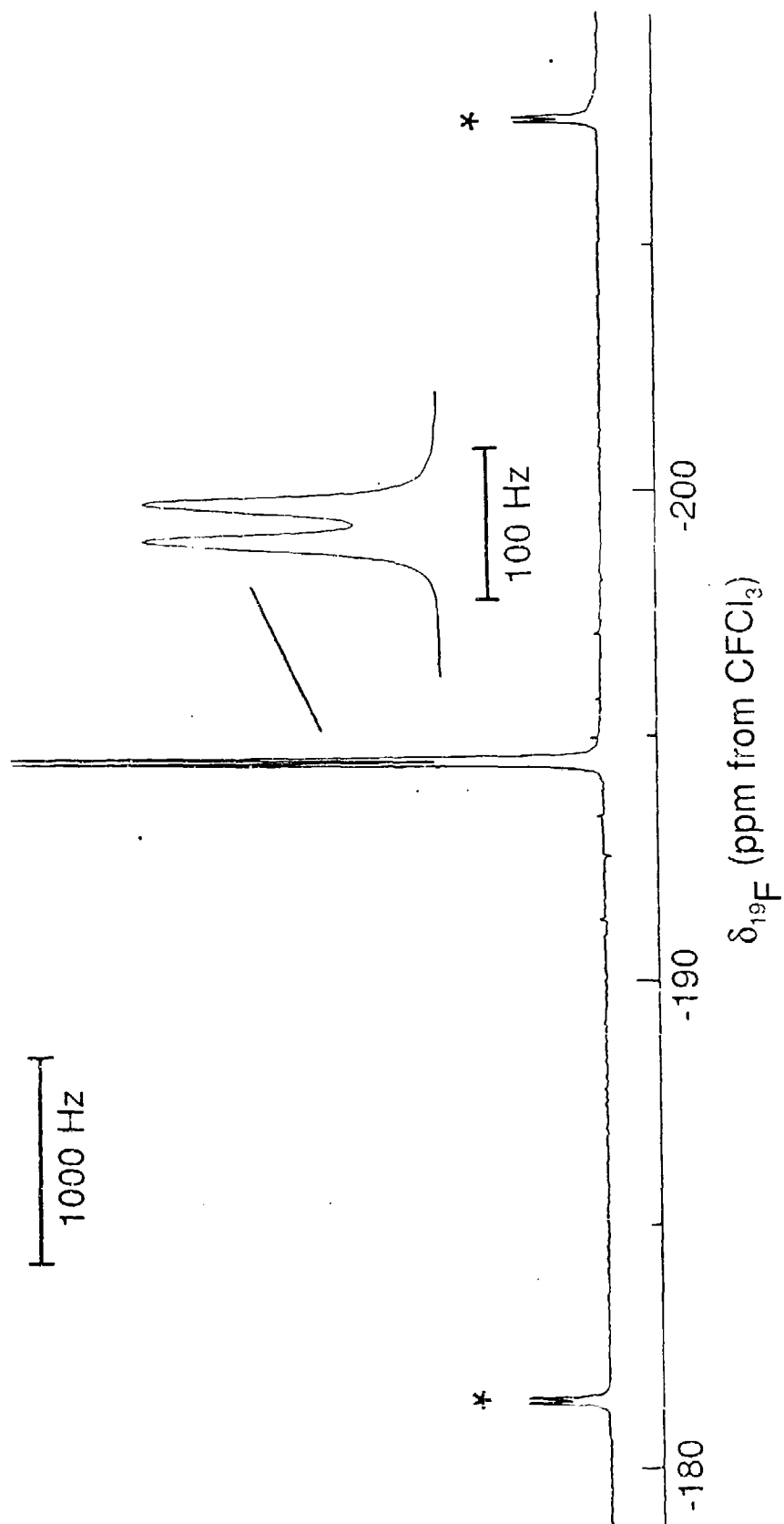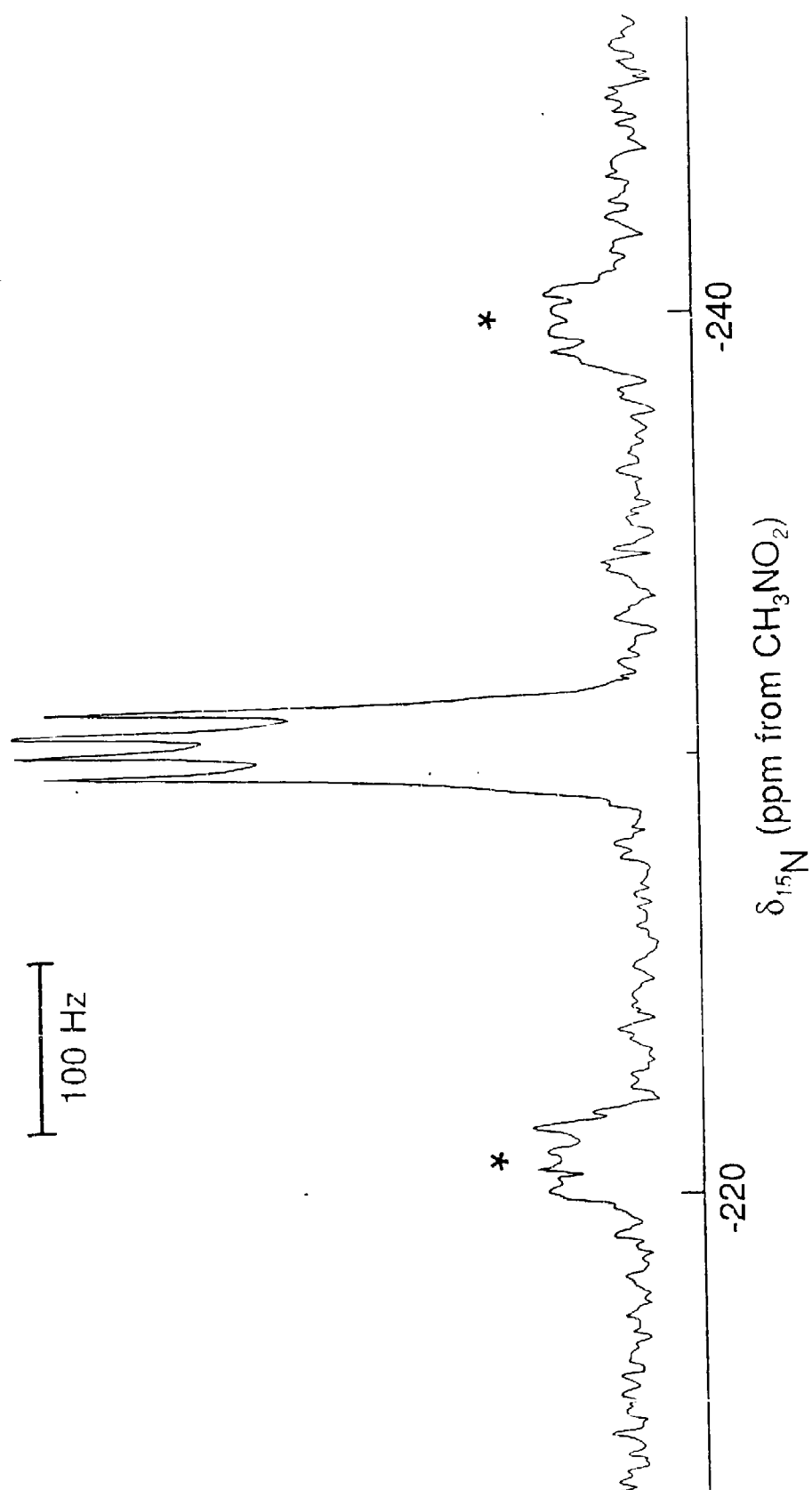
48.   Pure Appl. Chem. 1972, 29, 627; 1976, 45, 217.

$$^{1}\text{H} - {}^{13}\text{C} \equiv {}^{14/15}\text{N} - {}^{129}\text{Xe} - {}^{19}\text{F}$$

$\oplus$

$\delta_{129}Xe$ (ppm from XeOF$_4$)

1000 Hz

a

-1500   -1550   -1600

$\delta_{^{129}Xe}$ (ppm from $XeOF_4$)

1000 Hz

-1550

-1600

b

96

$\delta_{129}Xe$ (ppm from $XeOF_4$)

97

$\delta_{^{19}F}$ (ppm from $CFCl_3$)

100 Hz

1000 Hz

*

*

-180

-190

-200

100 Hz

*

*

$\delta_{^{15}N}$ (ppm from CH_3NO_2)

-240

-220

99

20 Hz

*

*

*

*

δ_{1H} (ppm from $(CH_3)_4Si$)

5.0   4.8   4.6   4.4

100

100 Hz

$\delta_{13}C$ (ppm from $(CH_3)_4Si$)

a

$H\text{-}^{12}C\equiv^{14}N\text{-Xe-F}^+AsF_6^-$

$\nu(^{12}C\equiv^{14}N)$

$\nu(H\text{-}^{12}C)$

$H\text{-}^{12}C\equiv^{15}N\text{-Xe-F}^+AsF_6^-$

$\nu(^{12}C\equiv^{15}N)$

$\nu(H\text{-}^{12}C)$

$H\text{-}^{13}C\equiv^{14}N\text{-Xe-F}^+AsF_6^-$

$\nu(^{13}C\equiv^{14}N)$

$\nu(H\text{-}^{13}C)$

INTENSITY

3200   3100   2200   2100

$\Delta\nu$, cm^{-1}

103

b

INTENSITY

$\Delta\nu$, cm^{-1}

104

The Fluoro(perfluoropyridine)xenon(II) Cations, C_5F_5N–XeF+ and 4-CF$_3$C$_5$F$_4$N–XeF+; Novel Examples of Xenon as an Aromatic Substituent and of Xenon–Nitrogen Bonding

Adel A. A. Emara and Gary J. Schrobilgen*

Department of Chemistry, McMaster University, Hamilton, Ontario L8S 4M1, Canada

The fluoro(perfluoropyridine)xenon(II) cations, 4-RC$_5$F$_4$N–XeF+ (R = F or CF$_3$), have been observed in HF and BrF$_5$ solutions (stable up to −30 °C) and their AsF$_6$− salts have been isolated from BrF$_5$ solutions; low temperature Raman and [129]Xe, ^{19}F, and [14]N n.m.r. spectroscopic results are consistent with planar cations in which the xenon atom is co-ordinated to the aromatic ring through the lone pair of electrons on the nitrogen.

Compounds containing xenon–nitrogen bonds have only been characterized relatively recently and include the neutral species FXeN(SO$_2$F)$_2$,[1,2] Xe[N(SO$_2$F)$_2$]$_2$,[2,3] and Xe[N-(SO$_2$CF$_3$)$_2$]$_2$,[4] and the cations XeN(SO$_2$F)$_2$+,[5] F[XeN-(SO$_2$F)$_2$]$_2$+,[2,5] and the recently reported series of nitrile cations R'C≡N–XeF+ (R' = H, CH$_3$, CH$_2$F, C$_2$H$_5$, C$_2$F$_5$,

C$_3$F$_7$, C$_6$F$_5$).[6] In this communication we report the synthesis and characterization of two novel xenon–nitrogen bonded cations which, thus far, represent unique examples of noble gas atoms functioning as aromatic ring substituents.

Equimolar amounts of XeF+AsF$_6$− and the perfluoropyridine 4-RC$_5$F$_4$N (R = F or CF$_3$), react in anhydrous HF at −30

Table 1. N.m.r parameters for the 4-RC$_5$F$_4$N–XeF$^+$ (R = F or CF$_3$) cations.[a]

|	Chemical shifts/p.p.m.[b]				Coupling constants/Hz		
	$\delta(^{129}Xe)$	$\delta(^{14}N)$	$\delta(^{19}F)$	$J(F-F)$		$^1J(^{129}Xe-^{19}F)$	$^1J(^{129}Xe-^{14}N)$
C$_5$F$_5$N–XeF$^+$ (HF; –30 °C)[c]	–1871.9	–208	–148.3 F(1)	24.6 F(1)F(2)		5936	236
			–89.7 F(2)	–21.2 F(2)F(2')			
			–158.0 F(3)	17.6 F(2)F(3)			
			–115.4 F(4)	–14.4 F(2')F(3')			
				2.0 F(3)F(3)			
				–19.5 F(3)F(4)			
C$_5$F$_5$N–XeF$^+$ (BrF$_5$; –30 °C)[c]	–1922.5		–139.6 F(1)	25.3 F(1)F(2)		5926	c
			–88.0 F(2)	[d]			
			–153.9 F(3)				
			–110.1 F(4)				
4-CF$_3$C$_5$F$_4$N–XeF$^+$ (HF; –15 °C)[c]	–1802.6		–153.8 F(1)	25.8 F(1)F(2)		5977	238
			–88.7 F(2)	[d]			
			–136.2 F(3)				
			–60.9 CF$_3$				
4-CF$_3$C$_5$F$_4$N–XeF$^+$ (BrF$_5$; –50 °C)[c]	–1853.4		–144.6 F(1)	25.8 F(1)F(2)		5963	c
			–86.8 F(2)	–19.9 F(2)F(2)			
			–132.6 F(3)	12.5 F(2)F(2)			
			–59.7 CF$_3$	–19.3 F(2')F(3')			
				–2.7 F(3)F(3)			
				–20.4 F(3)F(CF$_3$)			

[a] Spectra recorded without an external lock (field drift < 1 Hz h^{-1}) at an external field strength B_0 = 5.8719 T using 9 mm o.d FEP sample tubes. The corresponding spectrometer frequencies were 69.563 MHz (^{129}Xe), 18.075 MHz (^{14}N), and 235.361 MHz (^{19}F). [b] Spectra were referenced with respect to neat liquid external standards at 24 °C: XeOF$_4$ (^{129}Xe), CH$_3$NO$_2$ (^{14}N), and CFCl$_3$ (^{19}F). A positive chemical shift denotes a resonance occurring to high frequency of the reference compound. [c] For equilibrium reaction mixtures of XeF$_2$ and 4-RC$_5$F$_4$NH$^+$AsF$_6^-$ the following ^{19}F environments were also observed: (i) R = F, –30 °C, HF solvent: HF (–196.0 p.p.m.), XeF$_2$ [–200 p.p.m., $w_{1/2}$ 435 Hz, $^1J(^{129}$Xe–^{19}F) 5660 Hz]. AsF$_6^-$ [–69.4 p.p.m., broad saddle-shaped resonance arising from partial quadrupole collapse of $^1J(^{75}$As–^{19}F)], and C$_5$F$_5$NH$^+$ [F(2) –100.2 p.p.m., F(3) –158.6 p.p.m., F(4) –108.6 p.p.m.]; (ii) R = F, –30 °C, BrF$_5$ solvent: HF (–199.4 p.p.m., $w_{1/2}$ 240 Hz), BrF$_5$ (quintet, 273.7 p.p.m.; doublet, 136.5 p.p.m.; ^2J(FF) 76.5 Hz), XeF$_2$ [δ (^{19}F) –187.4 p.p.m., $\delta(^{129}$Xe) –1629.2 p.p.m, $^1J(^{129}$Xe–^{19}F) 5643 Hz], AsF$_6^-$ (–64.0 p.p.m., $w_{1/2}$ 1780 Hz), C$_5$F$_5$NH$^+$ [F(2) –96.8 p.p.m., F(3) –154.5 p.p.m., F(4) –103.2 p.p.m.]; (iii) R = CF$_3$, –20 °C, HF solvent: HF (–196.6 p.p.m.), AsF$_6^-$ [–68.9 p.p.m., broad saddle-shaped resonance arising from partial quadrupole collapse of $^1J(^{75}$As–^{19}F)], 4-CF$_3$C$_5$F$_4$NH$^+$ [F(2) –98.5 p.p.m., F(3) –136.1 p.p.m., CF$_3$ –60.7 p.p.m.]; (iv) R = CF$_3$, –50 °C, BrF$_5$ solvent: HF (–193.1 p.p.m., $w_{1/2}$ 150 Hz), BrF$_5$ (quintet, 273.2 p.p.m.; doublet, 135.8 p.p.m.; ^2J(F–F) 76.4 Hz], XeF$_2$ [$\delta(^{19}$F) –188.2 p.p.m., $\delta(^{129}$Xe) –1589.0 p.p.m., $^1J(^{129}$Xe–^{19}F) 5654 Hz], AsF$_6^-$ (–63.7 p.p.m., $w_{1/2}$ 980 Hz), 4-CF$_3$C$_5$F$_4$NH$^+$ [F(2) –86.2 p.p.m., F(3) –131.8 p.p.m., CF$_3$ –59.5 p.p.m.]. [d] Although observed, intra-ring F–F couplings are not reported. [c] The spin-spin coupling $^1J(^{129}$Xe–^{14}N) is quadrupole collapsed in BrF$_5$ solvent at –30 and –50 °C.
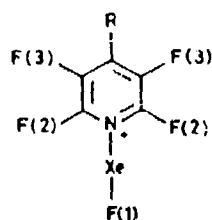

(6; R = F(4) or CF$_3$)

to –20 °C according to equation (1) and equilibria (2) and (3) to give the novel Xe–N bonded cations, 4-RC$_5$F$_4$N–XeF$^+$, as the AsF$_6^-$ salts in solution. At –30 °C these solutions consisted of equilibrium mixtures of XeF$_2$, 4-RC$_5$F$_4$-

$$4\text{-RC}_5\text{F}_4\text{N} + (n + 1)\text{HF} \rightarrow 4\text{-RC}_5\text{F}_4\text{NH}^+(\text{HF})_n^- \quad (1)$$
$$\quad (1) \qquad\qquad (2) \qquad\qquad\qquad (3)$$

$$(3) + \text{XeF}^+\text{AsF}_6^- \rightleftharpoons 4\text{-RC}_5\text{F}_4\text{NH}^+\text{AsF}_6^- + \text{XeF}_2 + n(2) \quad (2)$$
$$\qquad\qquad (4) \qquad\qquad (5)$$

$$(4) + (5) \rightleftharpoons 4\text{-RC}_5\text{F}_4\text{N–XeF}^+\text{AsF}_6^- + (2) \quad (3)$$
$$\qquad (6)$$

NH$^+$AsF$_6^-$, and 4-RC$_5$F$_4$N–XeF$^+$AsF$_6^-$ (determined by n.m.r. spectroscopy) (Table 1). Removal of HF solvent by pumping at –50 °C resulted in white solids which Raman spectroscopy at –196 °C also showed to be mixtures of 4-RC$_5$F$_4$N–XeF$^+$AsF$_6^-$, XeF$_2$, and 4-RC$_5$F$_4$NH$^+$AsF$_6^-$.

An alternative approach which lead to isolation of the Xe–N bonded cations allowed stoicheiometric amounts of XeF$_2$ and the perfluoropyridinium cations, as their AsF$_6^-$ salts, to react in HF and BrF$_5$ solvents at –30 °C according to equilibrium (3). The equilibria in both solvents were again monitored by ^{129}Xe, ^{19}F, and ^{14}N n.m.r. spectroscopy. In BrF$_5$, formation of 4-RC$_5$F$_4$N–XeF$^+$AsF$_6^-$ was more strongly favoured than in HF solvent; the equilibrium ratio [4-RC$_5$F$_4$NXeF$^+$]/[4-RC$_5$F$_4$NH$^+$] being 0.25 and 2.1 in HF and BrF$_5$ solvents, respectively, at –30 °C for R = F and 3.7 for R = CF$_3$ in BrF$_5$ at –50 °C [K_F = 4.5 at –30 °C and K_{CF_3} = 13.6 at –50 °C in BrF$_5$ for equilibrium (3)]. Consequently, removal of BrF$_5$ solvent under vacuum at –30 °C yielded white solids corresponding to 4-RC$_5$F$_4$N–XeF$^+$AsF$_6^-$ salts.

The Raman and n.m.r. spectroscopic findings confirm the formulations of the compounds isolated from BrF$_5$ solution as AsF$_6^-$ salts possessing cation structures in which a xenon atom is co-ordinated to the aromatic perfluoropyridine ring (6), thus providing the first examples of compounds in which the
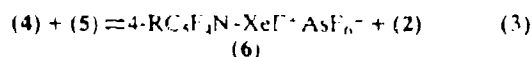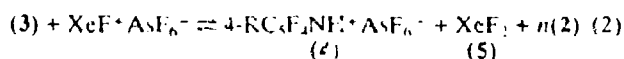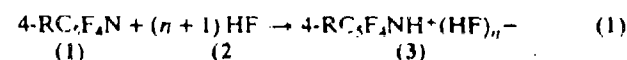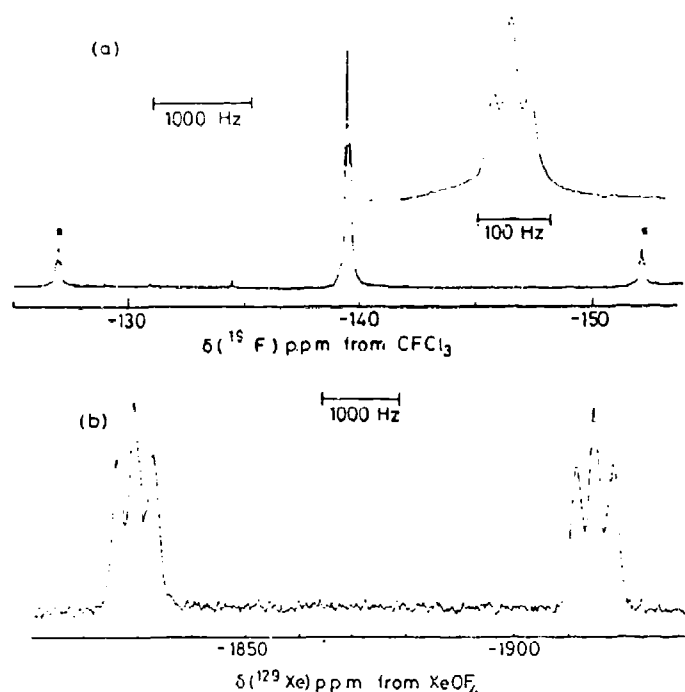
Figure 1. N.m.r. spectra of the $C_5F_5N-XeF^+$ cation at $-30\,^{\circ}C$: (a) the ^{19}F n.m.r. spectrum (235.361 MHz; solvent BrF_5) depicting the fluorine-on-xenon(II) region of the spectrum and ^{129}Xe satellites (denoted by asterisks) arising from spin–spin coupling of the terminal fluorine-on-xenon to natural abundance ^{129}Xe, $^1J(^{129}Xe-^{19}F)$ ($I = \frac{1}{2}$; 26.4%), the 1,2:1 triplet fine structure on the central line and the satellites is assigned to $^3J[F(1)-F(2)]$; (b) the ^{129}Xe n.m.r. spectrum (69.563 MHz; solvent HF) depicting the doublet arising from $^1J(^{129}Xe-^{19}F)$ and partially quadrupole collapsed 1:1:1 triplets arising from xenon directly bonded to the nitrogen of the pyridine ring, $^1J(^{129}Xe-^{14}N)$.

noble gas atoms serve as aromatic substituents. In addition to lines arising from the AsF_6^- anions [v_1 (a_{1g}) 677, 680 cm^{-1}; $v_2(e_g)$ 577 cm^{-1}; $v_5(t_{2g})$ 375 cm^{-1}], several key frequencies have been assigned. The Xe–N stretching frequencies can only be tentatively assigned to weak bands at 367(2) (R = F) and 367(12) (R = CF_3) cm^{-1} [cf. 422 cm^{-1} in $FXeN(SO_2F)_2$] while the F–Xe–N bends are assigned to moderately strong bands at 158(13) (R = F) and 162(13) (R = CF_3) cm^{-1}. The intense bands in the Raman spectra of the salts occur at 528(100) (R = F) and 524(100) cm^{-1} (R = CF_3) and are assigned to Xe–F stretching frequencies. These frequencies are higher than that of $FXe-N(SO_2F)_2$ (506 cm^{-1}) and lower than in the recently reported nitrile cations, $R'C\equiv N-XeF^+$ (564 and 565 cm^{-1} for R' = H and Me, respectively), reflecting the intermediate base strengths of $4-RC_5F_4N$ with respect to the Lewis acid XeF^+. The latter point is corroborated by comparison of the ^{129}Xe and ^{19}F chemical shifts of the Xe–F groups within a well established trend in which $\delta(^{19}F)$ increases in frequency with increasing covalency of the Xe–ligand bond, while $\delta(^{129}Xe)$ is observed to decrease. The nuclear spin–spin couplings $^1J(^{129}Xe-^{19}F)$ (doublet), $^1J(^{129}Xe-^{14}N)$ (partially quadrupole collapsed 1:1:1 triplet), and $^4J(F_1-F_2)$ (1:2:1 triplet) also support the proposed cation structures in solution (Figure 1). Owing to the higher viscosity of BrF_5, $^1J(^{129}Xe-^{14}N)$ is quadrupole collapsed at -50 and $-30\,^{\circ}C$ but is observed in HF at -15 and $-30\,^{\circ}C$. The magnitude of $^1J(^{129}Xe-^{14}N)$ is consistent with a one-bond $^{129}Xe-^{14}N$ coupling. On the assumption that the Fermi contact contribution to the $^{129}Xe-^{14}N$ spin–spin coupling is dominant, a comparison of the reduced coupling constants, $^1K(Xe-N)_1 = 0.983 \times 10^{22}$ and $^1K(Xe-N)_{CF_3} = 0.991 \times 10^{22}$ N A^{-2} m^{-3}, with those in

which the nitrogen atom σ-bonded to xenon is sp hybridized ($R'C\equiv N-XeF^+$ 1.297—1.393 $\times$ 10^{22} N A^{-2} m^{-3}) and sp^2 hybridized [$FXe-N(SO_2F)_2$ 0.913 $\times$ 10^{22}] is also consistent with bonding between the sp^2 hybridized nitrogens of the perfluoropyridines and xenon.

Other pyridine derivatives and nitrogen bases are currently being investigated as potential electron-pair donors towards noble gas cations. X-ray crystallographic studies of the fluoro(perfluoropyridine)xenon(II) cations are also underway in this laboratory.

References

1 J. F. Sawyer, G. J. Schrobilgen, and S. J. Sutherland. *Inorg. Chem.*, 1982, **21**, 4064.
2 D. D. DesMarteau, R. D. LeBlond, S. F. Hossian, and D. Nothe, *J. Am. Chem. Soc.*, 1981, **103**, 7734.
3 G. A. Schumacher and G. J. Schrobilgen. *Inorg. Chem.*, 1983, **22**, 2178.
4 J. Foropoulos and D. D. DesMarteau, *J. Am. Chem. Soc.*, 1982, **104**, 4260.
5 R. Faggiani, D. K. Kennepohl, C. J. L. Lock, and G. J. Schrobilgen. *Inorg. Chem.*, 1986, **25**, 563
6 A. A. A. Emara and G. J. Schrobilgen, *J. Chem. Soc., Chem. Commun.*, 1987, 1644

SECTION I. Trifluoro-s-triazine Adducts of XeF⁺ AND XeOTeF₅⁺; Novel Xe-N Bonding

INTRODUCTION

General Criteria Required for Ligands to Bond to Xenon

Numerous attempted preparations and successful syntheses of Xe-O compounds have provided sufficient data for the formulation of several general guidelines for selecting a ligand that may be suitable for bonding to xenon. Ligands exhibiting the following criteria generally satisfy the condition that the ligand must be capable of withstanding the high electron affinity of xenon in its positive formal oxidation states:

1. the ligand should form a moderate to strong monoprotic acid,

2. each ligand has a high effective group electronegativity,

3. each ligand exists as a stable anion in alkali metal salts,

4. each group forms a positive chlorine derivative.

For example, $FXeOTeF_5$ and $Xe(OTeF_5)_2$ and the precursor acid, $HOTeF_5$, and its alkali metal salts M^+OTeF_5 and the chlorine derivative $ClOTeF_5$ are known.

Xenon Nitrogen Chemistry

It was not until 1974, that the first xenon-nitrogen compound was prepared.[1] The general approach was to use a ligand satisfying the criteria listed above. To this end, a nitrogen ligand made highly

electronegative by substitution with electron withdrawing SO_2F groups was selected. The reaction was shown to proceed according to equation (1).

$$CF_2Cl_2$$
$$XeF_2 + HN(SO_2F)_2 \longrightarrow F-Xe-N(SO_2F)_2 + HF \quad (1)$$
$$0°C, 4 \text{ days}$$
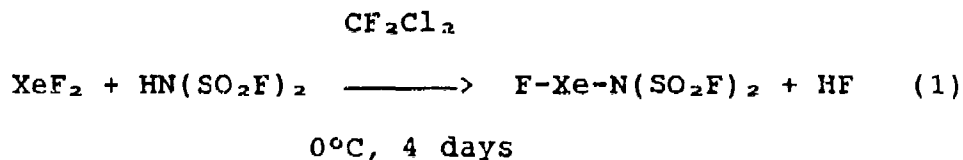
Owing to the instability of the product, the imidodisulfurly derivative was not fully characterized until 1982 when definitive evidence for Xe-N bonding was obtained in the form of the low- temperature crystal structure[2] (Figure 1). Several other compounds containing Xe-N-$(SO_2X)_2$ (X = F, CF_3) were also prepared (Table 1), however, the aforementioned method was limited by the number of suitable electron withdrawing groups which could be attached to nitrogen to provide a sufficiently electronegative nitrogen ligand.

Lewis Acid Behavior of XeF⁺ and KrF⁺

In 1987, the discovery that XeF⁺ had Lewis acid properties, and, as such, would undergo reactions with nitrogen bases to form adducts,[7] significantly broadened the scope of xenon-nitrogen chemistry, and noble-gas chemistry in general (Annual Report, May 1, 1987 - April 30, 1988 and references therein). In these acid-base reactions, XeF⁺ functions as an electron-pair acceptor towards the lone pair on the nitrogen base of specific ligands, provided the ligand can withstand oxidation by XeF⁺. The electron affinity of XeF⁺ is

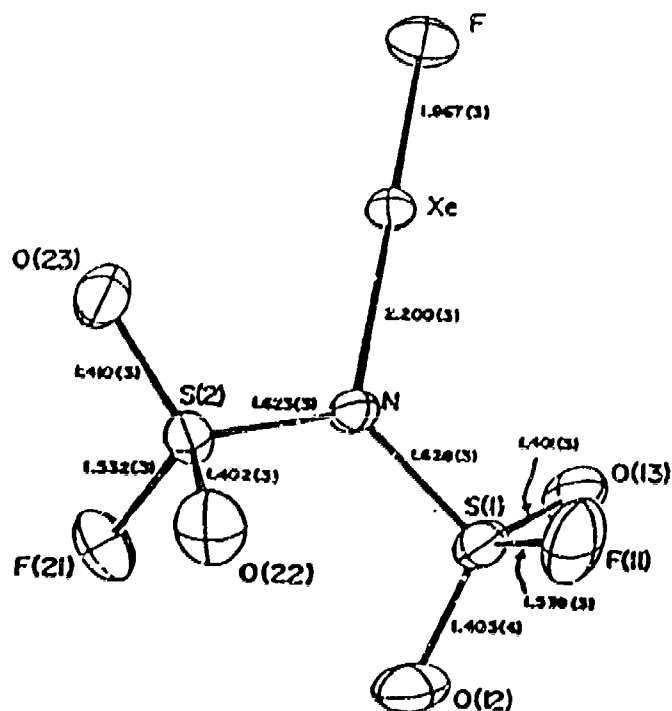Figure 1. Crystal structure of F-Xe-N(SO₂F)₂.

110

Table 1.

Xe-N Derivatives of the $N(SO_2X)_2$ Group $(X = F, CF_3)$

Compounds	Reference
$FXeN(SO_2F)_2$	2
$[XeN(SO_2F)_2]^+AsF_6^-$,	3
$[XeN(SO_2F)_2]^+SbF_{16}^-$	3
$F[XeN(SO_2F)_2]_2^+AsF_6^-$	3,4
$Xe[N(SO_2F)_2]_2$	5
$Xe[N(SO_2CF_3)_2]_2$	6

Table 2.

Ionization Potentials of Some Nitrogen Containing Ligands

Compound	1st Ionization Potential (eV)	Reference
$CF_3C\equiv N$	13.90	9
$HC\equiv N$	13.59	10
$CH_2FC\equiv N$	13.00 ± 0.1	11
$CF_3C\equiv N$	12.60	9
$CHF_2C\equiv N$	12.40	12
$CH_3C\equiv N$	12.19 ± 0.005	13
$s-C_3F_3N_3$	11.50	14
$CH_3N\equiv C$	11.32	15
C_5F_5N	10.08	16

estimated to be 10.9 eV,[8] accordingly ligands are required to have first ionization potentials exceeding 11 eV if they are to be capable of forming stable adducts. Examination of the known first adiabatic ionization potentials of several nitrogen containing ligands provides insight into which ligands are likely to be suitable candidates for adduct formation (Table 2).

The method of adduct preparation is generally straight forward and involves the interaction of stoichiometric amounts of $XeF^+AsF_6^-$ and a suitable organic nitrogen base in anhydrous HF solvent or the interaction of a stoichiometric amount of a protonated base salt with XeF_2 in HF or BrF_5 solvents. Brief warming to -30 to -20°C is generally sufficient to effect reaction and dissolution in the solvent without significant decomposition. Vacuum pumping at -50 to -30°C, resulted in the isolation of white solids, many of which are not stable above -10°C. Using this approach a large number of new xenon-nitrogen compounds were recently prepared, including adducts with per-fluoroalkylnitrile cations[7] (Figure 2) and perfluoropyridine cations[17] (Figure 3). Solid samples of a large number of these compounds have been characterized by low-temperature laser Raman spectroscopy and solutions of the adducts in HF and/or BrF_5 have been examined by ^{19}F, [129]Xe, and ^{14}N NMR spectroscopy.

Another cationic noble-gas species which was believed to exhibit Lewis acid properties was KrF^+ which has an estimated electron affinity of 13.2 eV.[32] Consequently, it was desirable to test the hypothesis by allowing KrF^+ to react with a suitable oxidatively resistant ligand using the synthetic methods outlined above. Unfortunately, KrF^+ proved to be more difficult to work with owing to the fact that its salts are unstable near room temperature. In

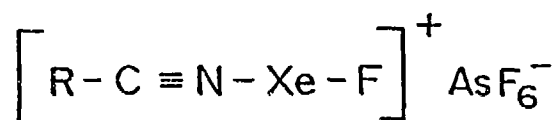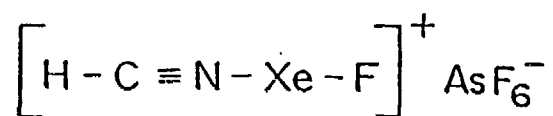$$\left[H-C \equiv N-Xe-F \right]^{+} AsF_6^{-}$$

$$\left[R-C \equiv N-Xe-F \right]^{+} AsF_6^{-}$$

Figure 2.   Hydrogen cyanide, alkylnitrile and perfluoroalkylnitrile
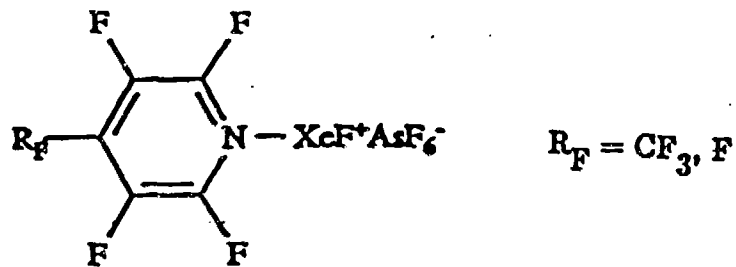adducts of XeF$^+$AsF$_6$$^-$.

$R_F = CF_3, F$

Figure 3. Perfluoropyridine adducts of XeF$^+$AsF$_6$$^-$.

addition, KrF^+ undergoes autocatalytic redox reactions in HF solvent. In view of these properties, the interaction of neutral KrF_2 with $HC\equiv NH^+AsF_6^-$ (1st IP of $HC\equiv N$, 13.59 eV) in BrF_5 was attempted. The reaction proceeded according to equation (2) resulting in the formation of $HC\equiv N-KrF^+AsF_6^-$, the first species containing a krypton-nitrogen bond.[18]

$$KrF_2 + HC\equiv NH+AsF_6^- \longrightarrow [HC\equiv N-Kr-F]^+AsF_6^- + HF \qquad (2)$$
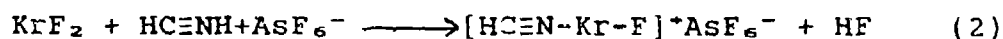
The Trifluoro-s-Triazine Adduct of XeF^+

The first ionization potential of trifluoro-s-triazine, s-$C_3F_3N_3$, (11.50 eV) indicated that it should resist oxidation by XeF^+ and form a stable Xe-N adduct (Table 2). The synthesis of the trifluoro-s-triazine adduct of XeF^+ was consequently attempted using HF as the solvent at -10°C. The presence of fluorinated ring byproducts from this reaction demonstrated that trifluoro-s-triazine is subject to solvolysis in HF, and attempts to prepare the compound in other solvents also proved unsuccessful. Accordingly, the direct reaction of solid $XeF^+AsF_6^-$ with liquid trifluoro-s-triazine in absence of solvent was attempted. The synthesis of s-$C_3F_3N_2N-XeF^+$ has recently been reported,[19] (see Section II) and is formed in the reaction of s-$C_3F_3N_3$ with $XeF^+AsF_6^-$ according to equation (3)

$$(3)$$

114
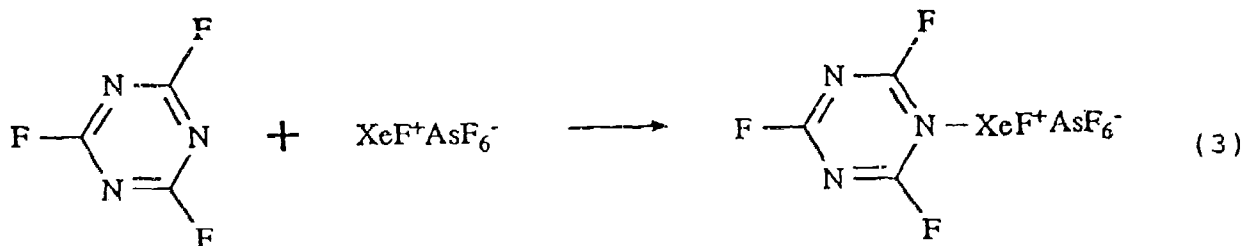
The compound was characterized by low-temperature laser Raman spectroscopy, ^{19}F and [129]Xe NMR spectroscopy.

Unlike other Xe-N compounds, the trifluoro-s-triazine adduct exhibited remarkable stability at room temperature. In addition, the solid XeF^+ appeared to react with a second mole of trifluoro-s-triazine during the reaction, a feature unique to this system and the subject of a portion of the present report.

Purpose and Scope of Present Work

In the present work we have undertaken to prepare noble-gas compounds containing novel Xe-N bonds. In general electronegative nitrogen organic bases with first ionization potentials greater than the electron affinity of XeF^+ (10.9 eV)[18] have proved to be suitable ligands for adduct formation. Trifluoro-s-triazine fulfills this criterion and exhibits resistance to oxidation. Moreover, the XeF^+ adduct of $s-C_3F_3N_3$ has demonstrated remarkable stability at room temperature. For these reasons $s-C_3F_3N_3$ was selected as the ligand to test the possibility of forming new Xe-N compounds from other suspected xenon Lewis acids, namely XeF_3^+ and $XeOTeF_5^+$.

In addition, the potential binding of a second mole of trifluoro-s-triazine to the xenon Lewis acid, XeF^+, was examined using low-temperature laser Raman spectroscopy.

EXPERIMENTAL

Apparatus and Materials

The majority of compounds prepared and used in this work are air and moisture sensitive, accordingly manipulations were carried out under anhydrous conditions. Non-volatile air-sensitive solids, $XeF^+AsF_6^-$, $XeOTeF_5^+AsF_6$, $XeF_3^+SbF_6^-$, $Xe(OTeF_5)_2$, $Sb(OTeF_5)_3$, $XeOTeF_5^+Sb(OTeF_5)_6^-$ were weighed and transferred to reaction vessels in a dry box (Vacuum Atmospheres Model DLX; <0.01 ppm H_2O and <0.1 ppm O2). Volatile reactants and solvents were transferred using glass or metal vacuum lines.

Preparation and Purification of Starting Materials

Solvents. All solvents were transferred on a metal vacuum line through all fluoroplastic connections. The former was constructed of 316 stainless steel, nickel, Teflon and Kel-F.

Sulfurylchlorofluoride, SO_2ClF (Columbia Organic Chemicals), was purified by distillation onto SbF_5 to remove SO_2 contaminate, as previously described.[20] Subsequently the solvent was distilled (from SbF_5), into a glass storage bulb, equipped with a Rota-Flo valve, containing dry KF to remove residual SbF_5 and HF. The purified solvent was used directly from this vessel.

Bromine pentafluoride, BrF_5, (Ozark Mahoning) was purified as described earlier[21] and stored over dry KF in a 3/4" Kel-F storage vessel equipped with a Kel-F valve.

Anhydrous hydrogen fluoride, HF, (Harshaw Chemical Co.) was

purified by treatment with.5 atmospheres of F_2 gas in a nickel can for a period of 1 month, converting residual water to HF and O_2 gas. After the specified time period, the excess F_2 gas was removed under vacuum at -196°C. The anhydrous HF was subsequently warmed to room temperature and vacuum distilled into a dry Kel-F storage vessel equipped with a Kel-F valve and stored at room temperature until used.

Trifluoro-s-Triazine. Trifluoro-s-triazine, $s-C_3F_3N_3$ (Armageddon Chemicals, Durham, N.C.) was treated prior to use, by transferring it to a glass bulb containing anhydrous CaH_2 powder (British Drug Houses) in a fume hood. Trifluoro-s-triazine was transferred on a glass vacuum line equipped with J. Young 6mm glass/FEP valves (Figure 4) using a glass vacuum distillation apparatus equipped with J. Young 4mm glass/FEP valves (Figure 5). To avoid contamination of samples with CaH_2, trifluoro-s-triazine was always transferred to an intermediate preweighed evacuated glass bulb prior use in syntheses.

Xenon Cations Salts, $Xe(OTeF_5)_2$ and $Sb(OTeF_5)_3$. Preparations of $XeF^+AsF_6^-$,[22] $XeF_3^+SbF_6^-$,[23] $XeOTeF+AsF_6^-$,[24] $Xe(OTeF_5)_2$[25] and $Sb(OTeF_5)_3$[26] are described elsewhere.

to pump

$\frac{1}{4}$"

20 cm

A

B

C
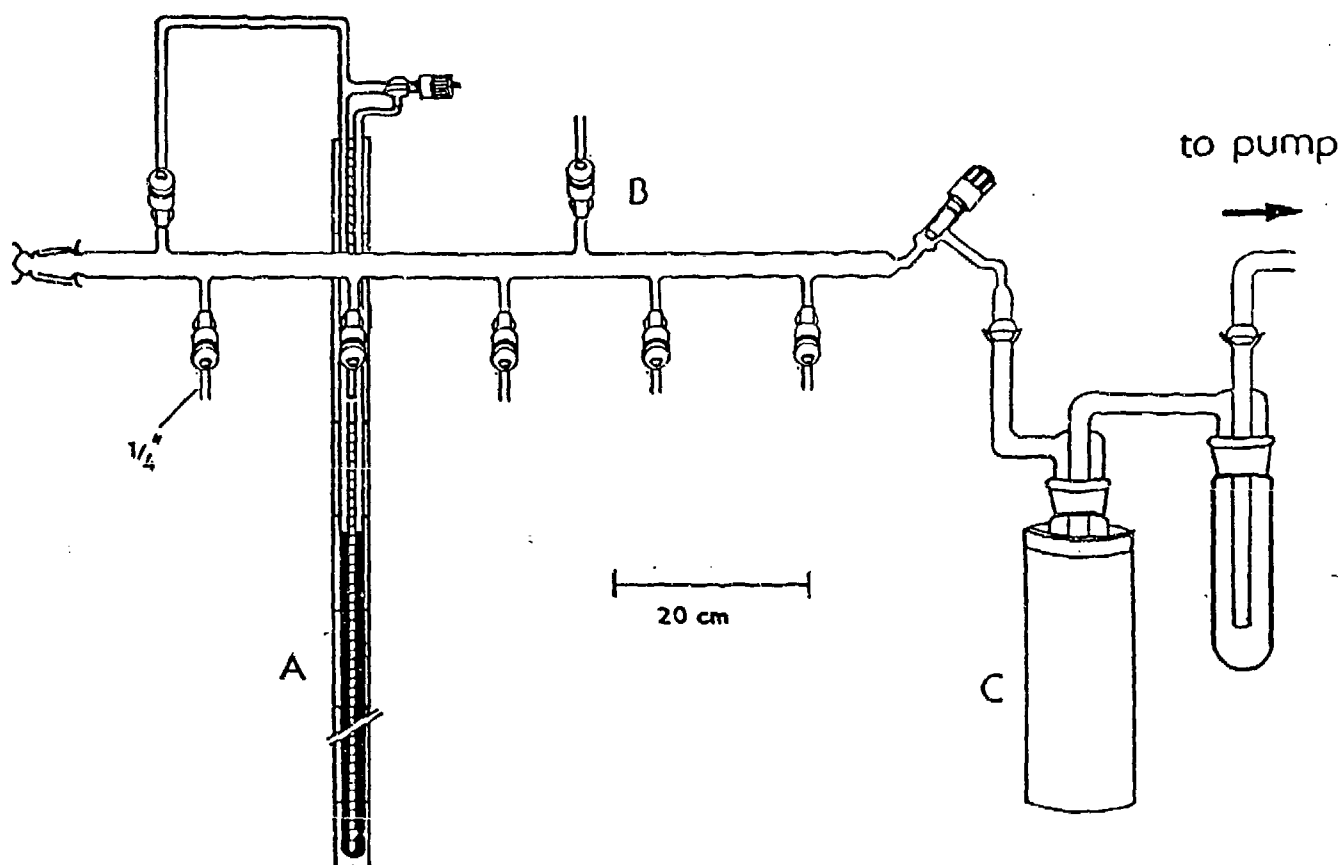
Figure 5.   Glass grease-free vacuum line; (A) manometer, (B) dry
   nitrogen inlet, (C) liquid nitrogen trap.

118

s-$C_3F_3N_2$N-XeF$^+$AsF$_6^-$.   In a typical preparation 0.850 g (6.294 mmol) of s-$C_3F_3N_3$ was transferred to an evacuated glass bulb using a glass vacuum distillation apparatus (Figure 6a) attached to a glass vacuum line. XeF$^+$AsF$_6^-$, (0.281 g, 1.852 mmol), was weighed into a 1/4" o.d FEP reaction vessel equipped with a Kel-F valve in a dry box. Trifluoro-s-triazine was vacuum distilled onto the solid at -196°C (Figure 6b).   The sample was allowed to warm to room temperature and left to react for 2 hrs. with periodic agitation to effect even distribution of the liquid throughout the solid.   Reaction was generally apparent within 20 min. of mixing at room temperature, resulting in the formation of a fine white solid suspended in excess trifluoro-s-triazine. Upon completion of the reaction, the sample was pumped under vacuum at room temperature for 40 min. to remove excess s-$C_3F_3N_3$.   The yield was 0.8489 g (96.7%) and the product was stable indefinitely at room temperature.   A Raman sample was prepared according to the methods described later in this section, as were solutions of the product in HF and BrF$_5$ for examination by ^{19}F NMR and ^{129}Xe NMR spectroscopy.

Preparation of the Higher Adducts x   s-$C_3F_3N_3$:   XeF$^+$AsF$_6^-$ (x > 1). In typical preparations of the title compounds, the weight of s-$C_3F_3N_3$ required for the desired stoichiometry was vacuum distilled into an evacuated glass bulb. The required amount of XeF$^+$AsF$_6^-$ was
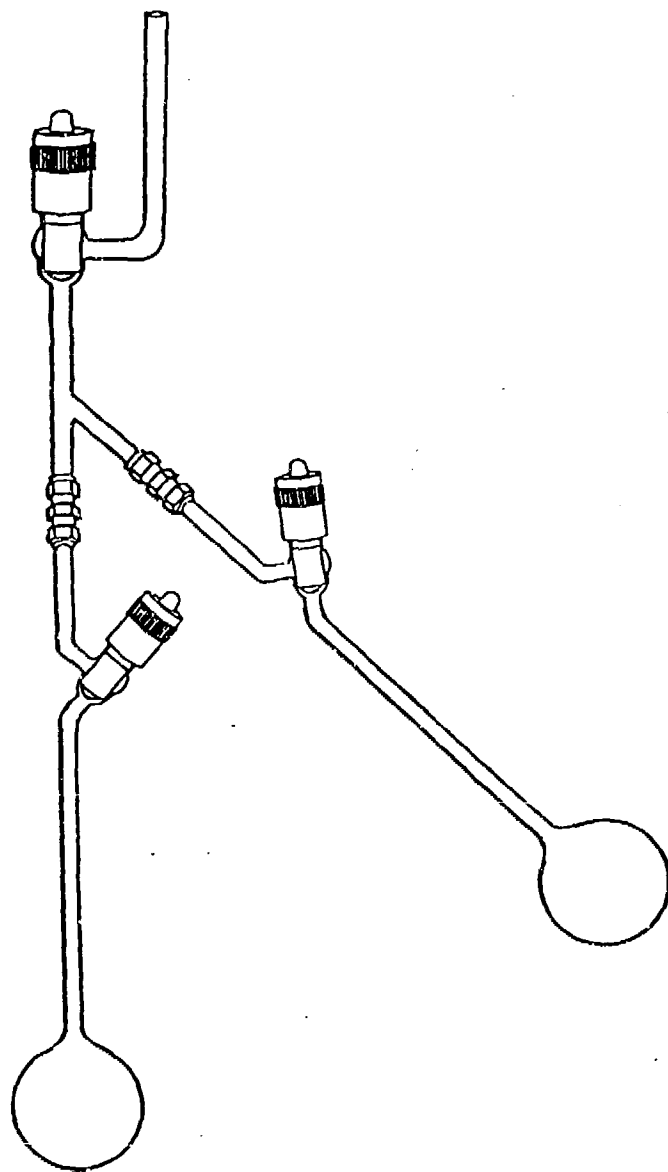
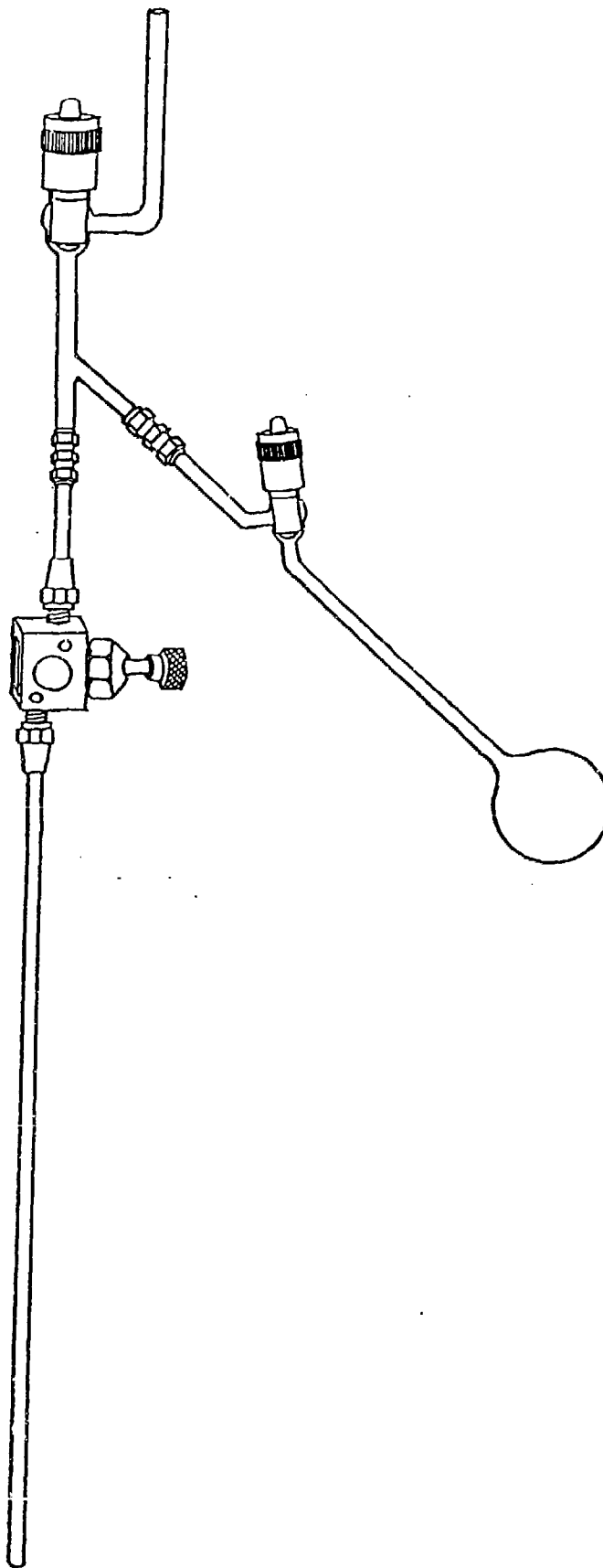Figure 6a. Vacuum distillation apparatus for purification of
s-$C_3F_3N_3$.

Figure 6b. Glass vacuum distillation apparatus for the preparation of
trifluoro-s-triazine adducts of XeF$^+$ and XeOTeF$_5^+$.

ubsequently weighed into a 1/4" o.d. FEP tube in a dry box. Trifluoro-s-triazine was distilled onto the solid and the reaction was allowed to proceed for 2 hrs. The amounts of $XeF^+AsF_6^-$ and $s-C_3F_3N_3$ used in each reaction as well as the appearance of the mixture after 2 hrs. are listed in Table 3.

Upon completion of the reaction, the reaction tube was heat sealed under vacuum at -196°C and subsequently examined by low-temperature Raman spectroscopy.

Preparation of $s-C_3F_3N_2N-XeOTeF_5^+AsF_6^-$. The title compound was prepared from $XeOTeF_5^+AsF_6^-$ according to equation (4).

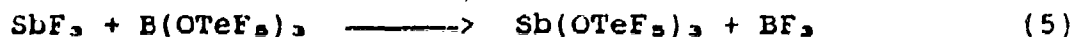$$XeOTeF_5^+AsF_6^- + s-C_3F_3N_3 \longrightarrow s-C_3F_3N_2N-XeOTeF_5^+AsF_6^- \qquad (4)$$
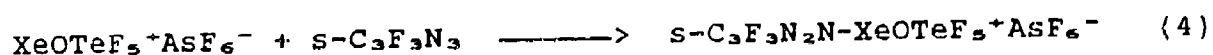
Solid $XeOTeF_5^+AsF_6^-$ (0.3379 g, 0.6047 mmol) was weighed into a 1/4" FEP o.d. tube in a dry box and excess $s-C_3F_3N_3$ (0.5686 g, 4.212 mmol) was distilled into an evacuated glass bulb on a glass vacuum line. Trifluoro-s-triazine was distilled onto solid $XeOTeF_5^+AsF_6^-$ and the mixture was warmed to -10°C. A color change from yellow to off-white was immediate and the reaction was allowed to proceed for an additional 10 min. at -10°C and 5 min. at 0°C. The mixture was subsequently pumped under vacuum at room temperature for 20 min. to remove excess $s-C_3F_3N_3$. The product was an extremely fine white solid which was stable at room temperature. The yield was 98.7% based on a 1:1 combining for $XeOTeF_5^+AsF6$ and $s-C_3F_3N_3$. Solid samples for Raman

Table 3. Preparation of the adducts, x s-$C_3F_3N_3$: $XeF^+AsF_6^-$; amounts of reagents and appearance of products.

x	s-$C_3F_3N_3$ (g)	s-$C_3F_3N_3$ (mmol)	$XeF^+AsF_6^-$ (g)	$XeF^+AsF_6^-$ (mmol)	Appearance of Products
1.243	0.2834	2.097	0.5724	1.687	dry white solid
1.497	0.3374	2.498	0.5649	1.665	dry white solid
2.317	0.4460	3.303	0.4833	1.425	dry white solid
3.007	0.3669	2.717	0.3052	0.8998	dry white solid
4.951	0.6662	4.933	0.3880	0.9646	suspension of white solid in liquid s-$C_3F_3N_3$

spectroscopy, and ^{19}F NMR and ^{129}Xe NMR samples in BrF_5 solvent were prepared as described later in this section.

Preparation of $XeOTeF_5^+Sb(OTeF_5)_6^-$. The title compound was prepared by the following series of reactions:

$$SbF_3 + B(OTeF_5)_3 \longrightarrow Sb(OTeF_5)_3 + BF_3 \qquad (5)$$

$$3XeF_2 + 2B(OTeF_5)_3 \longrightarrow 3Xe(OTeF_5)_2 + 2BF_3 \qquad (6)$$

$$2Xe(OTeF_5)_2 + Sb(OTeF_5)_3 \longrightarrow XeOTeF_5^+(SbOTeF5)6- + Xe \qquad (7)$$
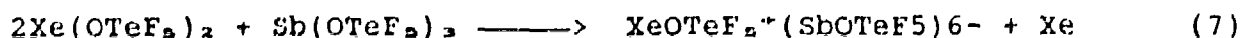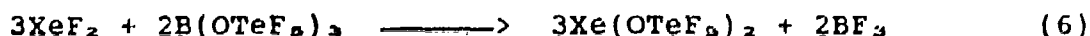
$Xe(OTeF_5)_2$ (3.409 g, 5.601 mmol) and $Sb(OTeF_5)_3$ (2.315 g, 2.763 mmol) were weighed in a dry box, then combined in a 1/2" o.d. FEP tube equipped with a Kel-F valve and maintained at $-196°C$. The tube was transferred to a metal vacuum line where SO_2ClF was distilled onto the cold solids. The mixture was slowly warmed from $-40°C$ to $-10°C$. However, the reaction was slow, consequently the temperature was raised to $0°C$ resulting in the generation of a bright orange solution and steady evolution of xenon gas. The evolved xenon gas was bled off periodically, and the reaction deemed to be complete when xenon evolution had ceased. Upon completion of the reaction, the mixture was pumped under vacuum at $0°C$ until a pale orange powder was obtained, then further pumped at room temperature for an additional hr. The yield of the product was 96.3%. A solid Raman sample, and solutions of the product dissolved in SO_2ClF for examination by ^{19}F NMR, were prepared by methods described later in this section.

Preparation of s-C$_3$F$_3$N$_2$N-XeOTeF$_5$$^+$Sb(OTeF$_5$)$_6$$^-$.   The title compound was prepared from XeOTeF$_5$$^+$Sb(OTeF$_5$)$_6$$^-$ in a manner analogous to the synthesis of s-C$_3$F$_3$N$_2$N-XeOTeF$_5$$^+AsF_6$$^-$.   XeOTeF$_5$$^+$Sb(OTeF$_5$)$_6$$^-$ (0.5197 g, 0.2702 mmol) and excess s-C$_3$F$_3$N$_3$ were combined in a 1/4" o.d. FEP tube equipped with a Kel-F valve and warmed to -20°C at which point an immediate color change from orange/yellow to off-white occurred.   The reaction was allowed to proceed for 5 min. and was then pumped under vacuum at 0°C for 20 min. to remove excess trifluoro-s-triazine.   The product was an extremely fine off-white grey solid, yield 98.6%.   The solid Raman sample as well as a sample dissolved in SO$_2$ClF for ^{19}F NMR spectroscopy were subsequently prepared from this material.

Reaction of XeF$_3$$^+SbF_6$$^-$ with Trifluoro-s-Triazine.   In a typical reaction solid XeF$_3$$^+SbF_6$$^-$, (0.3183 g, 0.7490 mmol) was transferred to a 1/4" o.d. FEP reaction vessel equipped with a 316 stainless steel metal valve (Figure 7) and attached to a glass vacuum distillation apparatus by means of Air Drome AN fittings.   It was necessary to use a metal valve and fittings as solid XeF$_3$$^+SbF_6$$^-$ is a potent oxidant which is known to attack and rupture Kel-F.   Excess trifluoro-s-triazine (0.5276 g, 3.907 mmol) was vacuum distilled onto solid XeF$_3$$^+SbF_6$$^-$ using a glass vacuum line,
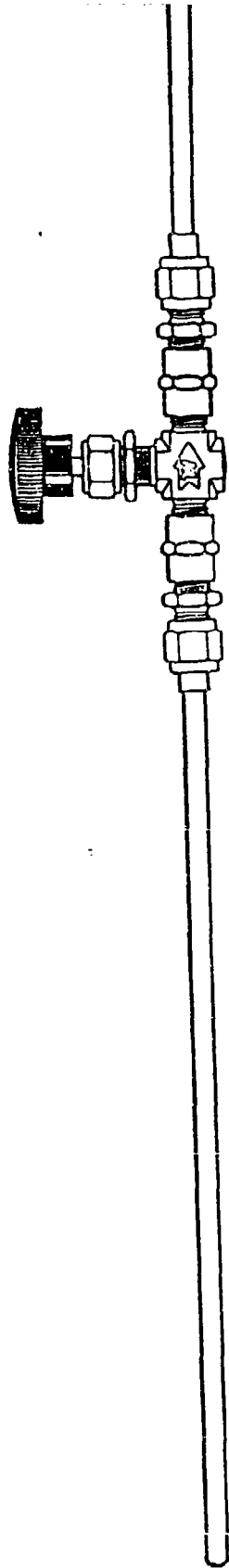
Figure 7.   Metal valve assembly used for reactions involving $XeF_3{}^+SbF_6$.

126

and the samples were warmed to -30°C at which point a color change from yellow to white occurred within 5 min. The sample was warmed further to 0°C, and allowed to react for a further 30 min. Upon completion of the reaction, the samples were pumped at 0°C for 20 min. to remove excess $s-C_3F_3N_3$. The product was stable at room temperature. Samples for ^{19}F NMR, ^{129}Xe NMR and Raman spectroscopy were prepared according to the methods described later in this section.

Nuclear Magnetic Resonance Spectroscopy

Several different containers were used for NMR samples depending on the nucleus under investigation and the solvent used:

Nucleus	Solvent	Sample Tube Materials and Dimensions
^{121}Sb	SO_2ClF	9 mm o.d. FEP tube for insertion into Wilmad thin wall 10 mm o.d. precision glass tube
^{129}Xe	BrF_5 SO_2ClF	9 mm o.d. FEP tube for insertion into Wilmad thin wall 10 mm o.d. precision glass tube
^{19}F	HF	4 mm o.d. FEP tube for insertion into Wilmad thin wall 5 mm o.d. precision glass tube
^{19}F	BrF_5 SO_2ClF	Wilmad precision 5 mm o.d. medium wall glass tube

Solid samples were transferred to NMR tubes in a dry box and sufficient solvent was distilled onto the solid to effect dissolution. The tubes were subsequently heat sealed under vacuum between -196 °C, and stored

in liquid nitrogen. All spectra were recorded on a Bruker WM-250 pulse spectrometer at an external applied field strength of 5.8719 Telsa. The observed frequencies for ^{19}F, ^{129}Xe and ^{121}Sb were 235.36, 69.50 and 59.86 MHz, respectively. NMR spectra were referenced externally at 24°C using the following reference substances: $CFCl_3$ (neat ^{19}F), $XeOF_4$ (neat, ^{129}Xe), $Et_4N^+SbF_6^-$ (0.1 M in $CH_3C\equiv N$). Free induction decays were accumulated in a 16K or 32K memory with spectral width settings between 10 and 25 KHz yielding data point resolutions of 1.6 to 6.0 Hz. The number of scans obtained varied with each sample, with ^{19}F spectra generally requiring 500-2000 scans, and ^{121}Sb and ^{129}Xe spectra requiring between 1000 and 10000 scans for sufficient signal to noise.

Laser Raman Spectroscopy

Excluding reaction mixtures X $s-C_3F_3N_3C3F3N3$: XeF^+ where X > 1, all Raman spectra were obtained from solid samples in sealed precision medium wall glass NMR tubes (Wilmad 5 mm o.d.) A Coherent Nova 90-5 argon ion laser, providing up to 5 W at 514.5 nm was used as the excitation source in conjunction with a Spex Industries Model 14018 double monochromator equipped with 1800-grooves/mm holographic grating. The spectra were accumulated using a RCA C 31034 phototube detector combined with a pulse count system (Hamner NA11) consisting of a pulse amplifier analyzer (Hamner NC-11), and a rate meter (Hamner N-708 A). Spectra were recorded using a Texas Instruments Model FS0ZWBA strip chart recorder. The spectrometer was periodically calibrated by recording the discharge lines from an argon lamp over the spectral range of interest, and the Raman shifts quoted are estimated to be

accurate to ±1 cm^{-1}. Slit widths were set to 150, 200, 200, 150 mμ and all spectra were recorded at a chart speed of 0.5 cm^{-1}/s with gains between 10K and 100K, and time constants between 0.25 and 1.0 s. The approximate power of the beam at the sample ranged from 0.60 to 0.93 w.

Sample tubes were mounted vertically in an unsilvered Pyrex glass Dewar filled with liquid nitrogen such that the angle between the incident beam and the sample was 45° (Figure 8). In cases where immersion in liquid nitrogen was insufficient to prevent decomposition at the site of excitation the sample was rotated to effect increased cooling.

LIQUID N$_2$

SAMPLE

DETECTOR

UNSILVERED DEWAR

LASER BEAM
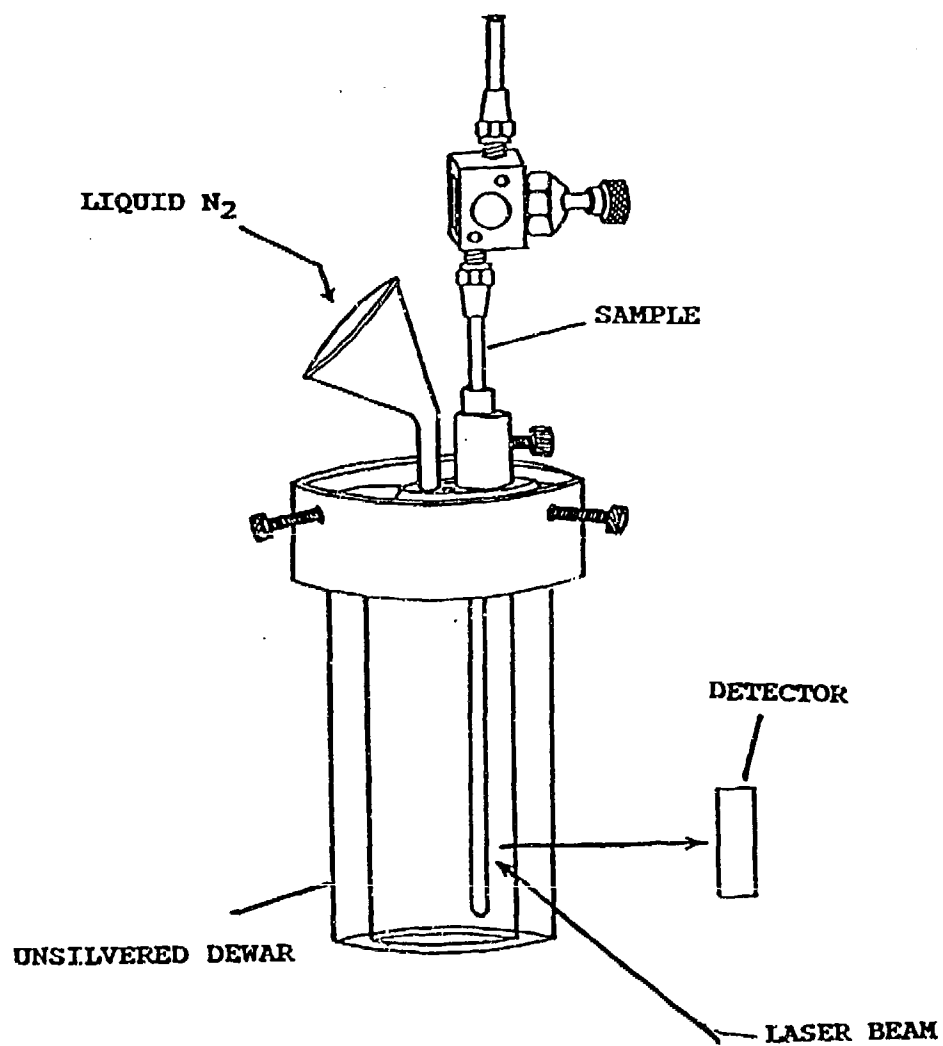
Figure 8. Sample holder for recording laser Raman spectra at -196 °C.

RESULTS AND DISCUSSION

INVESTIGATION OF $(C_3F_3N_2N)_2-XeF^+AsF_6^-$

As noted in the introduction, the reaction of trifluoro-s-triazine with XeF^+ resulted in solid white products, even when a significant excess of liquid $s-C_3F_3N_3$ was employed. It was speculated that at least two moles of $s-C_3F_3N_3$ may be coordinated to Xe(II). To investigate this possibility further, a series of x $s-C_3F_3N_3$: $XeF^+-AsF_6^-$ reaction mixtures was prepared. Since removal of excess $s-C_3F_3N_3$ from the products by pumping under vacuum at room temperature invariably resulted in the formation of the thermally stable 1:1 adduct, $s-C_3F_3N_2N-XeF^+AsF_6^-$, the reaction mixtures were heat sealed under vacuum in FEP tubes at -196 °C, and subsequently examined by low-temperature Raman spectroscopy.

Raman Spectra

A comparison of the Raman spectra for the reaction mixtures (Table 4) with the spectrum for $s-C_3F_3N_2N-XeF^+AsF_6^-$ (Section II) indicated that there was a definite change in the most intense band, characteristic of the Xe-F stretch from 544 in $s-C_3F_3N_2N-XeF^+AsF_6^-$ to 560 cm^{-1} upon addition of excess $s-C_3F_3N_3$ (Figure 9). This high-frequency shift of the Xe-F stretch is indicative of strengthening in the Xe-F bond, resulting from increased Xe-F character in the resonance structure of the adduct

$$F-Xe-L \rightleftharpoons F-Xe^+ L^-$$

Table 4. Some key Raman frequencies $XeF^+AsF_6^-$ and $s-C_3F_3N_2N-XeF^+AsF_6^-$ ·X $s-C_3F_3N_3$

Frequency, cm^{-1}		Assignment
$s-C_3F_3N_2NXeF^+AsF_6^-$	$s-C_3F_3N_2NXeF^+AsF_6^-$ ·X $s-C_3F_3N_3$ [a]	
1504(10)	1510	a_1, sym breathing
648(20)	648,641	a_1 ring breathing, all atoms in phase
553(53)	--	a_1, Xe-F
544(100)	560	a_1, Xe-F
156(23)	157	b_1, b_2, δ(C-N-Xe)
110(15)	94	b_1, b_2, δ(N-Xe-F)

[a] Peak positions invariant for $s-C_3F_3N_2NXeF^+AsF_6^-$·x $s-C_3F_3N_3$ adducts, but the intensity varied.

132
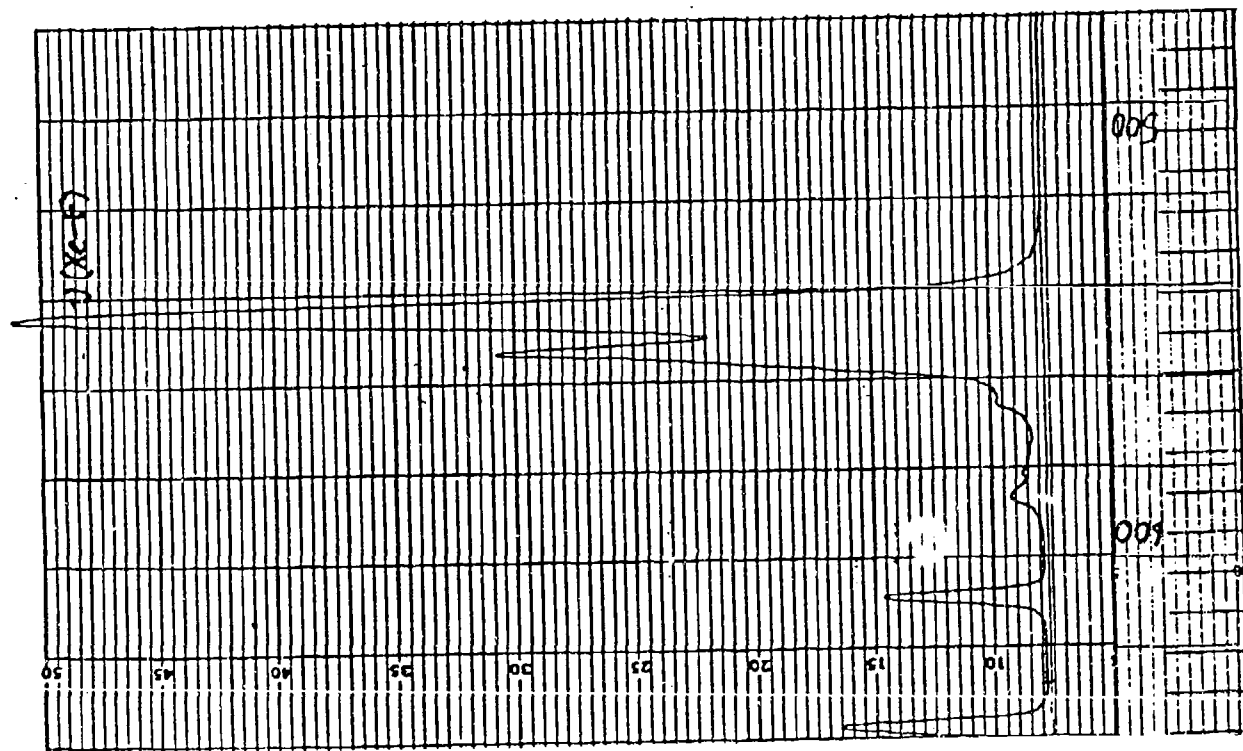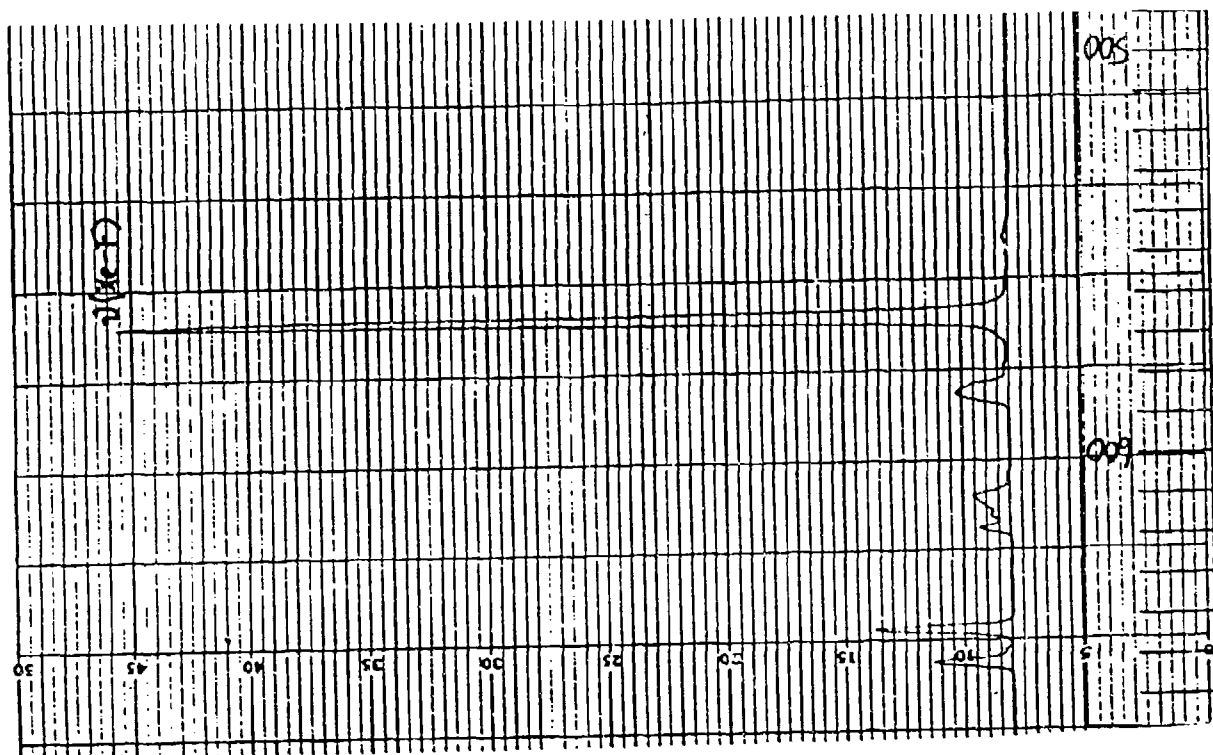
RAMAN SPECTRA OF 3 $C_3F_3N_3$ + $XeF^+AsF_6^-$ SYSTEM

RAMAN SPECTRUM OF $C_3F_3N_2N-XeF^+AsF_6^-$

Figure 9. Raman Xe-F stretch of s-$C_3F_3N_2N-XeF^+AsF_6^-$ and s-$C_3F_3N_2N-XeF^{+'}$ x s-$C_3F_3N_3$.

Other vibrational frequencies associated with the $s-C_3F_3N_2NXeF^+$ cation were also found to be shifted.

In general, the spectra obtained for the different x:1 ratios were very similar, the major difference being relative peak intensities, with little apparent change in peak positions. Unfortunately, the peak intensities were shown to vary while scanning the spectra, preventing a rigourous analysis of the effect of increasing the ratio of trifluoro-s-triazine XeF^+. The variation of peak intensities is thought to arise from dissociation of the more weakly bonded excess $s-C_3F_3N_3$ adducts in the laser beam. No such intensity variation was observed in the spectrum of the 1:1 adduct $s-C_3F_3N_2N-XeF^+AsF_6^-$.

One prominent spectral feature which deserves special mention is the fact that even as x approached 1, the most intense peak, corresponding to the Xe-F, stretch occurred at 560 cm^{-1}, and was invariant. However, below the 1:1 ratio, only one Xe-F stretch at 544 cm^{-1} was present, corresponding to that of $XeF^+AsF_6^-$. These results are significant in that they indicate a product with a different Xe-F bond was formed even when little excess trifluoro-s-triazine was present. Consequently, the formation of a simple $(C_3F_3N_2N)_2-XeF^+$ monomer is unlikely, since it does not account for the change in bonding at x:1 ratios less than 2. To explain these results it is necessary to postulate the formation of a polymer in which each XeF^+ is bonded to two trifluoro-s-triazine rings and which immediately converts, under vacuum, to the monomeric 1:1 adduct $s-C_3F_3N_2N-XeF^+AsF_6^-$ upon removal of excess trifluoro-s-triazine. One possible structure

134

for such a polymer is suggested below [Structure (I)]. Branching in the polymer is unlikely because it could only occur where XeF^+ was bonded to three $s-C_3F_3N_3$ molecules, consequently one can only account for the higher adducts by postulating the formation of cyclic $s-C_3F_3N_2NXeF^+AsF_6^- \cdot x \ s-C_3F_3N_3$ polymers.
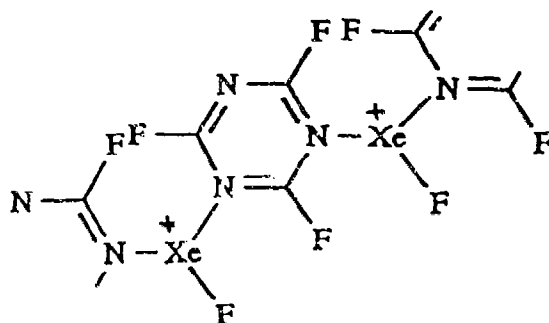
I

If polymeric $s-C_3F_3N_2NXeF^+AsF_6^- \cdot x \ s-C_3F_3N_3$ structures do exist, they might be expected to have the novel AX_3E_3 VSEPR arrangement of lone pairs and bond pairs about the central xenon atom. Two representations of this geometry are given by Structures (II) and (III). Of the two possibilities, Structure (II) is more likely because it minimizes the lone pair - lone pair repulsions relative to the only other alternative, the facial isomer represented by Structure (III). In either case, the binding of the second mole of trifluoro-s-triazine to Xe should result in a lowering of the electric field gradient at the xenon nucleus sufficient to significantly decrease the quadrupole splitting in the ^{129}Xe Mössbauer spectrum. Presently, ^{129}Xe Mössbauer studies are pending; it is expected that they may provide further

insight into the local environment of xenon in the s-$C_3F_3N_2N$-$XeF^+AsF_6^-$ ·x s-$C_3F_3N_3$ systems.
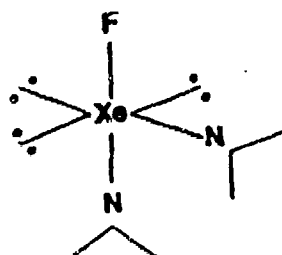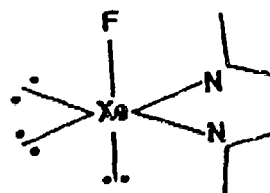
II   III

REACTION OF XeF$_3^+$SbF$_6^-$ WITH TRIFLUORO-s-TRIAZINE

In light of the resistance to oxidation exhibited by the trifluoro-s-triazine ligand, the direct reaction of the ligand with a salt of the Xe(IV) cation, XeF_3^+, was attempted. The salt, $XeF_3^+SbF_6^-$, was selected in the hope that it, like $XeF^+AsF_6^-$, would exhibit Lewis acid characteristics, providing a means of preparing the first example of Xe(IV) bonded to nitrogen. The XeF_3^+ cation is, however, a more potent oxidant than XeF^+ and could possibly oxidize the base upon adduct formation.

^{19}F and ^{129}Xe NMR Spectroscopy

The ^{19}F and ^{129}Xe chemical shifts and coupling constants of

the products in BrF$_5$ (Table 5) gave no evidence for the formation of the desired compound, s-C$_3$F$_3$N$_2$N-XeF$_3$$^+SbF_6$$^-$. In fact, the ^{129}Xe spectrum shows no peaks in the Xe(IV) region (-663 to +595 ppm), and a doublet in the Xe(II) region with a chemical shift similar to that of s-C$_3$F$_3$N$_2$N-XeF$^+$AsF$_6$$^-$ (Figure 10). Furthermore, the chemical shifts and splittings in the F-on-C region of the ^{19}F spectrum (one triplet (1F), one doublet of doublets (2F), Figures 11 and 12), and the F-on-Xe region (triplet with ^{129}Xe satellites, Figure 13) correspond to those obtained for s-C$_3$F$_3$N$_2$N-XeF$^-$ (Figures 14 and 15), indicating Xe(IV) has undergone a two electron reduction to Xe(II) to form of s-C$_3$F$_3$N$_2$N-XeF$^+$SbF$_6$$^-$(Table 5). It should be noted that the ^{129}Xe is an NMR-active nucleus having 26.44% natural abundance. Consequently, 26.44% of the fluorines bonded to Xe couple with ^{129}Xe to produce satellites which, owing to shielding anisotropy, do not exhibit the fine structure of the central multiplet (Figures 13 and 15).

The oxidized product of two trifluoro-s-triazine molecules coupled through nitrogen [Structure (IV)] accounts for the remaining multiplets in the ^{19}F spectrum (Table 5), and the reaction was determined to proceed according to equation (8).
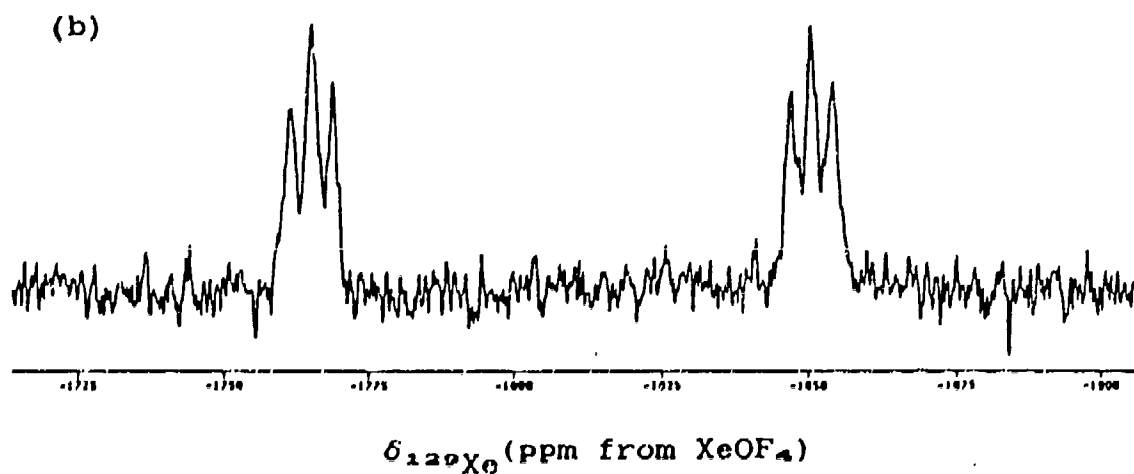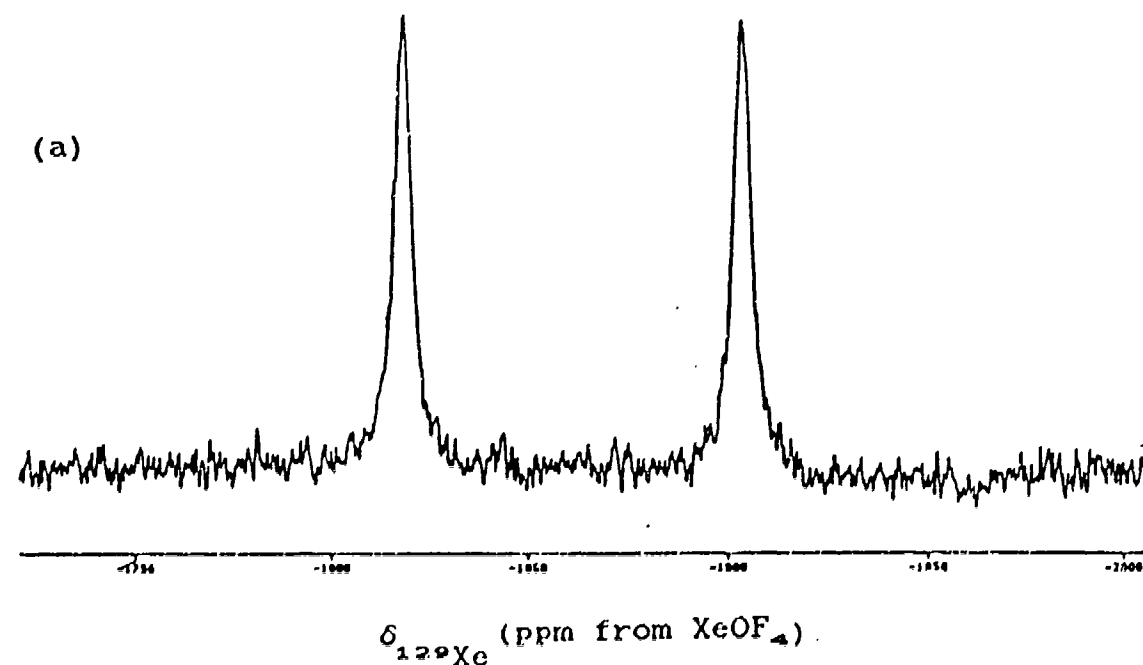
(8)

$$XeF_3^+SbF_6^- + 3\ s\text{-}C_3F_3N_3 \xrightarrow{-20^\circ C}$$
$$s\text{-}C_3F_3N_2N\text{-}XeF^+SbF_6^- +$$

137

(a)

$\delta_{129_{Xe}}$ (ppm from XeOF$_4$)

(b)

$\delta_{129_{Xe}}$ (ppm from XeOF$_4$)
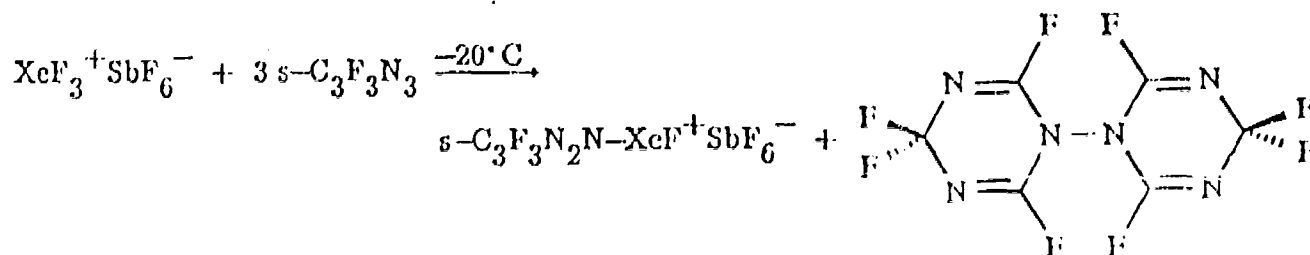
Figure 10. ^{129}Xe spectrum (69.563 MHz) of s-C$_3$F$_3$N$_2$N-XeF$^+$AsF$_6^-$ in (a) BrF$_5$ at -50°C illustrating quadrupole collapse of the ^{129}Xe-^{14}N coupling and a doublet arising from $^1J[^{129}$Xe-^{14}N], and (b) HF at -5°C showing $^1J[^{129}$Xe-^{19}F] and the partially quadrupole collapsed 1:1:1 multiplet arising from $^1J[^{129}$Xe-^{14}N] coupling.

138
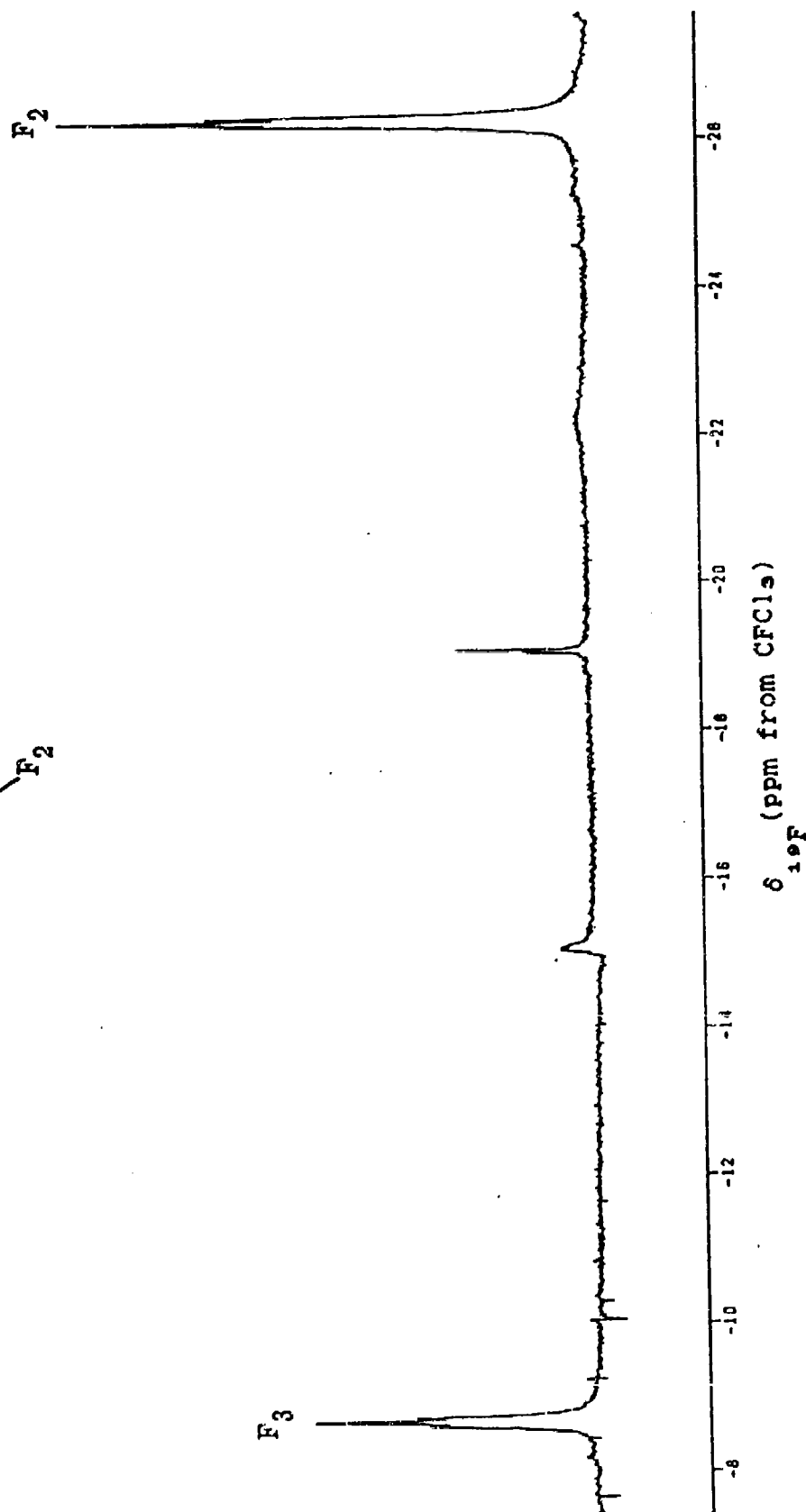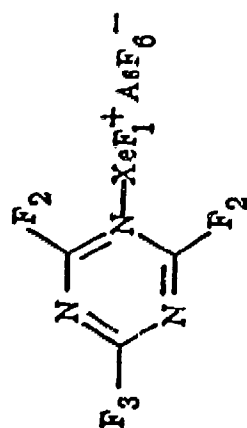
Figure 11. ^{19}F NMR spectrum (235.361 MHz) of s-$C_3F_3N_2N$-XeF$^+$AsF$_6^-$ in BrF$_5$ at

−36°C, F-on-C region.

139
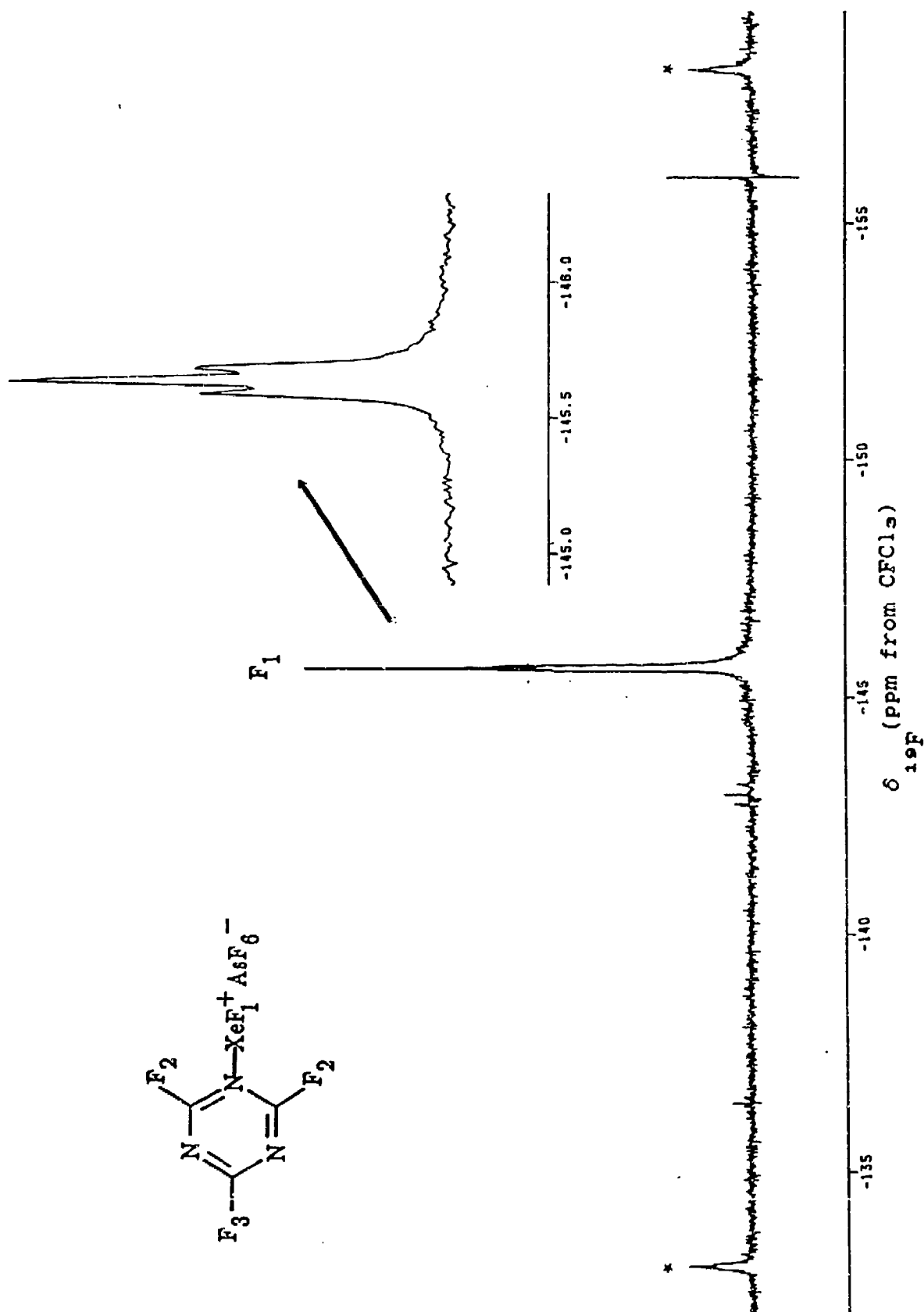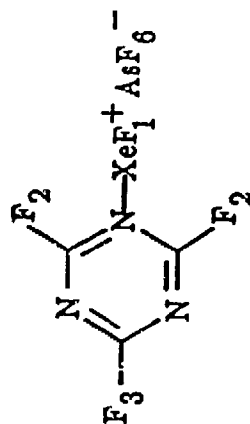
Figure 12. ^{19}F NMR spectrum (235.361 MHz) of $s\text{-}C_3F_3N_2N\text{-}XeF^+AsF_6^-$ in BrF_5 at $-36°C$, F-on-Xe region. Asterisks (*) denote ^{129}Xe satellites.

140

Table 5. NMR parameters for s-$C_3F_3N_2N$–$XeF^+AsF_6^-$ and products resulting from the reaction of $XeF_3^+SbF_6^-$ with trifluoro-s-triazine.[a]

Sample	Species	$\delta^{19}F$ ppm	$\delta^{129}Xe$ ppm	Coupling Consts. Hz
s-$C_3F_3N_2N$–Xe, $^-AsF_6^-$	s-$C_3F_3N_2N$–XeF^+	F(1),-145.6 [D,1F]	-1862 [D]	$^4J[F(1)-F(2)]$,10.9
		F(2),-26.2 [T,2F]		$^4J[F(2)-F(3)]$,13.3
		F(3),-8.7 [T,1F]		$^1J[^{19}F-^{129}Xe]$,5932
s-$C_3F_3N_3$ + $XeF_3^+SbF_6^-$ rxn. prods.	s-$C_3F_3N_2N$–XeF^+	F(1),-145.0 [D,1F]	-1858 [D]	$^4J[F(1)-F(2)]$,11.6
		F(2),-25.4 [d.d.,2F]		$^4J[F(2)-F(3)]$,14.6
		F(3),-8.1 [T,1F]		$^1J[^{19}F-^{129}Xe]$,5917
	(C3F4N2N-)2	F(1'),-36.9 [T,4F]		$^4J[F(1')-F(2')]$,17.4
		F(2'),-19.6 [d.o.t.,2F]		$^4J[F(1')-F(3')]$,16.4
		F(3'),+5.7 [d.o.t.,2F]		$^2J[F(2')-F(3')]$,32.3

[a] Recorded in BrF_5 solvent at -50°C.

Figure 13. ^{19}F NMR spectrum (235.361 MHz) of products resulting from the reaction of $XeF_3^+SbF_6^-$ with trifluoro-s-triazine in BrF_5 at $-50°C$, F-on-C region.

142
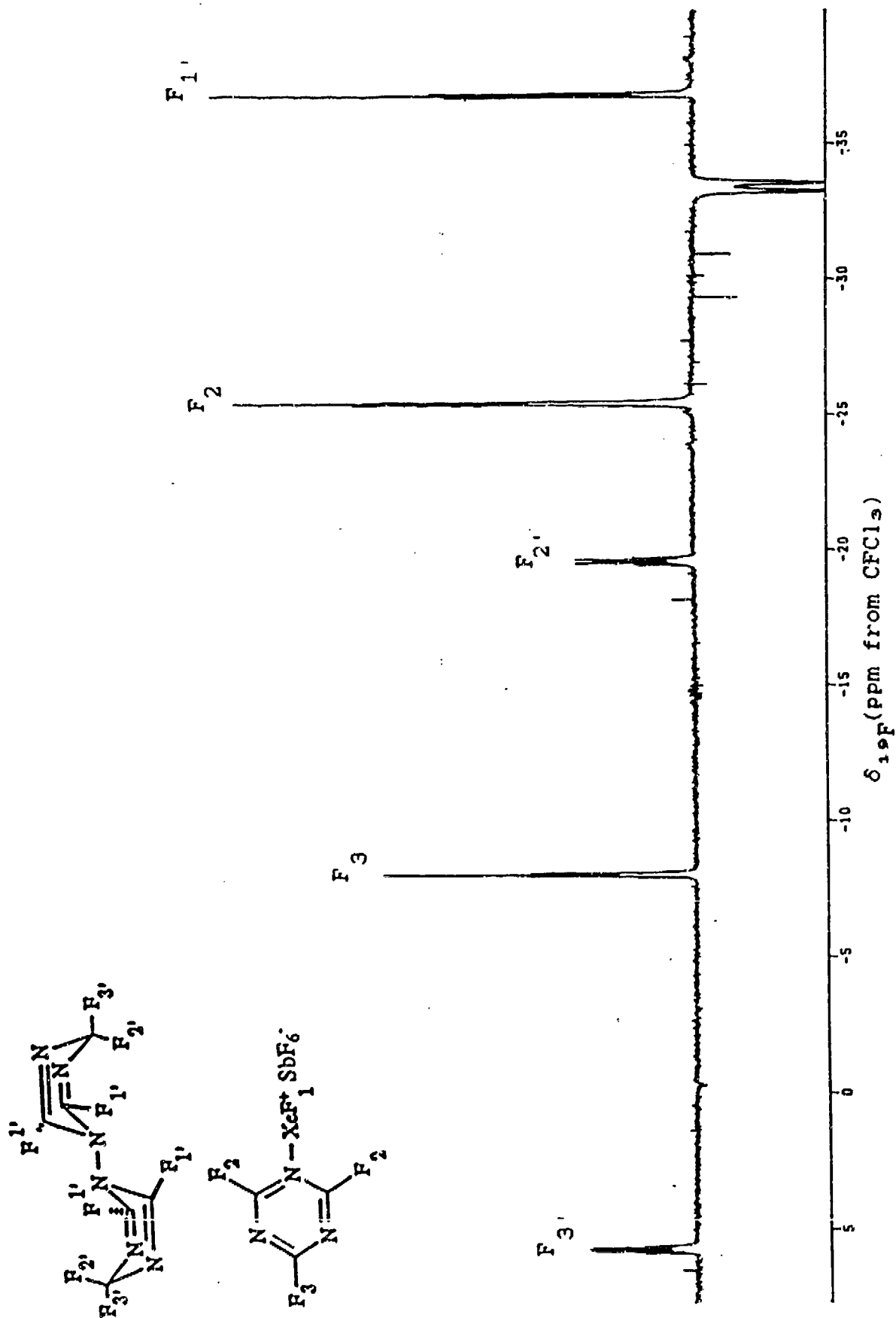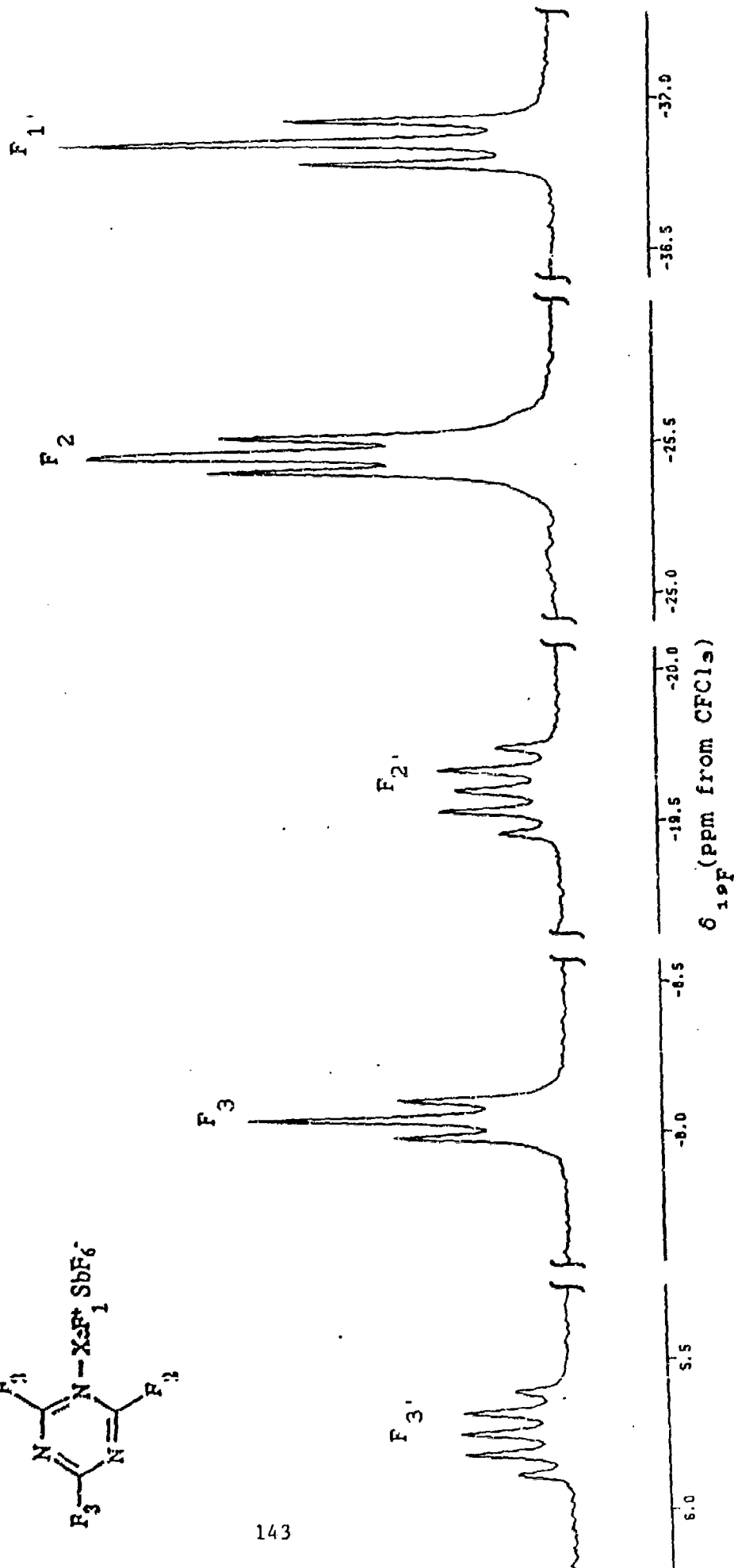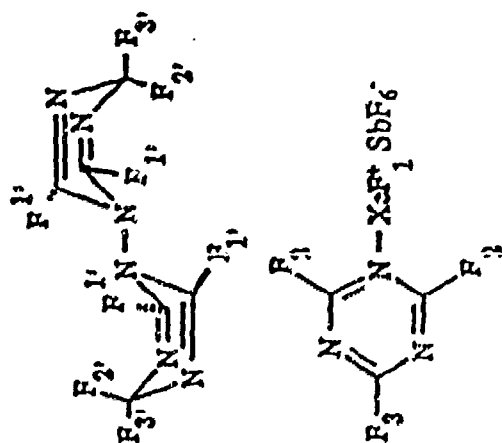
Figure 14. ^{19}F NMR spectrum (235.361 MHz) of products resulting from the reaction of $XeF_3^+SbF_6^-$ with trifluoro-s-triazine in BrF_5 at $-50°C$, F-on-C region expansion.
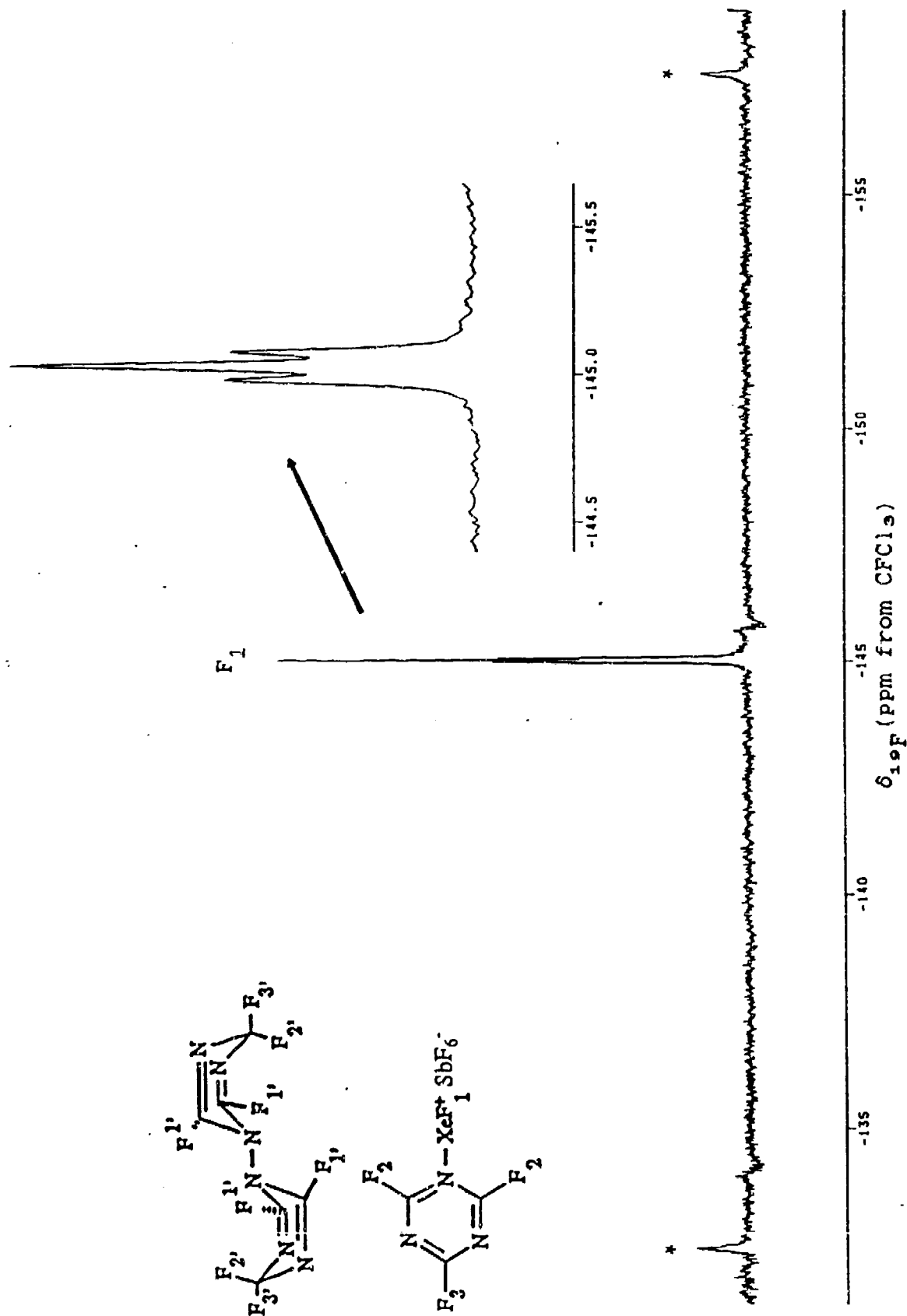
Figure 15. ^{19}F NMR spectrum (235.361 MHz) of products resulting from the reaction of $XeF_3^+SbF_6^-$ with trifluoro-s-triazine in BrF_5 at $-50°C$, F-on-Xe region. Asterisks (*) denote ^{129}Xe satellites.

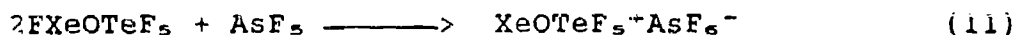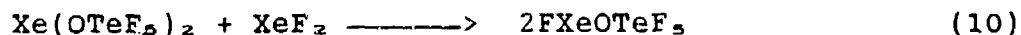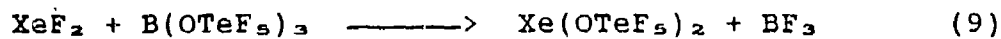
Energy calculations performed on the coupled ring product using the computer program MODEL indicate the minimum energy conformation is one with two fused boat forms of the coupled six membered rings depicted by Structure (IV). This geometry accounts for the presence of three multiplets in the ^{19}F NMR spectrum arising from three non-equivalent fluorines and their accompanying spin-spin couplings (Figures 11 and, Figure 12).
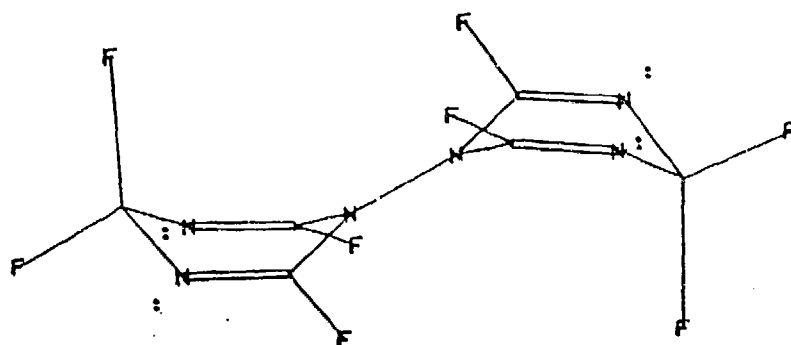
IV

COMPOUNDS CONTAINING NOVEL N-Xe-O LINKAGES

In addition to XeF^+, $XeOTeF_5^+$ has been known for some time and is expected to exhibit Lewis acid properties. The salt, $XeOTeF_5^+AsF_6^-$, can be prepared in good yield according to the following series of reactions:

$$XeF_2 + B(OTeF_5)_3 \longrightarrow Xe(OTeF_5)_2 + BF_3 \qquad (9)$$

$$Xe(OTeF_5)_2 + XeF_2 \longrightarrow 2FXeOTeF_5 \qquad (10)$$

$$2FXeOTeF_5 + AsF_5 \longrightarrow XeOTeF_5^+AsF_6^- \qquad (11)$$

Because the XeOTeF$_5^+$ cation readily undergoes solvolysis in HF and BrF$_5$, the only solvents suitable for the preparation of the previous series of Xe-N adducts, its potential use as a Lewis acid has never been investigated.[24] Fortunately, the direct interaction of XeOTeF$_5^+$AsF$_6^-$ with trifluoro-s-triazine requires no solvent, and XeOTeF$_5^+$AsF$_6^-$ has been used to prepare s-C$_3$F$_3$N$_2$N-XeOTeF$_5^+$AsF$_6^-$, the first compound with an N-Xe-O linkage, according to equation (12).
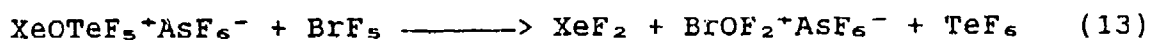
$$XeOTeF_5^+AsF_6^- + s-C_3F_3N_3 \longrightarrow s-C_3F_3N_2N-XeOTeF_5^+AsF_6^- \quad (12)$$
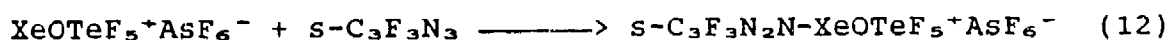
^{19}F and ^{129}Xe NMR Spectroscopy

The product, s-C$_3$F$_3$N$_2$N-XeOTeF$_5^+$AsF$_6^-$, proved to be insoluble in SO$_2$ClF and was subject to solvolysis in HF. Accordingly, it was necessary to use BrF$_5$ solvent for NMR sample preparation, though the XeOTeF$_5^+$ group undergoes solvolysis with BrF$_5$ resulting in the production of TeF$_6$ and bromine oxofluorides, equation (13).

$$XeOTeF_5^+AsF_6^- + BrF_5 \longrightarrow XeF_2 + BrOF_2^+AsF_6^- + TeF_6 \quad (13)$$

Fortunately, reaction of s-C$_3$F$_3$N$_2$N-XeOTeF$_5^+$AsF$_6^-$ with the solvent was slow and incomplete at -50°C, and peaks indicative of the novel cation could be identified in the ^{19}F spectrum (Table 6).

The ^{19}F NMR spectrum of the compound was quite complex owing to the fact that the equatorial and axial fluorines of the -OTeF$_5$

Table 6. NMR parameters for s-$C_3F_3N_2N$-$XeOTeF_5^+AsF_6^-$, s-$C_3F_3N_2N$-$XeOTeF_5^+Sb(OTeF_5)_6^-$ and $XeOTeF_5^+Sb(OTeF_5)_6^-$

Compound	Species	$\delta^{19}F$ (ppm)	$\delta^{129}Xe$ (ppm)	Coupling Consts. (Hz)
s-$C_3F_3N_2N$-$XeOTeF_5^+$ AsF_6^-	s-$C_3F_3N_2N$-$XeOTeF_5^+$ AsF_6^-	F(2),-26.8[a] [D,2F] F(3),-9.0 [T,1F] AB_4, F_{ax},-48.4 F_{eq},-43.1	-2250[b] [S]	$^4J[F(2)-F(3)]$,14.4 $^2J[F_{ax}-F_{eq}]$,177.4 $^1J[F_{eq}-^{125}Te]$,3723
	s-$C_3F_3N_2N$-$XeF^+AsF_6^-$	F(1'),-145.0 [T,1F] F(2'),-26.0 [d.d.,2F] F(3'),-8.3	-1863 [D]	$^4J[F(1')-F(2')]$,11.3 $^4J[F(2')-F(3')]$,14.6 $^1J[^{19}F-^{129}Xe]$,5898
	TeF_6	^{19}F,-53.3 [S]		$^1J[^{19}F-^{125}Te]$,3739 $1J[^{19}F-^{123}Te]$,3102
	AsF_6^-	^{19}F,-64.6 [S]		
$XeOTeF_5^+$ $Sb(OTeF_5)_6^-$[e]	$XeOTeF_5^+$	XeOTeF5, AB_4,[c] F_{ax}, -46.0 F_{eq}, -40.7	-1457[d] [D]	$^2J[F_{ax}-F_{eq}]$,-274.7
	$Sb(OTeF_5)_6^-$	$Sb(OTeF_5)_6^-$ AB_4, ^{19}F, -42.4		
s-$C_3F_3N_2N$-$XeOTeF_5^+$ $Sb(OTeF_5)_6^-$	s-$C_3F_3N_2N$-$XeOTeF_5^+$	F(2),-25.6[f] [D,2F] F(3),-9.1 [T,1F] $XeOTeF_5^+$ AB_4, F_{ax},-47.1 F_{eq},≈-42.3		$^4J[F(2)-F(3)]$,14.5 $^1J[^{19}F-^{129}Xe]$,24.78 $^2J[F_{ax}-F_{eq}]$,≈187 $^1J[F_{eq}-^{125}Te]$,3719
	$Sb(OTeF_5)_6^-$	AB_4 ^{19}F,-42.6		$^1J[^{19}F-^{125}Te]$,3558 $^1J[^{19}F-^{123}Te]$,2951

[a] BrF_5, -55°C. [b] BrF_5, -51°C. [c] SO_2ClF, -51°C. [d] SO_2ClF, 25°C. [e] ^{121}Sb spectrum obtained in SO_2ClF at 25°C. $\delta^{121}Sb$, -13.21 ppm, broad singlet. [f] spectrum obtained in SO_2ClF at -51°C after warming to room temperature.
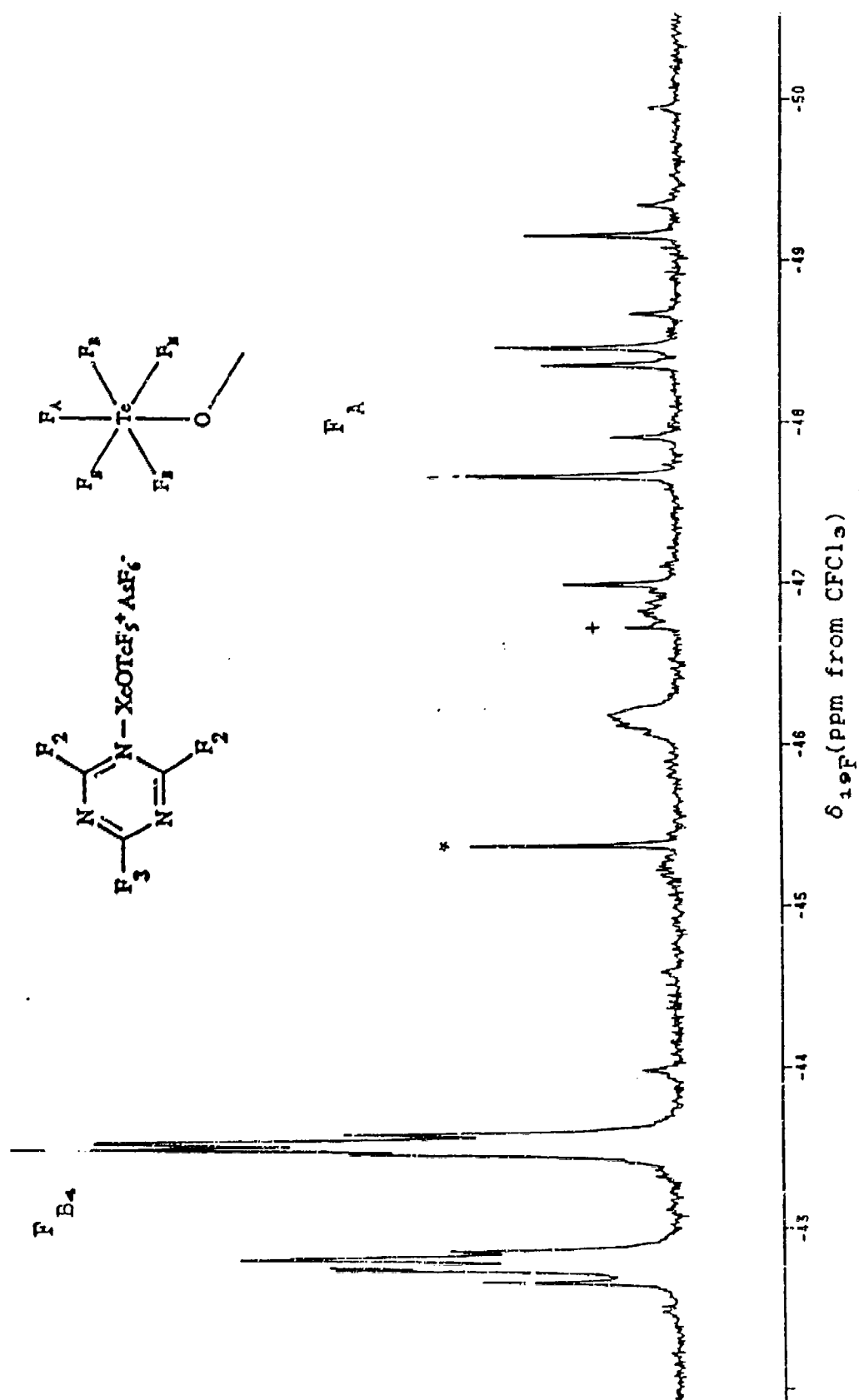
Figure 16. ^{19}F NMR spectrum (235.361 MHz) of $s\text{-}C_3F_3N_2N\text{-}XeOTeF_5^+AsF_6^-$ and byproducts of solvolysis in BrF_5 -55°C, AB_4 region. Plus signs (+) denote ^{125}Te satellites of TeF_6. Asterisks (*) denote ^{123}Te satellite of TeF_6.

148
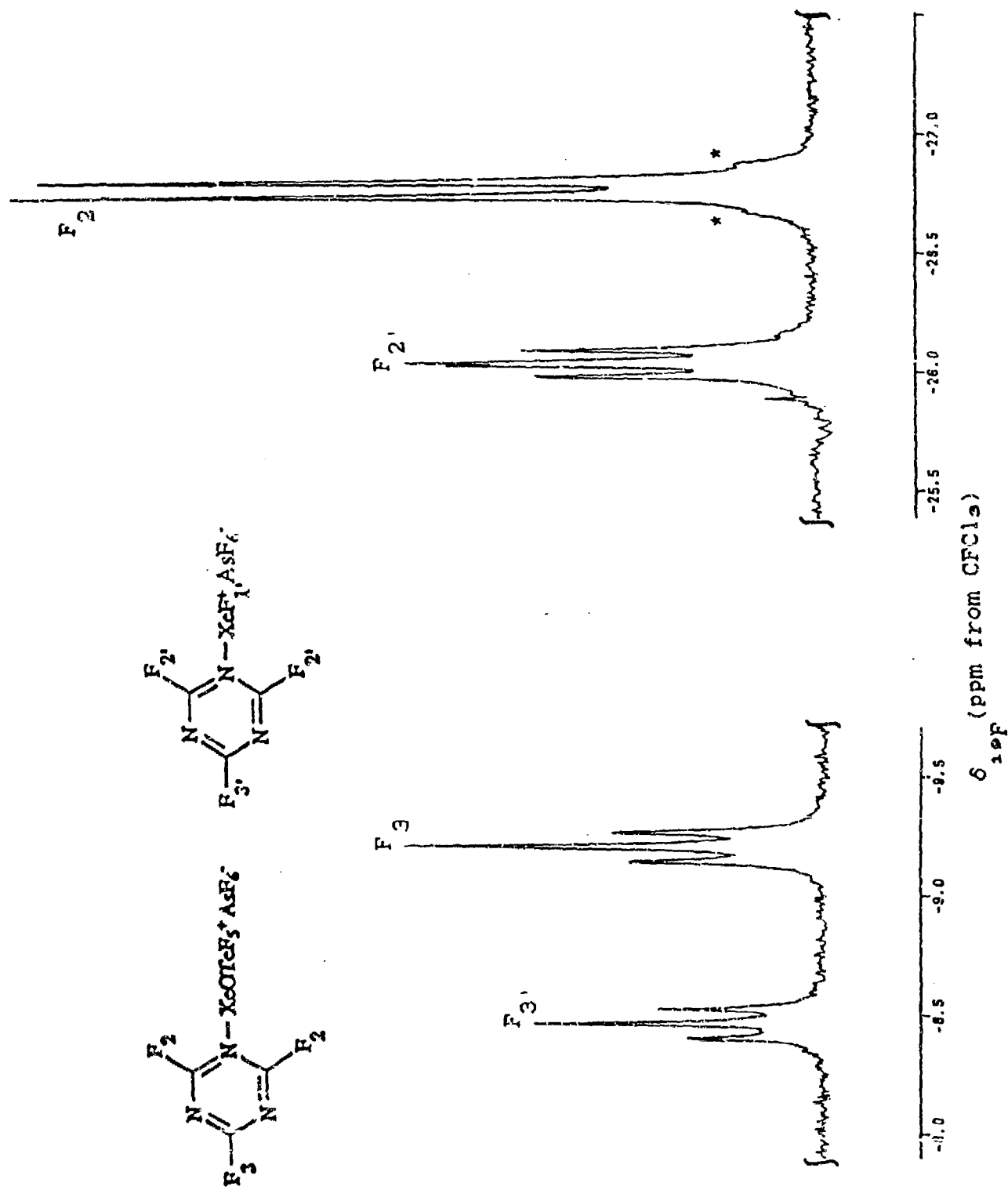
Figure 17. ^{19}F NMR spectrum (235.361 MHz) of s-C$_3$F$_3$N$_2$N-XeOTeF$_5$[+]AsF$_6$[-] and byproducts of solvolysis in BrF$_5$ -55°C., F-on-C region expansions. Asterisks (*) denote [129]Xe satellites.
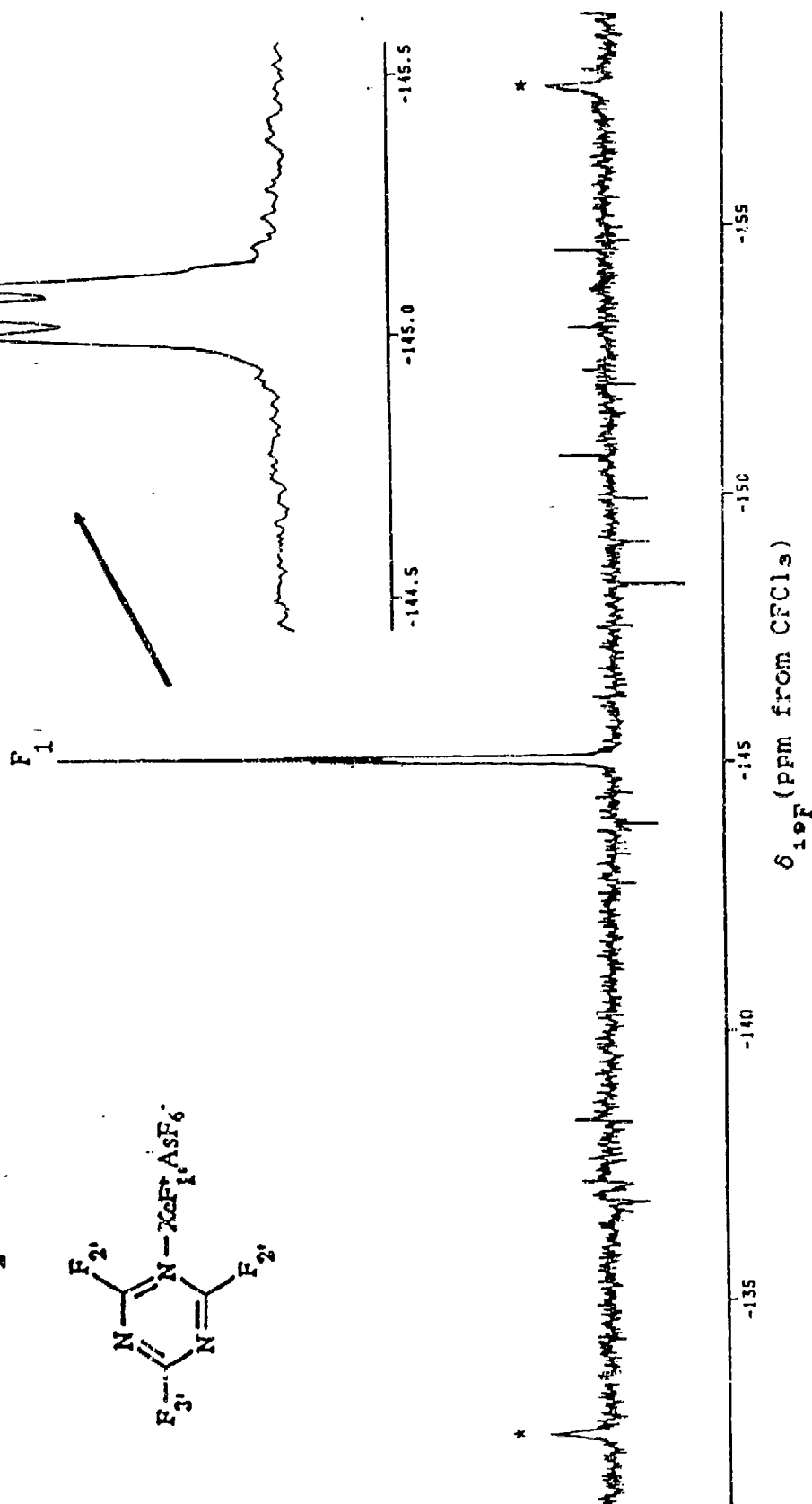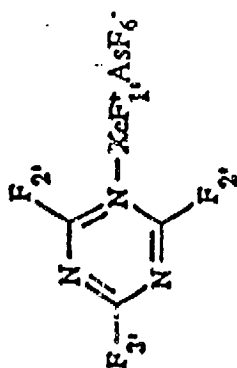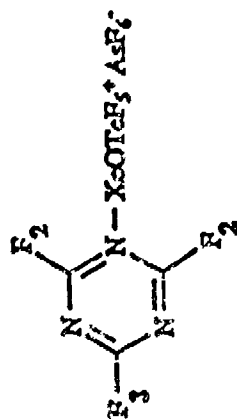
Figure 18. ^{19}F NMR spectrum (235.361 MHz) of s-$C_3F_3N_2N$-Xe$OTeF_5^+AsF_6^-$ and byproducts of solvolysis in BrF$_5$ -55°C, F-on-Xe region. Asterisks (*) denote ^{129}Xe satellites.

group give rise to an AB_4 spin system consisting of 25 transitions (Figure 16). It is interesting to note that line 1 of the AB_4 pattern, which denotes the chemical shift for the lone axial fluorine, is sharper than the rest of the peaks, as is predicted by theory.[27] In addition to the AB_4 pattern, the spectrum of s-$C_3F_3N_2N$-$XeOTeF_5^+AsF_6^-$ gave rise to two multiplets in the F-on-C region; a doublet with ^{129}Xe satellites, and a triplet (Figure 17).

Additional multiplets arising from TeF_6, s-$C_3F_3N_2N$-$XeF^+AsF_6^-$ (Figures 17 and 18 and Table 9) and a broad peak attributed to BrF_3 were also present (Figure 16). Satellites arising from coupling of ^{19}F with ^{125}Te and ^{123}Te (Table 6) are evident for the strong TeF_6 peak.

$XeOTeF_5^+Sb(OTeF_5)_6^-$

Although s-$C_3F_3N_2N$-$XeOTeF_5^+AsF_6^-$ was successfully prepared, the $XeOTeF_5^+AsF_6^-$ Lewis acid could not be used in other Xe-N adduct preparations for lack of a suitable solvent. Other potential ligands such as nitriles and pyridines could not be allowed to react as neat compounds owing to their previously demonstrated thermal instabilities at or near room temperature. To address this problem $XeOTeF_5^+Sb(OTeF_5)_6^-$ was prepared in the hope that the decreased polarity of the $Sb(OTeF_5)_6^-$ anion relative to AsF_6^- anion would facilitate its low-temperature dissolution in SO_2ClF (m.p., -124°C), an inert, low-polarity solvent. It was hoped this synthetic approach would allow the formation of adduct species with $XeOTeF_5^+$ and other more reducing nitrogen bases at low temperatures.

$XeOTeF_5^+Sb(OTeF_5)_6^-$, the first fully substituted $OTeF_5$ salt

151

prepared to date, was prepared using the redox synthesis described by equation (14).

$$2Xe(OTeF_5)_2 + Sb(OTeF_5)_3 \longrightarrow XeOTeF_5^+Sb(OTeF_5)_6^- + Xe \qquad (14)$$
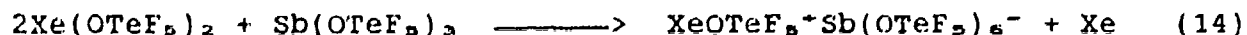
Dissolution of the product in SO_2ClF at $-50°C$ resulted in the formation of a bright orange solution and demonstrated the high solubility of $XeOTeF_5^+Sb(OTeF_5)_6^-$ in SO_2ClF at low temperatures. Chemical shifts and coupling constants obtained using ^{19}F, ^{129}Xe and ^{121}Sb NMR confirm the presence of $XeOTeF_5^+Sb(OTeF_5)_6^-$ (Table 6). The ^{19}F NMR of the product was very complex, owing to the presence of two AB_4 patterns arising from the $-OTeF_5$ groups on Xe and Sb (Figure 19). Although the AB_4 spin system for the $OTeF_5$ group on $XeOTeF_5^+$ was better resolved than that for the anion, owing to incomplete resolution of the individual transitions in the B_4 region of the cation spectrum, only approximate chemical shifts and coupling constants for the axial and equatorial fluorines of the cation could be obtained (Table 6). The AB_4 pattern arising from the $Sb(OTeF_5)_6^-$ anion was very severe, and only one approximate chemical shift for the two fluorine environments could be obtained (Table 6). Owing to the severity of the latter AB_4 pattern, a high-field NMR instrument will likely have no significant effect on the observed resolution, and it is expected that computer simulation will be necessary to obtain even approximate chemical shifts and coupling constants. Tellurium-125 satellites for the AB_4 pattern of the anion were also observed (Figure 19).

The ^{129}Xe spectrum of the $XeOTeF_5^+Sb(OTeF_5)_6^-$ consisted of a

XeOTeF₅⁺Sb(OTeF₅)₆⁻

A: F(A) of XeOTeF₅⁺

B: F(B₄) of XeOTeF₅⁺
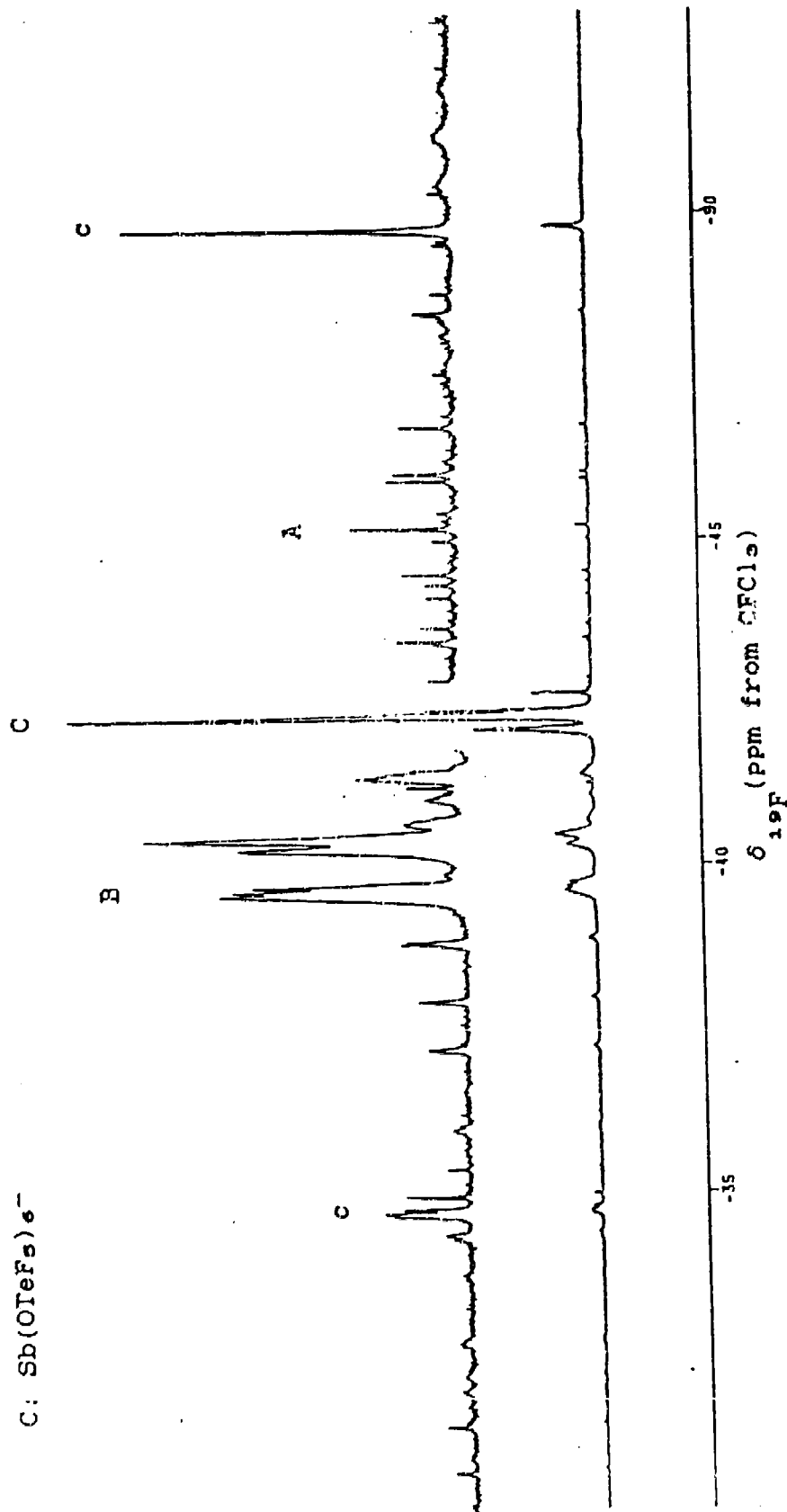
C: Sb(OTeF₅)₆⁻

Figure 20. ¹⁹F NMR spectrum (235.361 MHz) of XeOTeF₅⁺Sb(OTeF₅)₆⁻ in SO₂ClF at 25°C, AB₄ region. Lower case letters denote ¹²⁵Te satellites of Sb(OTeF₅)₆⁻ anion.

153

broad quadrupole collapsed peak at -1457 ppm, which is within the expected range for Xe(II). The ^{121}Sb NMR spectrum was also a broad singlet, (-13.21 ppm, W_4 = 1650 Hz) resulting from partial relaxation of ^{121}Sb in a near-octahedral environment of six OTeF$_5$ groups.

s-C$_3$F$_3$N$_2$N-XeOTeF$_5^+$Sb(OTeF$_5$)$_6^-$

The Lewis acid properties of XeOTeF$_5^+$Sb(OTeF$_5$)$_6^-$ were studied by allowing the solid to react with trifluoro-s-triazine at 0°C. The reaction was immediate, and proceeded according to equation (14)

$$\text{XeOTeF}_5{}^+\text{Sb(OTeF}_5)_6{}^- + \text{s-C}_3\text{F}_3\text{N}_3 \longrightarrow$$

$$\text{s-C}_3\text{F}_3\text{N}_2\text{N-XeOTeF}_5{}^+\text{Sb(OTeF}_5)_6{}^- \quad (14)$$
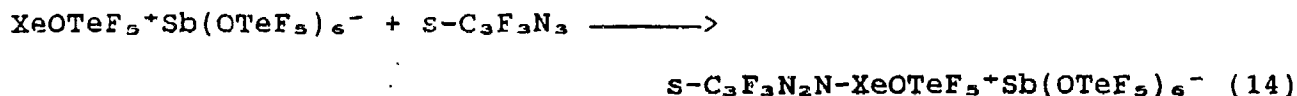
The product proved to be soluble in SO$_2$ClF at low temperatures, and the ^{19}F NMR confirmed the presence of s-C$_3$F$_3$N$_2$N-XeOTeF$_5^+$Sb(OTeF$_5$)$_6^-$ (Table 6). Owing to the presence the two AB$_4$ spin systems, the ^{19}F NMR spectrum was again very complex (Figure 20). The AB$_4$ pattern for the Sb(OTeF$_5$)$_6^-$ anion was severe, and only one ^{19}F chemical shift could be obtained in addition to the tellurium satellite couplings ^{1}J[^{19}F-^{125}Te] and ^{1}J[^{19}F-^{123}Te] (Table 6). The AB$_4$ pattern corresponding to XeOTeF$_5^+$ was better resolved, and it was possible to determine chemical shifts for the axial and equatorial fluorine environments in addition to approximate values for ^{2}J[^{19}F-^{125}Te] (Table 6). Fortunately, the multiplets arising from fluorines bonded to carbon (Figure 21) were well resolved, occurring at significantly higher frequencies than the
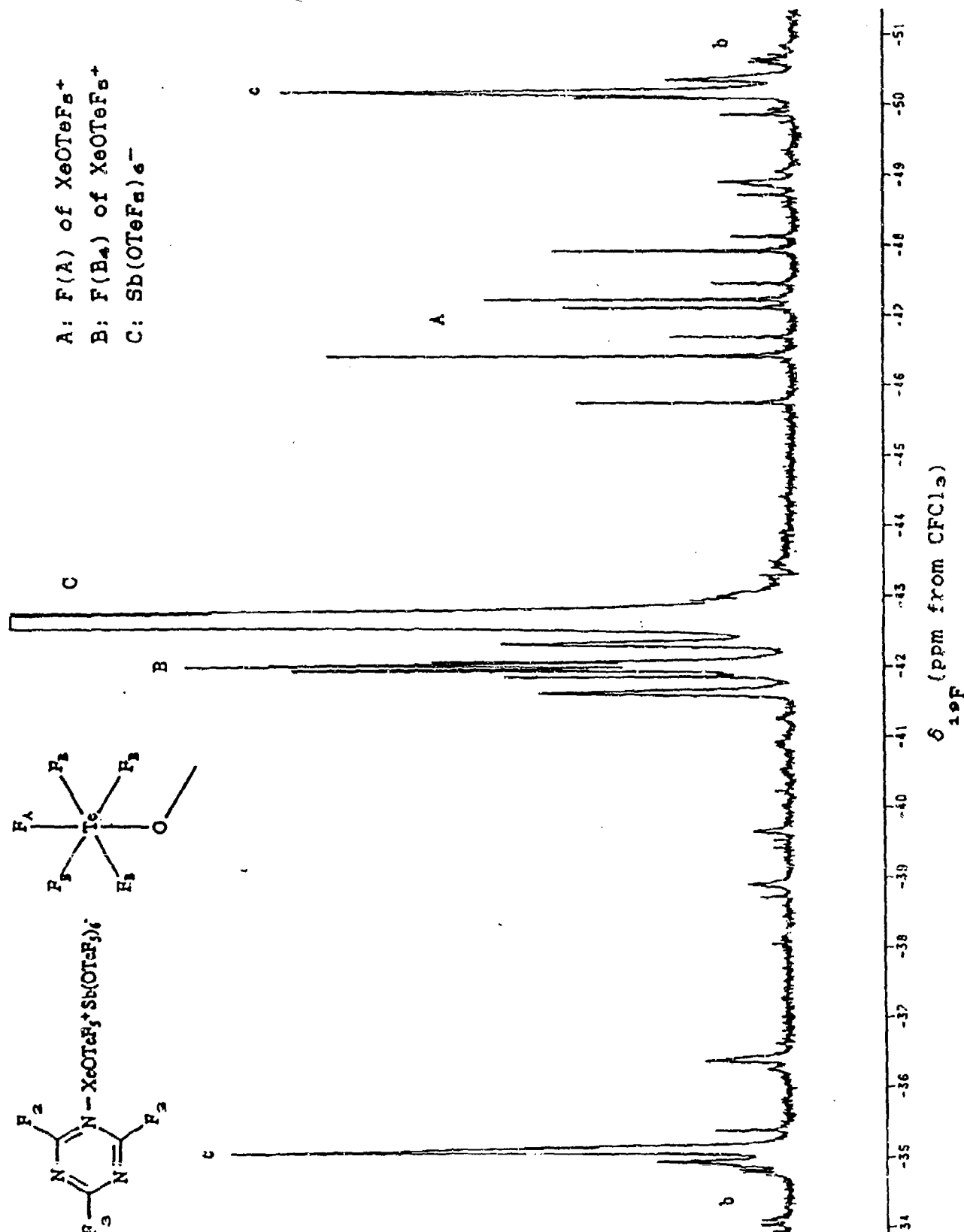
154

Figure 20. ^{19}F NMR spectrum (235.361 MHz) of $XeOTeF_5^+Sb(OTeF_5)_6^-$ in SO_2ClF at 25°C. AB_4 region. Lower case letters denote ^{125}Te satellites of $Sb(OTeF_5)_6^-$ anion.

A: F(A) of $XeOTeF_5^+$
B: F(B₄) of $XeOTeF_5^+$
C: $Sb(OTeF_5)_6^-$

$\delta_{^{19}F}$ (ppm from $CFCl_3$)

Figure 21. ^{19}F NMR spectrum (235.361 MHz) of s-C$_3$F$_3$N$_2$N-XeOTeF$_5$$^+$Sb(OTeF$_5$)$_6$$^-$ in SO$_2$ClF at 25°C, F-on-C region. Asterisks (*) denote ^{129}Xe satellites.

complex AB_4 patterns, thus affording ready measurement of the coupling constants and chemical shifts (Table 6). Xenon-129 NMR spectroscopy studies are presently pending.

It should be noted that some evidence for the presence of byproducts was obtained, however, it is believed that decomposition occurred when the sample was warmed to 25°C prior to obtaining the spectrum at -50°C. Future work will consequently entail ^{19}F NMR characterization of $s-C_3F_3N_2N-XeOTeF_5^+Sb(OTeF_5)_6^-$ at temperatures not exceeding -30°C.

Raman Spectroscopy

The Raman spectrum for $s-C_3F_3N_2N-XeF^+AsF_6^-$ was assigned on the basis of the vibrational assignments for of $s-C_3F_3N_3$ under D_{3h} symmetry, $3A_1' + 4A_2' + 5E' + 2A_2'' + 2E''$.[27] Formation of the XeF^+ adducts of trifluoro-s-triazine lowers the ring symmetry from D_{3h} to C_{2v}, accordingly, 21 bands ($3N - 6$, $N = 9$) for the triazine moiety of $s-C_3F_3N_2N-XeF^+AsF_6^-$ are expected, $8A_1 + 4B_1 + 7B_2 + 2A_2$. In addition, the XeF^+ moiety gives rise to 6 bands, [Xe-F stretch, A_1; Xe-N stretch, A_1; $\delta(N-Xe-F)$, B_1; $\delta(N-Xe-F)$, B_2; $\delta(C-N-Xe)$, B_1; $\delta(C-N-Xe)$, B_2] resulting in a total of 27 bands for $s-C_3F_3N_2N-XeF^+$ ($10A_1 + 6B_1 + 9B_2 + 2A_2$) (Table 7). The octahedral AsF_6^- anion is expected to give rise to three additional bands in the Raman spectrum, namely, $\nu_2(a_{1g})$, $\nu_2(e_g)$, and $\nu_5(t_{2g})$ (Table 7).

The vibrational Raman assignments for the $XeOTeF_5^+$ group in $s-C_3F_3N_2N-XeOTeF_5^+Sb(OTeF_5)_6^-$ and $s-C_3F_3N_2N-XeOTeF_5^+AsF_6^-$ are by analogy with $XeOTeF_5^+AsF_6^-$[24] (Table 7). In both cases the symmetries

Table 7

Raman Frequencies and Assignments for s-C₃F₃N₂N-XeF⁺AsF₆⁻, s-C₃F₃N₂N-XeOTeF₅⁺AsF₆⁻, s-C₃F₃N₂N-XeOTeF₅⁺Sb(OTeF₅)₆⁻ and XeOTeF₅⁺Sb(OTeF₅)₆⁻

frequency cm⁻¹

s-C₃F₃N₂N-XeF⁺AsF₆⁻	s-C₃F₃N₂N-XeOTeF₅⁺AsF₆⁻	s-C₃F₃N₂N-XeOTeF₅⁺Sb(OTeF₅)₆⁻	XeOTeF₅⁺Sb(OTeF₅)₆⁻	Assignment
1661(0.4),1621(1)	1625(1),1662(1)	1613(2)	—	ring mode, a, b ring stretching
1504(1)	1499(22)	1502(3)	—	ring mode, a, symmetric breathing
1252(1)	1249(1)	1249(2)	—	ring mode, C atom twist against N
1117(1),1112(4)	1138(18),1127(3)	1115(18),1127(4)	—	ring mode, a, b, C-F stretching
1015(9)	1010(22)	1008(16)	—	ring mode, a, ring breathing C and N out of plane
805(1)	804(1)	—	—	ring mode, b, out of plane stretch
745(2)	744(4)	—	—	ring mode, a, b, C-F wagging
	729(9),734(7)	—	—	a', ν asym(TeF₄), sym to plane of sym
721(1)	722(3)	—	—	a', ν asym(TeF₄), asym to plane of sym
	706(17),711(4),714(3)	703(14)	—	ring mode, a, b, C-F wagging
694(2)	699(4)			a', ν (TeF)
—	667(6)			ring mode, not assigned
648(20)	656(43)	655(60)	663(45)	a', ν sym(TeF₄), breathing
616(16)	644(97)	644(100)		a', ν sym(TeF₄), out of phase
565(3)	610(27)	608(24)		ring mode, a, ring breathing, all atoms in phase
	564(4)	564(5)		ring mode, not assigned
543(100)	—	—	—	ring mode, not assigned
467(100)			579(17)	a, ν Xe-F
410(2)	478(87)	478(87)		a', ν Xe-F
386(16)	402(21)	402(21)	413(36)	a', ν sym(Xe-O-Te)
325(5)				ring mode, not assigned
312(4)	318(9)		323(11)	ν(Sb-O-Te)
314(1)	312(9)			ring mode, e', C-F rocking
290(3)	305(10)			a', δ(F'TeF₄) in plane of symmetry
—	246(43)		306(28)	a, ν Xe-N
251(15)		c	253(13)	a', δ(TeF₄) in plane scissors
256(28)	230(4)			a', δ(TeF₄) sym to plane of symmetry
236(5)	202(2)		—	ring mode, not assigned
234(1)			—	ring mode, not assigned
200(2)	175(15)		171(25)	a', δ(OTeF₄) out of plane
172(37)	148(36)			a', δ(Xe-O-Te)
155(23)	126(46)		123(47)	b, b, δ(C-N-Xe)
133(40)	100(15)			δ(O-Xe-N)
120(52)				b, b, δ(N-Xe-F)
110(15)				
98(26)				
663(23)	748(23)	748(12)		
581(2) a	731(35)	743(12)		
372(6)	726(14)	732(10)		
371(5)	721(18)	725(21)		
	717(27)	716(54)		
	715(25) c	705(24)	c	
98(25)	706(39)	649(41)		
76(5) b	639(16) b	642(20)		
69(5)	240(11)	413(36)		
	91(44)	148(36)		
	77(29) b	136(34)		
	71(33)	123(47)		
	67(34)			

a AsF₆⁻ modes.   b External modes and/or low-frequency bending and torsional modes.   c Non-assigned modes arising from -OTeF₅ group.

158

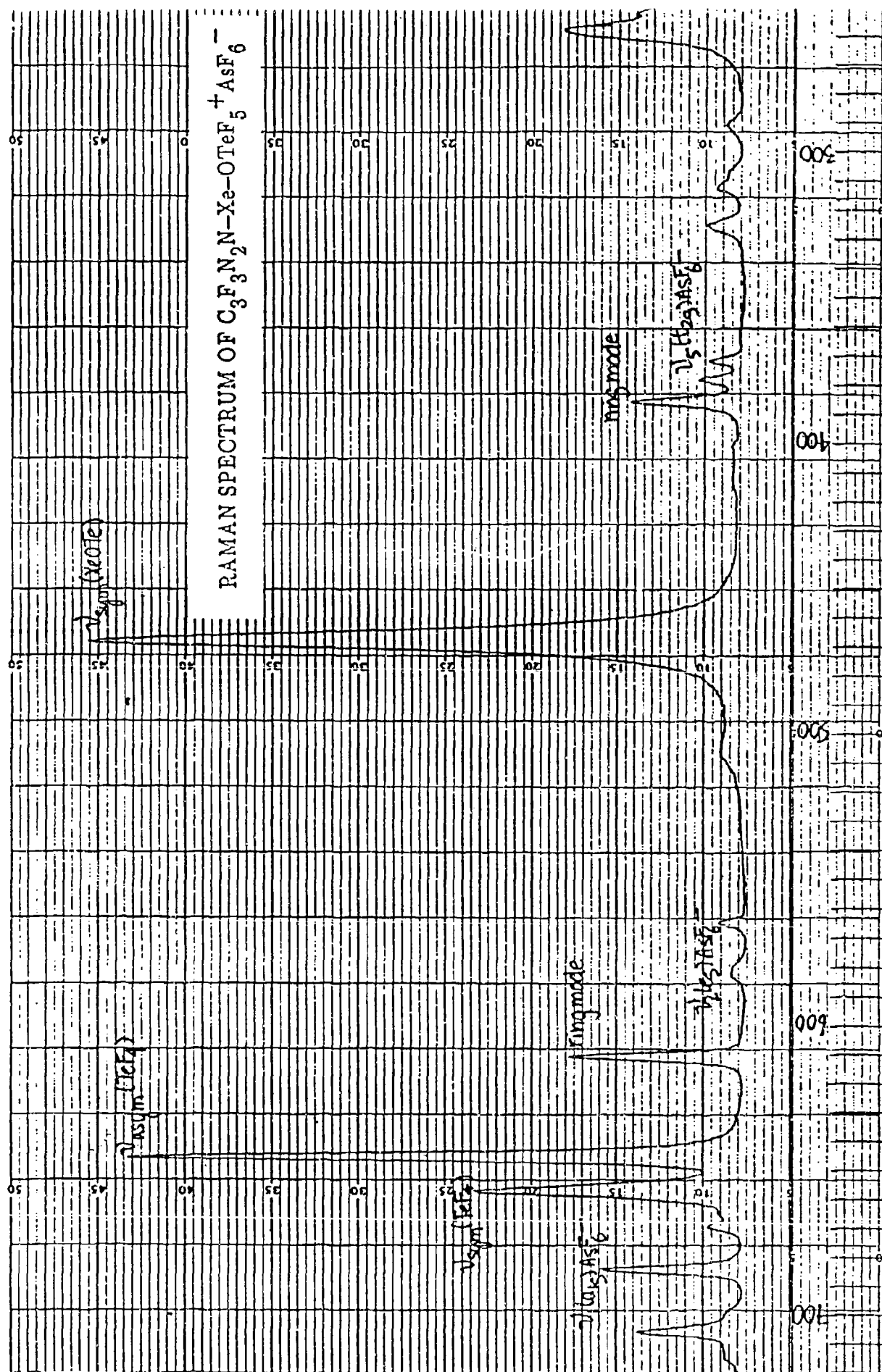RAMAN SPECTRUM OF $C_3F_3N_2N-Xe-OTeF_5^+AsF_6^-$

Figure 22. Raman Spectrum of $C_3F_3N_2N-XeOTeF_5^+AsF_6^-$

of the cations are assumed to be low (C_s or C_1); for the purposes of this discussion and labelling, C_s symmetry is assumed. In either case, all the modes associated with the $XeOTeF_5^+$ group are expected to be Raman active (11A' + 7A" under C_s and 18A under C_1).

The modes associated with the $OTeF_5$ group of the anion $Sb(OTeF_5)_6^-$ were very difficult to assign owing to their proximity to the $OTeF_5$ bands of $XeOTeF_5^+$. The only $Sb(OTeF_5)_6^-$ band assigned is that corresponding to the intense and strongly coupled Sb-O-Te stretches.

In general, one would expect the less electronegative $OTeF_5$ group (3.38 relative to 4.10 for F on the Allred-Rochow / Pauling scale)[29] to give rise to a more covalent Xe-N adduct than in the XeF+ analogue. Accordingly the increased electron donating ability of the $XeOTeF_5^+$ group relative to XeF^+ should result in overall shifts of bands to lower frequencies. However, many other factors, such as the site symmetry and the symmetry of the crystal environment also play a role in activities and, to a lesser extent, peak positions. Thus, comparison of the spectra of the $XeOTeF_5$ and $s-C_3F_3N_2N-$ moieties as well as the AsF_6^- anion in $s-C_3F_3N_2N-XeF^+AsF_6^-$, $s-C_3F_3N_2N-XeOTeF_5^+AsF_6^-$ and $s-C_3F_3N_2N-Xe-OTeF_5^+Sb(OTeF_5)_6^-$ show little variation enabling one to "transfer" the modes from $XeOTeF_5^+AsF_6^-$ and $s-C_3F_3N_2N-$ for the purpose of assignment of these compounds.

Among the major difficulties encountered when analyzing the Raman spectra for the three adducts was the fact that the low frequency Xe-N stretch is generally weak and therefore hard to assign. Consequently, the vibrational mode is expected to vary the most among the

three compounds, the Xe-N stretch, could not be definitively assigned. Although the Xe-O, Te-O and Sb-O stretches associated with these compounds was generally very intense, it is not possible to assign discrete stretching modes to the bands owing to strong coupling of stretching vibrations arising from atoms of nearly identical masses, i.e., Xe-O-Te and Sb-O-Te.

The spectrum for $XeOTeF_5^+Sb(OTeF_5)_6^-$ was poorly resolved by virtue of the nature of the compound itself, i.e., poor crystallinity. It was, however, possible to assign a number of modes including $OTeF_5$ modes and the intense and strongly coupled Xe-O-Te stretching modes all correlating well with those observed in the spectra of $s-C_3F_3N_2N-XeOTeF_5^+AsF_6^-$ and $s-C_3F_3N_2N-XeOTeF_5^+Sb(OTeF_5)_6^-$.

^{129}Xe Mössbauer Study of Xenon-Nitrogen Bonded Species and Related Species

We have recently added ^{129}Xe Mössbauer spectroscopy to our in-house arsenal of structural characterization techniques. In conjunction with establishing the capability in our laboratory, we have prepared a high quality sealed source, namely, $Na_5{}^{129}IO_6$. To date, we have remeasured a number of previously determined compounds as well as a number of new xenon(II) cations described in our previous Annual Technical Report (see Table 8).

In ^{129}Xe Mössbauer spectroscopy, only the quadrupole splitting is sufficiently sensitive to provide information relating to xenon-ligand atom bond covalency, and is therefore the parameter we are primarily concerned with. In general, the quadrupole splitting in xenon(II) species is seen to decrease with increasing covalency as determined from the ^{129}Xe NMR chemical shift and the Xe-F stretching frequency.

We have reported the reaction of $XeF^+AsF_6^-$ with trifluoro-s-triazine, $s-C_3F_3N_3$, leading to the formation of a new class of Xe-N bonded cation, $s-C_3F_3N_2N-XeF^+AsF_6^-$ in Section II. We propose to investigate the 2:1 cation described earlier in this report by Mössbauer spectroscopy. The Mössbauer spectrum of $s-C_3F_3N_2N-XeF^+AsF_6^-$ has been measured. The quadrupole splitting in $[s-C_3F_3N_2N-]_2XeF^+AsF_6^-$ ought to be significantly smaller than in the 1:1 cation or any other xenon(II) derivative presently known if the second nitrogen is coordinated to the xenon. If our speculations are confirmed, the

162

addition of this technique will prove invaluable in establishing the existence of the first compound known to possess an AX_3E_3 arrangement of bond pairs and lone pairs. The isolation of examples of solid fluoro(alkylnitrile) and fluoro(pyridine) xenon(II) cations in the course of these investigations have also provided us with further opportunities to measure their Mössbauer spectra (Table 8).

Table 8. ^{129}Xe Mössbauer data for Xenon derivatives

at 4.2 K·a

Compound	δ b	E_Q mm/s	Γ c mm/s	χ^2 d	
$Xe_2F_3{}^+AsF_6{}^-$	0.2(1)	41.7(2)	8.6(4)	0.89	
$XeF^+AsF_6{}^-$	0.2(7)	40.5(1)	9.5(3)	1.06	*
$HCNXeF^+AsF_6{}^-$	0.2(1)	40.2(3)	8.8(6)	0.82	*
XeF_2	0.0(2)	38.7(3)	9.6(7)	0.78	
$C_5F_5NXeF^+AsF_6{}^-$	0.2(1)	37.8(3)	7.2(7)	0.91	*
$FXeOSO_2F$	0.05(9)	37.8(2)	10.1(4)	0.92	*
$Xe(OSO_2F)_2$	0.3(9)	37.3(2)	10.5(4)	0.96	*
$CH_3CNXeF^+AsF_6{}^-$	0.1(1)	37.2(3)	8.1(5)	0.79	*
$C_3F_3N_2NXeF^+AsF_6{}^-$	0.0(1)	37.1(2)	7.3(4)	0.72	*
$Xe(OTeF_5)_2$	0.2(1)	36.0(3)	8.1(6)	0.83	
$Xe(OSeF_5)_2$	0.07(7)	35.4(1)	8.6(4)	0.78	*
$Xe[N(SO_2CF_3)_2]_2$	-0.5(2)	33.3(4)	7.3(10)	0.87	*
XeF_4	0.2(1)	40.6(2)	10.4(5)	0.69	
$Xe(OTeF_5)_4$	0.2(1)	35.2(2)	7.8(5)	0.78	
$O=Xe(OTeF_5)_4$	0.4(1)	15.8(2)	7.3(4)	1.01	
Na_4XeO_6	-0.4(10)	0	11.5(4)	0.82	

a The compounds being reported for the first time are
  denoted by an asterisk (*).
b Relative to hydroquinone clathrate.
c Full width at half height.
d Per degree of freedom.

Conclusions and Directions for Further Research

1. $XeF^+AsF_6^-$ may react with excess trifluoro-s-triazine to form polymeric $s\text{-}C_3F_3N_2N\text{-}XeF^+ \cdot x\ s\text{-}C_3F_3N_3\ x > 1$, [129]Xe Mössbauer studies may provide evidence for this novel bonding situation;

2. $XeF_3^+SbF_6^-$ is too potent an oxidizing agent to form a stable $Xe(IV)\text{-}N$ adduct with trifluoro-s-triazine;

3. $XeOTeF_5^+AsF_6^-$ has Lewis acid properties and, as such, can be used to prepare $s\text{-}C_3F_3N_2N\text{-}Xe\text{-}OTeF_5^+AsF_6^-$, the first compound containing an $N\text{-}Xe\text{-}O$ linkage;

4. The preparation and characterization of $XeOTeF_5^+Sb(OTeF_5)_6^-$ and $s\text{-}C_3F_3N_2N\text{-}XeOTeF_5^+Sb(OTeF_5)_6^-$ represents an important new development in noble-gas chemistry. The high solubility of $XeOTeF_5^+Sb(OTeF_5)_6^-$ and its trifluoro-s-triazine adduct in SO_2ClF are significant in that they indicate a means to prepare and characterize novel $Xe\text{-}N$ compounds in an inert, low-polarity solvent. The use of the Lewis acid $XeOTeF_5^+Sb(OTeF_5)_6^-$, as in the preparation of $s\text{-}C_3F_3N_2N\text{-}XeOTeF_5^+Sb(OTeF_5)_6^-$, may extend to the syntheses of numerous novel noble-gas compounds which would be protonated and/or fluorinated in BrF_5 and HF.

5. To a certain extent follow-up work stemming from this work has served to illustrate point (4) above. Cation adducts of the more easily oxidized nitrogen $CH_3C\equiv N$ and C_5F_5N (perfluoropyridine) have been stabilized at low temperatures in SO_2ClF solvents as the salts $CH_3C\equiv N\text{-}XeOTeF_5^+Sb(OTeF_5)_6^-$ and $C_5F_5N\text{-}XeOTeF_5^+Sb(OTeF_5)_6^-$.[49]

REFERENCES

1. R.D. LeBlond and D.D. DesMarteau, J. Chem. Soc., Chem. Commun, 1974, 555

2. J.F. Sawyer, G.J. Schrobilgen and S.J. Sutherland, Inorg. Chem., 1982, 21, 4064.

3. R. Faggiani, D.K. Kennepohl, C.J.L. Lock and G.J. Schrobilgen, Inorg. Chem., 1986, 25, 563.

4. D.D. DesMarteau, R.D. LeBlond, S.F. Hossian, D. Nothe, J. Amer. Chem. Soc., 1981, 103, 7734.

5. G.A. Schumacher and G.J. Schrobilgen, Inorg. Chem., 1983, 22, 2178

6. J. Foropoulos and D.D. DesMarteau, J. Am. Chem. Soc., 1982, 104, 4260.

7. A.A.A. Emara and G.J. Schrobilgen, J. Chem. Soc., Chem. Commun., 1987, 1644.

8. G.J. Schrobilgen, J. Chem. Soc., Chem. Commun., 1988, 863.

9. H. Bock, R. Dammel and D. Lentz, Inorg. Chem., 1984, 23, 1535.

10. V.H. Piebler and S.K. Liston, J. Chem. Phys., 1968, 48, 4765.

11. G.P. van der Kelen and P.J. DeBievre, Bull. Soc. Chim. Belg., 1960, 82, 1555.

12. G.P. van der Kelen and P.J. DeBievre, Bull. Soc. Chim. Belg., 1960, 82, 1555.

13. D.M. Rider, G.W. Ray, E.J. Darland and G.E. Lero, J. Chem. Phys., 1981, 74, 1652.

14. C.R. Brundle, M.B. Robin and N.A. Keubler, J. Amer. Chem. Soc., 1972, 94, 1466.

15. P. Rosums, H. Stafast and H. Bock, Chem. Phys. Lett., 1975, 34, 275.

16. C.R. Brundle, M.B. Robin and N.A. Keubler, J. Amer. Chem. Soc., 1972, 94, 1466.

17. A.A.A. Emara and G.J. Schrobilgen, J. Chem. Soc., Chem. Commun., 1988, 257.

18. G.J. Schrobilgen, J. Chem. Soc., Chem. Commun., 1988., 863.

19. G.J. Schrobilgen, J. Chem. Soc., Chem. Commun., 1988, 1506.

20.   R.J. Gillespie, A. Netzer and G.J. Schröbilgen, Inorg. Chem.,
        1974, 13, 1455.

21.   G.J. Schrobilgen, J.H. Holloway, P. Granger, C. Brevard, Inorg.
        Chem., 1978, 17, 980.

22.   R.J. Gillespie and B. Landa, Inorg. Chem., 1973, 12, 1383.

23.   R.J. Gillespie and G.J. Schrobilgen, Inorg. Chem., 1973, 12,
        1772.

24.   N. Keller and G.J. Schrobilgen, Inorg. Chem., 1981, 20, 2118.

25.   R.G. Syvret, Ph.D. Thesis, McMaster University, 1985.

26.   D. Lentz and K. Seppelt, Z. Anorg. Allg. Chem., 1983, 502, 83.

27.   R.K. Harris and K.J Packer, Inorg. Chem, 1961, 4736.

28.   J.E. Griffiths and D.E. Irish, Can. J. Chem., 1964, 42, 690.

29.   "Inorganic Chemistry", J.E. Huheey ed., Harper and Row, New
        York, 1983, 845.